Response to comments on "Retrieval of desert dust and carbonaceous aerosol emissions over Africa from POLDER/PARASOL products generated by GRASP algorithm" by Cheng Chen et al.

We would like to thank the two referees for their time reviewing the manuscript, and for the helpful feedback provided. Their comments allow us to improve the manuscript by better emphasizing its strength and are of important help to our future research. We have taken them into full consideration and made changes accordingly which we hope satisfying the reviewers. Their comments are repeated below along with our responses (in blue).

Response to comments by Referee #1

This is a solid contribution. My previous comments have been addressed. I recommend the publication of this paper as is.

Response: We appreciate the referee very much for these comments.

Response to comments by Referee #2

GENERAL COMMENTS:

The manuscript presents interesting and new results that contribute to the research field. The sensitivity tests are appropriate, the results presented are very good and the implementation of the posterior emissions in a different model confirms the quality of the results. More importantly, this work shows that it is possible to compute topdown estimates of emissions with a relatively high spatial and temporal resolution. The manuscript shows a detailed and complete work, but the quality of the figures and the general presentation of the text overshadow the work.

Despite the fact that English is not my mother tongue, I have found a large number of grammatical errors. Please correct carefully the English language to accomplish with the journal standards and to improve the readability of the manuscript. I have pointed out some of these errors in the minor changes section (only for the first pages of the manuscript).

In general, the figures are low quality for publication. Labels are small and captions are incomplete as they do not explain well the elements in the figures. In most of the maps there is no latitude/longitude labels, etc. Please follow the guidelines from https://www.atmospheric-chemistry-and-physics.net/for_authors/manuscript_preparation.html

Response: We thank the referee for detailed reviews and very helpful comments and remarks. We appreciate the referee's feedback and their recognition of the value that the study offers the scientific community. We will address their concerns to improve the precision, clarity and discussion of the manuscript.

The methodology section (3.1) is not clear. The notation is not consistent throughout the text and there are elements in the equations that are not explained. I would suggest to avoid details about the minimization procedure (they are already explained in Dubovik et al 2008) and to focus on the

improvements and differences with the Dubovik et al 2008 work.

Response: Indeed, this work is a continuation of the previous work by Dubovik et al. (2008). The results and community reaction on 2008 paper inspired the authors to continue the effort. This is why, in the text of this paper we tried to show clear link between 2008 and current work. From review comments we realized some deficiencies of our description. The section 3.1 was verified and corrected. The left only equations necessary to understand the changes what were implemented in GEOS-CHEM adjoin for this work: the adjoint operation for AOD and AAOD.

Basic information about the assimilation is missing in the manuscript.

Response: Section 3.1 provides the conceptual equations introducing the assimilation. We have somewhat revised the text to link the current work with assimilations overall assimilation activities. However, we think adding more introductory material would not correspond to the character of paper and we refer the readers to other more appropriate introductory papers.

The definitions and values of the error covariance matrices and the regularization parameter are nowhere stated. There is a whole subsection about the weights of the observational error covariance matrix without knowing the error covariance matrix. How do the authors account for the model error in their assimilation? How valid is the diagonal assumption of the observational error covariance matrix, knowing that the assimilated AOD and AAOD are issued from the same algorithm and measurements? Do the GRASP algorithm reports uncertainty of AOD and AAOD? Are these uncertainties taken into account in this work? Which are the uncertainties of the emissions factors? Are they the same for the different aerosol types, locations and seasons?

Response: We agree that the manuscript is not clear about definition of covariance matrices of measurements and contribution of *a priori* term. We have added some clarifications. Specifically, we recognize that at present covariance matrices of AOD and AAOD are not available and we use very simple assumptions about covariance matrices. We assume that covariance $\mathbf{C}_{\mathrm{obs}}$ matrix is diagonal and we introduce the relative weights for AOD and AAOD. The absolute values are not of importance since minimization procedure, in principle, does not require knowledge of the cost function absolute value.

Also, we used only very small contribution of *a priori* term (almost non), and we reported the value of regularization parameters. This is another weakness of the current study that is planned to be investigated in future efforts.

Reporting uncertainties of the posterior emissions would be an additional major contribution of this work, but in practice it is not always possible to compute them confidently. Would be possible to provide these values?

Response: We stated in the manuscript that we can't calculate uncertainties of retrieved emissions due to number of challenges. At the same time, we expected that conducted sensitivity tests provide some information how accurate retrieval can be expected. Therefore, based on the test results we make some estimation of the uncertainties.

SPECIFIC COMMENTS:

Title

Following the ACP guidelines, the title should not be capitalised in every word.

Response: Thanks for your suggestion. We revised the title as "Retrieval of desert dust and carbonaceous aerosol emissions over Africa from POLDER/PARASOL products generated by GRASP algorithm".

Short summary

I think that the qualifier "important" in "This study is an important contribution to" is out of place (and sounds like a subjective and personal appreciation that do not add information to the summary).

Response: Good suggestion. We revised the short summary as "This paper introduces a method to use satellite observed spectral AOD and AAOD to derive three types of aerosol emission sources simultaneously based on inverse modeling in a high spatial and temporal resolution. This study shows it is possible to estimate aerosol emissions and improve the atmospheric aerosol simulation using detailed aerosol optical and microphysical information from satellite observations."

P1 L14-17

Sentence too long. I suggest to split the sentence after "(OC) emissions" and continue with "AOD and AAOD from ... has been assimilated .. ".

Response: We revised this sentence as "In this paper, we use the GEOS-Chem based inverse modelling framework for retrieving desert dust (DD), black carbon (BC) and organic carbon (OC) aerosol emissions simultaneously. Aerosol Optical Depth (AOD) and Aerosol Absorption Optical Depth (AAOD) retrieved from the multi-angular and polarimetric POLDER/PARASOL measurements generated by the GRASP algorithm (hereafter PARASOL/GRASP) have been assimilated."

P1 L18

These tests show..

Response: Done.

P1 L19

Remove "For example"

Response: Done.

P1 L21

Please rephrase "...an additional about 1.8 times differences..."

Response: Thanks for your suggestion. It has been changed to "an additional factor of 1.8 differences".

P1 L24-25

Remove "GEOS-Chem inventory of". The inventory is not from GEOS-Chem, it is from Bond et al.

and GFED.

Response: Done.

P1 L29

Please change “independent of and more"

Response: Thanks for your suggestion. It has been changed to “that are completely independent measurements and more temporally frequent than PARASOL observations.”

P1 L31 – P2 L1

I am not sure if it is appropriate to list all the statistics (as acronyms) of the comparison in the abstract.

Response: Agreed. We have removed the statistics of the comparison in the abstract.

P2 L6-8

Despite it is cited in the next sentence, this sentence would improve with a reference.

Response: Thanks for your suggestion. We include a reference (Bond et al., 2013) to cite this introduction sentence.

P2 L14

“.. the role that atmospheric.. "

Response: Done.

P2 L15

Please clarify that it is about short-wave radiation. The measurements are not only due to aerosols, the interaction of light with molecules, surface and clouds is also important.

Response: Thanks for your suggestion. It has been corrected to “global mean direct shortwave radiative forcing”.

We are not completely sure what the reviewer means by sentence “The measurements are not only due to aerosols, the interaction of light with molecules, surface and clouds is also important”. Our discussion was about high uncertainly of radiative forcing estimation due to aerosol. We didn’t find any contradiction of our statements with the suggestion of the reviewer.

P2 L24

“aerosols"

Response: Done.

P2 L24

To my knowledge, sensors provide measurements, algorithms can provide retrievals.

Response: Thanks for your suggestion. It has been changed to “only a few satellite aerosol products can provide retrievals of AAOD”.

P2 L27-28

Reference needed. All the cited satellite retrievals of aerosols are based on visible, UV and near infrared measurements, so this sentence do not add new information. I would say that, given the current state of the instruments, algorithms and knowledge of the system, UV and polarimetric measurements are needed to better retrieve absorption properties of aerosols in the visible.

Response: Thanks for your suggestion. The sentence has been revised.

P2 L29

"high degree" sounds odd.

Response: Thanks for your suggestion. This sentence has been revised as "Despite their ability to provide global coverage in high spatial resolution, …"

P2 L30

Please change "answering question regarding" for something more specific.

Response: Thanks for your suggestion. It has been changed to "addressing question regarding".

P2 L30

"fates"?

Response: We think the word is used correctly.

P2 L31

I think that "incorporate" is not the best word

Response: Thanks for your suggestion. It has been changed to "rely on".

P3 L3

I would add aerosol processes... "of atmospheric and aerosol processes.."

Response: Done.

P3 L4

Please change "are found to"

Response: Thanks for your suggestion. It has been changed to "are expected to".

P3 L12

"i.e. fitting satellite observations and model estimates and by adjusting aerosol emissions". This sentence is not clear and it is inaccurate. Inverse modelling is also applied in mathematics, geophysics, etc (there are a lot of examples in the Tarantola (2005) book). Please be more concise in the definition of inverse modelling.

Response: Indeed, the "inverse modeling" is not well-defined term and allows various interpretations. In our understanding "inverse modeling" is related with assimilation effort where CTM (or similar models) fits observation. Here we follow interpretation by Bennett, (2002). We do not think that

“inverse modeling” should be considered as an equivalent to the term “inversion” in general. For example, Tarantola (2005) book does not use “inverse modeling” term.

P3 L13

Please avoid these kind of statements. The data is not inverted. Is the CTM (and the emission model/inventory) what is usually called “inverted".

Response: Thanks for your suggestion. This sentence has been revised as “For example, Dubovik et al. (2008) developed an algorithm for inverting CTM and implemented the approach to retrieve distributions of aerosol emissions using MODIS data.”

P3 L14

Please specify which kind of distributions: spatial? temporal? size distributions?

Response: Done.

P3 L17

The emissions are not from MODIS AOD.

Response: Good suggestion. It has been changed to “Huneeus et al. (2012, 2013) optimize global aerosol emissions using MODIS AOD with a simplified aerosol model (Huneeus et al., 2009).”

P3 L17-18

Please remove “works such as"

Response: Done.

P3 L3-26

This long sentence could be written better.

Response: Corrected.

P3 L26-27

Is not POLDER the name of the instrument? (and PARASOL the satellite/mission)?

Response: Corrected.

P3 L30

“decreases sharply.." This is true with respect to the wavelength. Wavelength is not the only way to account for the spectrum.

Response: Yes, we agree. By this sentence we discuss only spectral variability.

P3 L30-31

Please change “most strongly". “ubiquitously" sounds odd in this context.

Response: Revised.

P3 L31-32

Please decide : “shortwave", “short-wave" or “short wave". It could be possible to remove “shortwave" from here, as it is followed by “visible".

Response: Corrected.

P3 L34

I do not understand the point of this sentence. MODIS and MISR also provide AOD over bright surfaces. May be it is better to show the accuracy of GRASP retrievals over the desert.

Response: Actually, it is known problem and the first MODIS “Dark Target” algorithm did not provide any retrieval over bright surfaces. More recent algorithms, such as “Deep Blue”, provide retrieval over bright surface, however the accuracy of the retrieval is still limited. For example, Ångström exponent is uncertain and certainly SSA retrieval from MODIS.

This sentence has been revised as “The GRASP retrieval overcomes the difficulty of deriving aerosol over bright surfaces in the visible wavelengths and GRASP provides both AOD and AAOD even over desert that should help improve constraints of DD emissions over source regions, rather than having to rely on downwind observations (e.g., Wang et al., 2012).”

P4 L3-6

Should not this sentence go in the model description section?

Response: We believe that removing this sentence will reduce the clarity in explanation of the work done.

P4 Section 2.1:

Please check the grammar of this section.

Response: Done.

P4 L15-16

The variability has drawn the research? Please rephrase.

Response: Revised.

P4 L16-20

Sentence seems too long. I would prefer: Figure 1 shows the number of ..., the 28 AERONET sites,.. etc.

Response: Done.

P4 L23

“Northern Africa Sahara and Arabian Peninsula desert region"?

Response: Done.

P5 L7

Please remove or explain the word “forward".

Response: Done.

P5 L7

Please correct “with 47 layers vertical resolution"

Response: Thanks for your suggestion. It has been changed to “with 47 vertical layers”.

P5 L10

“consist of" sounds odd.

Response: Revised. This sentence has been revised as “Dust simulations in GEOS-Chem (Fairlie et al., 2007) combine the mineral dust entrainment and deposition (DEAD) model (Zender et al., 2003) with the GOCART dust source function (Ginoux et al., 2001).”

P5 L11

Please correct the grammar.

Response: Done.

P6 L2-6

Remove parenthesis in the citations of lines 2 and 3; check the grammar of the paragraph (“turbulent mixing of particles to the surface"? and all the line 5)

Response: Done.

P6 L7

Check “for all"

Response: Done.

P6 L8

“.. width for ..". Where are these parameters specified? Please add reference to the table if needed.

Response: Thanks for your suggestion. This sentence has been revised as “The modal (r_{mean}) and effective (r_{eff}) radius, and width (sigm) for each dry aerosol species and their optical properties is specified (see in Table 1).”

P6 L10 and L20

Hygroscopic, not hydroscopic

Response: Corrected.

P6 L14

Is it really necessary to write “aerosol particle"?. Only with “aerosol" (or particle) should be enough.

Response: Revised.

P6 L22, figure 2a

Why do the authors show Qext/r and not Qext?

Response: $Q_{ext}(\lambda)/r_e$ is the extinction efficiency normalized by particle effective radius, which indicates the particle extinction ability in consideration of particle size distribution assumption.

P7 L3

This is a personal blog. Please consider uploading the data as supplementary material.

Response: Thanks for your suggestion. We have removed this personal blog in the text and added the "Data availability" section at the end of the text.

P7 L10-13

The authors should clarify what "to model fully adequate" means.

Response: Revised.

Table 1.

Would be possible to add the parameters of the rest of the aerosols simulated? (SS and SU)

Response: Good suggestion. We have added the parameters of SS and SU in Table 1.

P8 L5

I suggest to change "is an efficient tool" to "can be used as a tool"

Response: Revised.

P8 L20-21

Please rephrase and avoid qualifiers as "highly versatile and accurate" without referring to appropriate validations.

Response: We agree. This sentence has been revised as "GRASP is a recently developed aerosol retrieval algorithm that processes properties of aerosol and land surface reflectance."

P9 L7-8

This sentence is not clear enough and it should be removed.

Response: Done.

P10 L4

Please specify which version of AERONET products. (2, 3?)

Response: We agree. AERONET Version 2 data are used in this study, and we have added this information in this sentence.

P10 - P13 Section 3.1

Please read the related general comment. This section is full of mistakes and imprecisions, so I will list

only some of them. The authors should note the $\mathbf{C}_{(.)}^{-1}$ are the inverse of the error covariance matrices and not the error covariance matrices. In this section there are several inconsistencies between the equations, and also in the text (for example, the matrix C of equation 5 is not the same as the one of equation 3. γ_r of eq. 3 is γ in eq. 4, Δf is not explained, etc). It is not clear what is K^{obs} (matrix of Jacobians? with respect to which variables? what are the "characteristics"?). The symbol J_p is important but it is not explained. The mass is written as M in the text and m in the equations. The definition of adjoint of L12-13 (P11) is vague and incomplete. An appropriate definition of adjoint operator can be found in the equation 2 of Talagrand and Courtier (1987).

Response: Section 3.1 has been revised. Though, we would like to note that we fully agree that Talagrand and Courtier give more rigorous definition. This paper is not aimed to provide fundamental discussion of this matter.

P12 L14

Here the authors state that the minimization is performed with the L-BFGS-B algorithm, but equation 3 described the minimization by using a simpler steepest descend algorithm. Do the authors use the algorithm of equation 3 or do they use L-BFGS-B with the gradient as equation 9?. Please clarify.

Response: We used GEOS-Chem, i.e. L-BFGS-B was used. We added clarifications in the text.

P14 L5

What is a "well-known qualitative tendency"?

Response: Revised.

P14 L10

The authors should clarify in which scenario (A, B, C, D, E) were these tests performed.

Response: Thanks for your suggestion. In this test, scenario C is used. We have added this information in the text. "The retrievals are conducted with option A and option B respectively (the inversion is conducted under Retrieval C scenario, see in the following sections), with other settings held constant."

P14 L18-19

This statement is in general not true. For example, taken the f function equal the identity in equation 3, the cost function is a quadratic function of S in Rn, and the problem is well-constrained (as J is a convex -and smooth- function, the problem has an unique solution), and the solution depends on the prior information.

Response: The text is improved to clarify our statement.

P15 L7-9

Please add an introductory paragraph before L9.

Response: Done.

Figure 7

Should not be divided by surface area?

Response: The "true" emission is defined at each grid box without consideration of the surface area of each grid box. So, we keep the amount of emission per grid box in Figure 7.

P17 L8-9, L16

Not using a priori knowledge of aerosol emissions implies much more than the B settings. It is not equivalent.

Response: We agree, and it has been revised.

P17 23

The false source generation is prevented only over ocean; but it is still allowed to generate a source in the wrong place and time. Please clarify.

Response: Revised.

P17 25

Why do not the authors show this ratio for the retrievals A and B? , how is the uncertainty of this ratio computed?

Response: This ratio, which is a mean of the ratios between retrieved emission $\boldsymbol{S}_{\text{retrieval}}$ and "true" emission $\boldsymbol{S}_{\text{true}}$ at all grid boxes over study area, can be used to evaluate the performance of the retrieval. However, Retrieval A and B show some limitations to capture the correct spatial distribution of emissions. So, there are some invalidate values to make this ratio for Retrieval A and B (e.g. $\boldsymbol{S}_{\text{retrieval}} > 0.0$ and $\boldsymbol{S}_{\text{true}} = 0.0$). The ratios of them would make no sense. And the uncertainty indicates the standard deviation of the mean ratio.

P18 , Section 3.2.3

Beyond the synthetic tests, how do the authors account for the (known) sub-daily emission variability of DD, BC and OC emissions?

Response: In the GEOS-Chem simulation, we adopt daily GFED3 biomass burning emission and monthly BOND inventory. So, the sub-daily BC and OC emission is constant. In the grid boxes, where the prior DD emissions are greater than zero ($\boldsymbol{S}_{0,DD} > 0.0$), we keep the sub-daily DD emission variability as prior DEAD dust model. However, the added background emissions over land grid boxes are sub-daily constant. In the inversion, we correct the DD emission using one scaling factor during a day.

P20 , Section 3.2.4

Which are the emissions used for the "retrieval E"? I would guess that they are the same as "retrieval C", but it is not clear. Are DU and OC included in this test? Is there any difference in retrieved DD and OC by changing the BC refractive index?

Response: Yes, the other settings for "Retrieval E" are the same with "Retrieval C" expect for BC refractive index. We have added this information in the text.

In the Retrieval E, we fix the same DD and OC emissions as that of "Retrieval C". We didn't retrieve DD and OC emissions in this test.

Figure 10:

Are these gridpoint values? Are they the accumulated emissions (16 days) of day-by day emissions? What is the grey area (20% of what?)?, the lines? What is "Y", "X", "R", etc.?

Response: Yes. This figure shows the grid-to-grid comparison of retrieved emissions (Retrieval C and Retrieval E) with the "true" BC emissions. The values are averaged over 16 days. And the grey area represents ±20% differences around the true values. "Y=kX" is the linear regression statistics between retrieved emissions (y-axis) with the "true" values (x-axis), and "R" is the correlation coefficient. We have added description to Figure 10 caption:

"Figure 10. Test of BC particle refractive index influence on the retrieval of BC emissions. The scatter plots are grid-to-grid comparison of retrieved 16 days averaged emissions (blue: Retrieval C; green: Retrieval E) with the "true" BC emissions. The shade grey area represents ±20% differences around the true values."

P21 L8-22

These conclusions about the idealised test are presented as a fact (and largely extrapolated to other contexts) without taking into account the nature of the synthetic measurements, and the limitations of the whole data assimilation system. I would suggest to present them as the authors' choice regarding the parameter configuration of the assimilation procedure.

Response: Done.

P21 L11

Why are needed 6 and not, for example, 5 wavelengths? Did the authors try with less wavelengths?

Response: we used maximum possible data, since reduction of the data hardly can bring serious advantages.

P21 L13

Please check the grammar

Response: Revised.

P21 L18

More stable and accurate than what? Where do the authors show the "stability" of the retrieval in the text? In which sense it is stable?

Response: Revised.

P21 L19

Please check the first sentence. It should not be inverted (retrievals sensitive to refractive index) ?

Response: Revised.

P21 L25

Why are not SS and SU included? Errors in the emission of these aerosols will impact the quality of the posterior emissions. How is this taken into account?

Response: We do not think that PARASOL data have sufficient information, however we will revisit this conclusion in future studies.

P21 L22 or L24

I would recommend to indicate that this configuration/parameters of the assimilation procedure will be used in Sections 4 and 5.

Response: Revised.

P21 L28

Even though a fixed number of iterations is a very practical stopping criterion, do the authors compute any diagnostic on the optimality of the cost function after 40 iterations?

Response: Revised.

P21 Section 4

Please indicate which BC Case (refractive index) is used in the results of Sections 4.1, 4.2, 4.3.1 and 4.3.3.

Response: Good suggestion. Case 1 BC refractive index is used in the results of this Section. We have added this information in the text.

P24 L13-14

Why could the coarse resolution of the model lead to the spectral differences of AAOD presented here?

Response: Because the PARASOL/GRASP retrieval of AAOD is at PARASOL original 6x7 km pixel, and then the PARASOL AAODs are aggregated into model 2.0° x 2.5° grid boxes. There could be different coverage of observations in different grid boxes.

P26 Section 4.3.1

How much of the DD reported in Figure 13 is produced in the Sahara? The retrieved emission seasonal cycle seems flat (but maybe it is only the scale of the plot). In comparison with other studies, would the authors think that the seasonal cycle is well captured?

Response: Our annual dust emission is 701 Tg over Africa and the Arabian Peninsula, which is agreed with the recent estimation by Escribano et al. (2017) that between 630 and 845 Tg over this area using observations from MODIS, MISR and PARASOL. Figure S1 shows the seasonal cycle of retrieved dust emission over Africa in comparison with that from prior GEOS-Chem model.

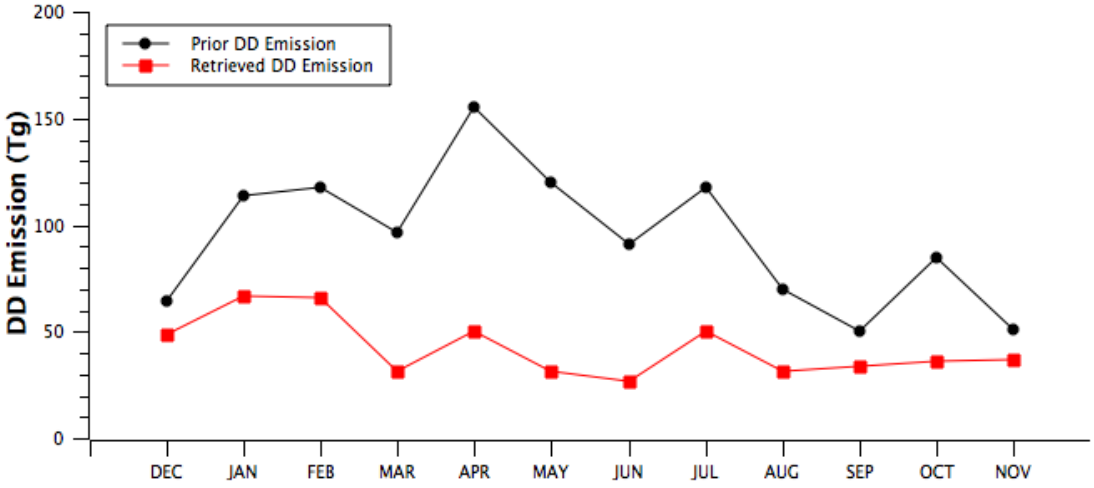

Figure S1. Comparison of monthly DD emission (unit: Tg) over Africa between prior model and retrieved emissions.

Figure 13.

The units are Tg/month or Tg?

Response: Corrected. It should be Tg.

P27 L11

This value is similar to the 3.4 factor of Kaiser et al 2012. I suggest to add and comment this reference in line 22. The authors have indicated that the difference between Case 1 and Case 2 retrievals is close to 1.8 for BC. This value have been computed in the sensitivity tests; but in this section the factor should be close to 8/3 (2.7). How do the authors explain this difference? Should not be better to include in the abstract and conclusion this value instead of the 1.8?

Response: Thanks for your suggestion. We have added Kaiser's 2012 paper on the discussion section 4.3.4. "Kaiser et al. (2012) also recommend correcting the carbonaceous aerosol emission (GFED3) with a factor 3.4 when using them in the global aerosol forecasting system."

Yes, the ratio of Case 1 and Case 2 BC emission from one-year real data inversion is ~2.3 (15.7/6.9), which is different from this ratio 1.8 in sensitivity test than conducted using 16 days synthetic data. This ratio is related to the intensity and spatial distribution of BC emission. Comprehensive tests should be done to analysis it in the future studies.

P27 L16-20

Please note that these values are not necessarily for the year 2008.

Response: The reviewer is probably correct, however we find it difficult to justify in this section since we show the data only for 2008.

P27 L27

Can the authors report the uncertainty of the retrieved emissions?

Response: Unfortunately, we can't calculate the uncertainties rigorously. Therefore, in estimation of uncertainties we can rely on the results of our numerical tests. We suggest that the errors in emission have similar magnitude as in the conducted tests.

P30 L5

Please indicate which BC case is used in this section.

Response: Thanks for your suggestion. In the posterior GEOS-Chem model simulation, we use Case 1 BC emission. We have added this information in the text. The difference of 2 cases of total BC emission is due to the different assumptions of BC particle absorbing ability. Thus, the GEOS-Chem posterior AAODs based on 2 cases of BC emissions, coupling with the 2 cases assumption of BC particle absorbing properties, show small differences (R=0.9, MAE=0.006, NMB=0.43%).

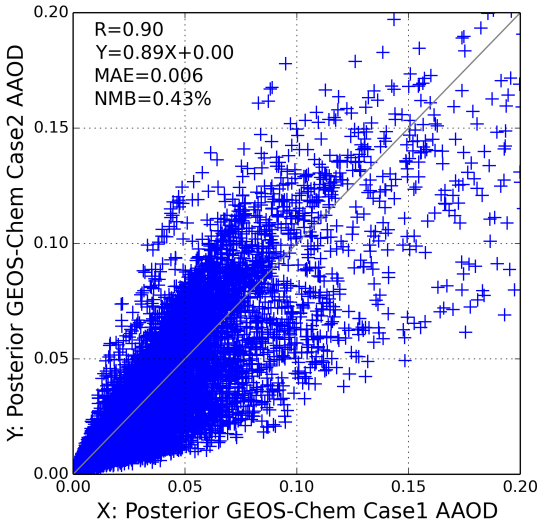

Figure S2. Comparison of posterior GEOS-Chem AAOD at 565nm based on 2 cases of BC emission. The correlation coefficient (R), mean absolute error (MAE), linear regression fit (Y=aX+b) and normalized mean bias (NMB) are provide in the top left corner.

Figure 18

The colour code of each square in the panels represent the number of pairs (observation, model) that fit in the square. The size of the squares are different in all the panels (in fact, some of them are not squares, despite the same limits of the x and y axes), so they are not comparable. The worst case is in the last column. The authors should write in the caption the size of the AAOD bins (and AOD for Figure 17). I strongly recommend to improve this figure.

Response: Good suggestion. The sizes of the AAOD bins in Figure 18 and AOD bins in Figure 17 have been added in the figure captions. And the Figure 18 has been changed to use the same size of the squares in the all panels.

P35 L22

This sentence should be written before (around line 10). Is the model sampled according to MODIS

availability?

Response: This sentence intended to indicate one possible reason that the posterior model AOD is a little lower than MODIS on monthly mean scale. Here, we used GEOS-5/GOCART model monthly mean value, which is averaged of all data during a month.

P36 L10-11

I could understand that these kind of measurements are more sensitive to the absorption properties, thus the retrieval of them is better constrained, but this first sentence of the paragraph implies that these are the only measurements sensitive to the absorption, which is a strong statement. Could you provide a reference on this?

Response: We agree, and the sentence has been revised.

P36 and P37

From panels a, b and c of Figure 21, it seems that the model/satellite comparison is not collocated. This could introduce errors in the analysis of the results, and it should be mentioned. Also, I would suggest to plot with transparent colour the missing data, and not with blue (which is equivalent to zero AAOD)

Response: Yes, the spatial distribution for model and satellite is not fully collocated. We use the OMI Level 3 monthly mean AAOD data (OMAERUV version 1.7.4) with a 0.5° x 0.5° spatial resolution, while the model AAOD is 2.0° x 2.5°. In panels a, b and c, we want to show the seasonal spatial pattern of AAOD from model and satellite, so we keep their best spatial resolution. In panel d and e, the grid-to-grid comparison between prior/posterior model and satellite AAOD is presented. In this comparison, the satellite AAOD is re-scaled to the model 2.0° x 2.5° resolution.

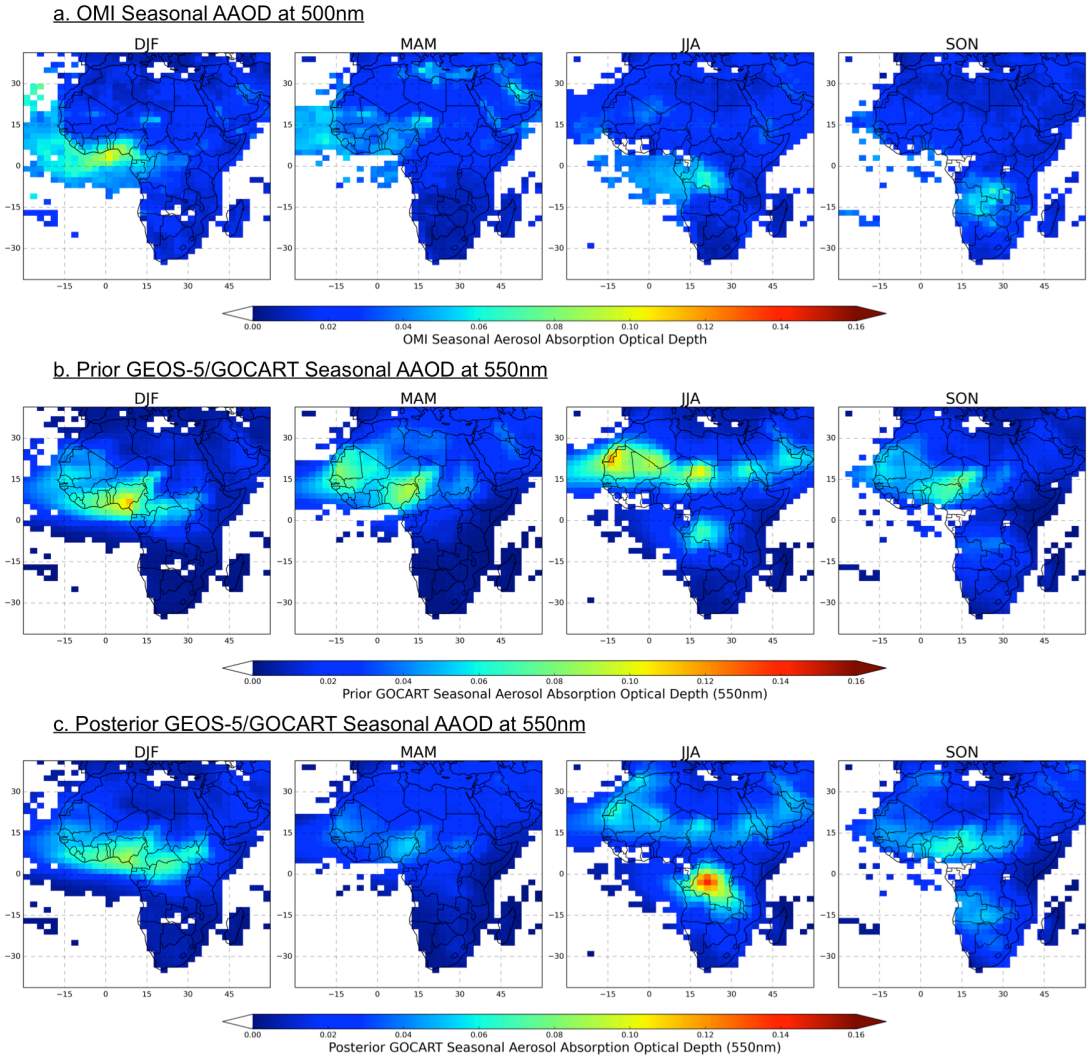

Figure S3. The collocated 2.0° x 2.5° seasonal AAOD from OMI (a), prior (b) and posterior (c) GEOS-5/GOCART simulation

P38 L17

Please rephrase this sentence to improve readability (It is not easy to figure out what a “800% lower" means).

Response: Revised.

References

Bennett A.F., Inverse Modeling of the Ocean and Atmosphere, Cambirge University Press, 220 p. 2002.

Bond, T. C., Doherty, S. J., Fahey, D. W., Forster, P. M., Berntsen, T., DeAngelo, B. J., Flanner, M. G., Ghan, S., Kärcher, B., Koch, D., Kinne, S., Kondo, Y., Quinn, P. K., Sarofim, M. C., Schultz, M. G., Schulz, M., Venkataraman, C., Zhang, H., Zhang, S., Bellouin, N., Guttikunda, S. K., Hopke, P. K., Jacobson, M. Z., Kaiser, J. W., Klimont, Z., Lohmann, U., Schwarz, J. P., Shindell, D., Storelvmo, T., Warren, S. G. and Zender, C. S.: Bounding the role of black carbon in the

climate system: A scientific assessment, J. Geophys. Res. Atmos., 118(11), 5380–5552, doi:10.1002/jgrd.50171, 2013.

Dubovik, O., Lapyonok, T., Kaufman, Y. J., Chin, M., Ginoux, P., Kahn, R. A. and Sinyuk, A.: Retrieving global aerosol sources from satellites using inverse modeling, Atmos. Chem. Phys., 8(2), 209–250, doi:10.5194/acp-8-209-2008, 2008.

Ginoux, P., Chin, M., Tegen, I., Prospero, J. M., Holben, B., Dubovik, O. and Lin, S.-J.: Sources and distributions of dust aerosols simulated with the GOCART model, J. Geophys. Res. Atmos., 106(D17), 20255–20273, doi:10.1029/2000JD000053, 2001.

Fairlie, T. D., Jacob, D. J. and Park, R. J.: The impact of transpacific transport of mineral dust in the United States, Atmos. Environ., 41(6), 1251–1266, doi:10.1016/j.atmosenv.2006.09.048, 2007.

Huneeus, N., Boucher, O. and Chevallier, F.: Simplified aerosol modeling for variational data assimilation, Geosci. Model Dev., 2(2), 213–229, doi:10.5194/gmd-2-213-2009, 2009.

Huneeus, N., Chevallier, F. and Boucher, O.: Estimating aerosol emissions by assimilating observed aerosol optical depth in a global aerosol model, Atmos. Chem. Phys., 12(10), 4585–4606, doi:10.5194/acp-12-4585-2012, 2012.

Huneeus, N., Boucher, O. and Chevallier, F.: Atmospheric inversion of SO2 and primary aerosol emissions for the year 2010, Atmos. Chem. Phys., 13(13), 6555–6573, doi:10.5194/acp-13-6555-2013, 2013.

Talagrand, O. and Courtier, P.: Variational assimilation of meteorological observations with the adjoint of the vorticity equations: Part I., Theory, Q. J. Roy. Meteor. Soc., 113, 1311–1328, 1987

Tarantola, A., Inverse problem theory and methods for model parameter estimation, Society for Industrial and Applied Mathematics, 2005.

Wang, J., Xu, X., Henze, D. K., Zeng, J., Ji, Q., Tsay, S.-C. and Huang, J.: Top-down estimate of dust emissions through integration of MODIS and MISR aerosol retrievals with the GEOS-Chem adjoint model, Geophys. Res. Lett., 39(8), L08802, doi:10.1029/2012GL051136, 2012.

Zender, C. S., Bian, H. and Newman, D.: Mineral Dust Entrainment and Deposition (DEAD) model: Description and 1990s dust climatology, J. Geophys. Res., 108(D14), 4416, doi:10.1029/2002JD002775, 2003.

~~Retrieval of Desert Dust and Carbonaceous Aerosol Emissions over Africa from POLDER/PARASOL Products Generated by GRASP Algorithm~~

Retrieval of desert dust and carbonaceous aerosol emissions over Africa from POLDER/PARASOL products generated by GRASP algorithm

Cheng Chen[1], Oleg Dubovik[1], Daven K. Henze[2], Tatyana Lapyonok ~~Lapyonak~~[1], Mian Chin[3], Fabrice Ducos[1], Pavel Litvinov[4], Xin Huang[4], Lei Li[1]

[1]Laboratoire d'Optique Atmosphérique (LOA), UMR8518 CNRS, Université de Lille1, Villeneuve D'ASCQ, 59655, France
[2]Department of Mechanical Engineering, University of Colorado, Boulder, Colorado, 80309, USA
[3]NASA Goddard Space Flight Center, Greenbelt, Maryland, 20771, USA
[4]GRASP-SAS, Remote Sensing Developments, Université de Lille1, Villeneuve D'ASCQ, 59655, France

Correspondence to: Cheng Chen (cheng1.chen@ed.univ-lille1.fr) and Oleg Dubovik (oleg.dubovik@univ-lille1.fr)

Abstract. Understanding the role atmospheric aerosols play in the earth-atmosphere system is limited by uncertainties in the knowledge of their distribution, composition and sources. In this paper, we use the GEOS-Chem based inverse modelling framework for retrieving desert dust (DD), black carbon (BC) and organic carbon (OC) aerosol emissions simultaneously. Aerosol Optical Depth (AOD) and Aerosol Absorption Optical Depth (AAOD) retrieved from the multi-angular and polarimetric POLDER/PARASOL measurements generated by the GRASP algorithm (hereafter PARASOL/GRASP) have been assimilated. First, the inversion framework is validated in a series of numerical tests conducted with synthetic PARASOL-like data. These tests show that the framework allows for retrieval of the distribution and strength of aerosol emissions. ~~For example,~~The uncertainty of retrieved daily emissions in error free conditions is bellow 25.8% for DD, 5.9% for BC and 26.9% for OC. In addition, BC refractive index is sensitive to BC emission retrieval, which could produce an additional ~~about 1.8 times~~ factor of 1.8 differences for total BC emission. The approach is then applied to one-year (December 2007 to November 2008) of data over the African and Arabian Peninsula region using PARASOL/GRASP spectral AOD and AAOD at six wavelengths (443, 490, 565, 670, 865 and 1020 nm). Analysis of the resulting retrieved emissions indicates 1.8 times overestimation of the prior DD online mobilization and entrainment model. For total BC and OC, the retrieved emissions show a significant increase of 209.9%~271.8% in comparison to the prior ~~GEOS-Chem inventory of~~ carbonaceous aerosol emissions. The model posterior simulation with retrieved emissions shows good agreement both with the AOD and AAOD PARASOL/GRASP products used in the inversion. The fidelity of the results is

evaluated by comparison of posterior simulations with measurements from AERONET that are completely independent measurements ~~of~~ and more temporally frequent than PARASOL observations. To further test the robustness of our posterior emissions constrained using PARASOL/GRASP, the posterior emissions are implemented in the GEOS-5/GOCART model and the consistency of simulated AOD ~~(prior: R=0.77, RMSE=0.14, MAE=0.09; posterior: R=0.81, RMSE=0.10, MAE=0.06)~~ and AAOD ~~(prior: R=0.65, RMSE=0.019, MAE=0.014; posterior: R=0.69, RMSE=0.015, MAE=0.011)~~ with other independent measurements (MODIS and OMI) demonstrates promise in applying this database for modelling studies.

1 Introduction

Atmospheric aerosols have a variety of sources and complex chemical compositions. Desert dust (DD) aerosol is one of the most abundant types of aerosol by mass, while the range of global dust emission estimates span a factor of about five (Huneeus et al., 2011). Primary carbonaceous aerosol, which consists of black carbon (BC) and organic carbon (OC) from combustion of fossil fuels, biofuels and biomass, has strong light absorption that can affect the energy balance of the earth-atmosphere system (Bond et al., 2013). High uncertainty in carbonaceous aerosol emissions (e.g., Bond et al., 2004) translates into a significant high uncertainty in evaluating their climate effects (Textor et al., 2006). The Intergovernmental Panel on Climate Change (IPCC) estimates the global mean direct shortwave radiative forcing due to primary carbonaceous aerosol of -0.1 w/m^2 in their 2001 report, in 2007 they raise it to 0.18 w/m^2, in the latest report (IPCC, 2013) the value comes to 0.31 w/m^2 (Myhre et al., 2013). Furthermore, desert dust and carbonaceous aerosols can have deleterious impacts on regional air quality and public health (Chin et al., 2007; Monks et al., 2009; Li et al., 2013). Thus, observations are needed to accurately evaluate their emissions in order to better understand the role that atmospheric aerosols play in the earth-atmosphere system (Bellouin et al., 2005).

Space-borne remote sensing instruments offer an integrated atmospheric column measurement of the amount of light scattering by aerosols through modification of diffuse and direct solar radiation. Numerous satellite observations of the spatial and temporal distribution of aerosols have been conducted in the last two decades (King et al., 1999; Kaufman et al., 2002; Lenoble et al., 2013). The satellite retrievals of Aerosol Optical Depth (AOD) and Aerosol Absorption Optical Depth (AAOD) are directly related to light extinction and absorption due to the presence of aerosol particles. AOD is a basic optical property derived from many earth-observation satellite sensors, such as AVHRR (Advanced Very High Resolution Radiometer), MODIS (Moderate Resolution Imaging Spectroradiometer), MISR (Multi-angular Imaging SpectroRadiometer) and POLDER (Polarization and Directionality of the Earth's Reflectances) (Goloub et al., 1999; Geogdzhayev et al., 2002; Kahn et al., 2009; Tanré et al., 2011; Levy et al., 2013). AAOD is another valuable product to quantify the solar absorption potential of aerosols; however, only a few satellite aerosol products ~~sensors~~ can provide retrievals of AAOD, and only with limited accuracy, for example OMI (Ozone Monitoring Instrument) on the Aura satellite making measurements in UV that have sensitivity to aerosol absorption (Torres et al., 2007; Veihelmann et al., 2007) ~~and POLDER on PARASOL (Polarization & Anisotropy of Reflectances for Atmospheric Sciences coupled with Observations~~

~~from a Lidar), because only ultraviolet (UV) and shortwave visible channels and polarimetric measurements are sensitive to aerosol absorption~~.

Despite their ability to provide global coverage in high spatial resolution ~~a high degree of spatial coverage~~, satellite measurements alone are not sufficient for addressing ~~answering~~ question regarding the distributions, magnitudes, and fates of aerosols in the atmosphere. These aspects can be studied using Chemical Transport Models (CTMs), which rely on ~~incorporate~~ meteorological data from external databases with atmospheric physics, considering the physical and chemical processes in the atmosphere, and allow modelling of detailed distribution of aerosol for any chosen time period (e.g. models by Balkanski et al., 1993; Chin et al., 2000; Takemura et al., 2000; Ginoux et al., 2001; Bessagnet et al., 2004; Grell et al., 2005; Spracklen et al., 2005; Mann et al., 2010) . However, CTM simulations are limited by uncertainties in knowledge of aerosol emissions characteristics, knowledge of atmospheric and aerosol processes, and the meteorological data used. As a result, even the most recent models are expected ~~found~~ to capture only the principal global features of aerosol. For example, among different models, quantitative estimates of average regional aerosol properties often disagree by amounts exceeding the uncertainty of remote sensing of aerosol observations (Chin et al., 2002, 2014, Kinne et al., 2003, 2006; Textor et al., 2006). Therefore, there are diverse and continuing efforts to harmonize and improve aerosol modelling by refining the meteorology, atmospheric process representations, emissions and other components (e.g. aerosol aging scheme, particle mixing state etc.) (Watson et al., 2002; Dabberdt et al., 2004; Generoso et al., 2007; Ghan and Schwartz, 2007; He et al., 2016; Wang et al., 2014a, 2016).

One of the most promising approaches for reducing model uncertainty is to improve the aerosol emission fields (that is input for the models) by inverse modelling, i.e. fitting satellite observations and model estimates and by adjusting aerosol emissions (e.g. Bennett, 2002). For example, Dubovik et al. (2008) developed an algorithm for inverting CTM ~~MODIS data~~ and implemented the approach to retrieve distributions of aerosol emissions using MODIS data. The algorithm was used to implement the first formal retrieval of global emission spatial and temporal distributions of fine mode aerosol from the MODIS fine mode AOD data. Wang et al. (2012) and Xu et al. (2013) use MODIS radiances to constrain aerosol sources over China. Huneeus et al. (2012, 2013) optimize global aerosol emissions ~~from~~ using MODIS AOD with a simplified aerosol model (Huneeus et al., 2009). However, as discussed in ~~works such as~~ Dubovik et al. (2008) and Meland et al. (2013), MODIS AOD (as well as currently available aerosol satellite data) contains only limited information to evaluate aerosol types, properties, or speciated emissions. Further, inconsistencies between representations of aerosol microphysics between the CTM and the aerosol retrieval algorithm can have significant influences on inverse modelling of aerosol sources (e.g. Drury et al., 2010; Wang et al., 2010). Therefore, the retrieval of aerosol emissions from satellite observations remains very challenging.

Recently new data set spectral AOD and AAOD was ~~The recently~~ generated using GRASP (General Retrieval of Atmosphere and Surface Properties) algorithm from POLDER/PARASOL (Polarization & Anisotropy of Reflectances for Atmospheric Sciences coupled with Observations from a Lidar) instrument ~~PARASOL/GRASP (General Retrieval of Atmosphere and Surface Properties) spectral AOD and AAOD data~~ (Dubovik et al., 2011, 2014; data available from ICARE

data distribution portal: http://www.icare.univ-lille1.fr/). Since several POLDER instruments were launched on different satellites, below in the text abbreviation of PARASOL satellite is used instead of instrument. The PARASOL/GRASP data present new opportunities for constraining DD, BC and OC sources because their optical properties vary dramatically in the spectrum of shortwave visible to near infrared (VIS-NIR) viewed by PARASOL. Polarimetric remote sensing measurements such as those from PARASOL have been postulated to provide much greater constraints on speciated aerosol emissions and microphysical properties (Meland et al., 2013). DD aerosols are dominated by coarse mode particles, and their AOD varies slightly in the VIS-NIR spectral range; in contrast, the AOD of fine mode dominated BC and OC aerosols decrease sharply in this spectral range. In addition, DD and OC particles absorb stronger in the UV and shortwave visible channels such as 443 nm, than in the rest of the visible spectrum, while BC particles are absorbing more ubiquitously (Sato et al., 2003). The GRASP retrieval overcomes the difficulty of deriving aerosol over bright surfaces in the ~~shortwave~~ visible wavelengths and GRASP provides both AOD and AAOD even over desert that~~, which~~ should help improve constraints of DD emissions over source regions, rather than having to rely on downwind observations (e.g., Wang et al., 2012).

Here we develop an inverse modelling approach to retrieve the spatial and temporal distributions of DD, BC and OC aerosol emissions simultaneously from PARASOL/GRASP spectral AOD and AAOD using the GEOS-Chem model (Bey et al., 2001) and its adjoint (Henze et al., 2007). Section 2 describes the model and data used in this study. The dust and carbonaceous aerosol model in the GEOS-Chem adjoint of Henze et al. (2007) is that of the GOCART (Goddard Chemistry Aerosol Radiation and Transport) model implemented in GEOS-Chem (Fairlie et al., 2007; Park et al., 2003), which is fully conceptually consistent with the aerosol model used in the inversion by Dubovik et al. (2008). The details of inverse modelling and performance evaluation of the inversion framework using numerical tests are presented in the Section 3. In order to interpret the retrieval results and improve our understanding of aerosol emissions, we retrieve one-year of daily DD, BC and OC emissions (see the Section 4). Evaluation of these inversion results using independent AERONET, MODIS and OMI observations, as well as implementation of the posterior emissions in the GEOS-5/GOCART model is presented in Section 5. Conclusions and discussion of the study's merits and limitations are considered in the Section 6.

2 Model and data description

2.1 Study Area

The study area (30°W-60°E, 40°S-40°N) is shown in Figure 1, which covers the whole of Africa and the Arabian Peninsula, comprising one of the largest dust source and biomass burning regions of the globe. The spatial and temporal variability of DD, BC and OC aerosols in this area has inspired ~~drawn~~ numerous researches (Duncan et al., 2003; Prospero and Lamb, 2003; Engelstaedter et al., 2006; Liousse et al., 2010; Zhao et al., 2010; Ginoux et al., 2012; Ealo et al., 2016). Figure 1 shows the number of PARASOL/GRASP retrievals per 0.1° x 0.1° grid box over a year (December 2007 to November 2008) and the 28 AERONET (AErosol RObotic NETwork) (Holben et al., 1998) sites used to evaluate GEOS-Chem model simulations and PARASOL/GRASP retrievals. Note that the GRASP algorithm performs aerosol retrievals at

PARASOL's native resolution of 6~7 km; each 0.1° grid box could thus have more than one GRASP retrieval, so the number of PARASOL/GRASP retrievals exceeds the number of days in some grid boxes of Figure 1. The number ~~amount~~ of GRASP algorithm (see in section 2.3) retrievals over the region of Northern Africa Sahara and the Arabian Peninsula desert is relatively high, whereas other regions have a reduced number of retrievals due to the presence of clouds.

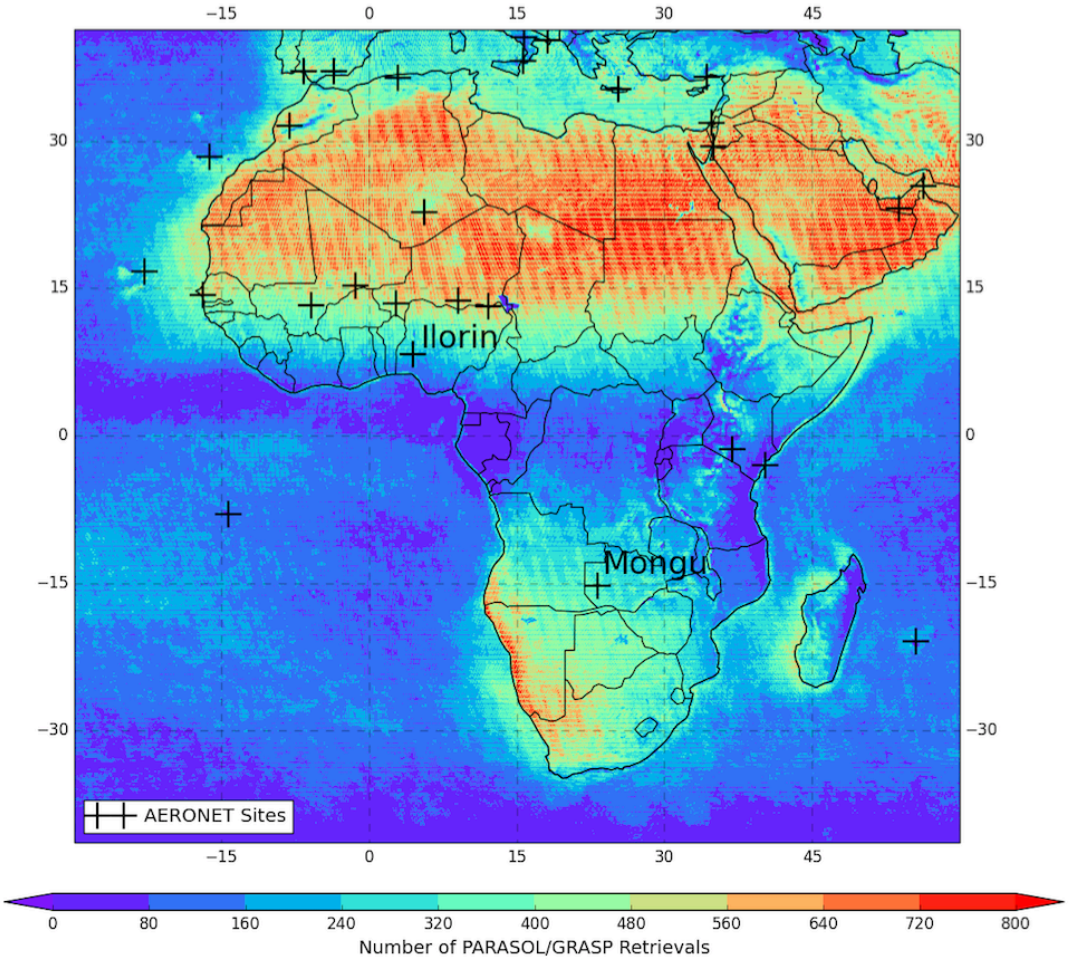

Figure 1. Distribution of PARASOL/GRASP AOD retrievals per 0.1° x 0.1° grid cell over a year (December 2007 to November 2008); the 28 AERONET sites used for validation are also shown with black cross.

2.2 GEOS-Chem model and its adjoint

GEOS-Chem is a global 3-dimensional chemical transport model driven by assimilated meteorological data from the NASA Goddard Earth Observing System Data Assimilation System (GEOS-DAS) (Bey et al., 2001). We use the GEOS-Chem (v9-02) model for ~~forward~~ aerosol simulation with 47 ~~layers~~ vertical layers ~~resolution~~ and 2° (latitude) x 2.5°

(longitude) horizontal resolution. DD, BC and OC aerosols are simulated in our study, including 7 size bins for resolving dust (Fairle et al., 2007), and total aerosol mass of black and organic carbon (Park et al., 2003). Dust simulations in GEOS-Chem (Fairlie et al., 2007) ~~consist of~~ combine the mineral dust entrainment and deposition (DEAD) model (Zender et al., 2003)~~, which is coupled~~ with the GOCART dust source function (Ginoux et al., 2001). The daily biomass burning sources ~~are calculating~~ are calculated from version 3 of Global Fire Emissions Database (GFED) inventory (van der Werf et al., 2006, 2010; Randerson et al., 2013). The monthly anthropogenic fossil fuel and biofuel BC and OC emissions are adopted from Bond inventory with base year 2000 (Bond et al., 2007). The sulphate (SU) and sea salt (SS) aerosol simulation in GEOS-Chem is described in ~~(~~Park et al. (2004)~~;~~ and Jaeglé et al.~~,~~ (2011). The standard aerosol dry deposition in GEOS-Chem is described in ~~(~~Wang et al. (1998)~~;~~ and Wesely, (1989), and accounts ~~accounting~~ for gravitational settling and turbulent mixing of particles to the ground layer ~~surface~~ (Pye et al., 2009; Zhang et al., 2001). Aerosol wet deposition in GEOS-Chem includes ~~is through~~ wet scavenging in convective updrafts as well as in- and below-cloud scavenging from convective and large scale precipitation (Liu et al., 2001).

The GEOS-Chem model assumes external mixing for ~~all~~ aerosol components with lognormal size distributions. The modal (r_{mean}) and effective (r_{eff}) radius, ~~diameter~~ and width (sigm) for each dry aerosol species and their optical properties are ~~is~~ specified (see in Table 1). The extinction and scattering coefficients are calculated from size distributions and refractive indices assuming spherical particles. Different aerosol species are considered to have ~~hydroscopic~~ hygroscopic growth rates as a function of ambient relative humidity (RH). The simulated aerosol masses are then converted to AOD (τ) and AAOD (τ_a) through the general relationship between aerosol optical depth and aerosol mass (Tegen and Lacis, 1996):

$$\tau(\lambda) = \sum_{i=1}^{n} \frac{3Q_{ext,i}(\lambda)}{4\rho_i r_{e,i}} m_i \quad (1)$$

$$\tau_a(\lambda) = \sum_{i=1}^{n} \frac{3Q_{abs,i}(\lambda)}{4\rho_i r_{e,i}} m_i \quad (2)$$

where n is the total number of aerosol components, i represents individual aerosol component, m is the aerosol mass, λ is wavelength, ρ is aerosol ~~particle~~ density, r_e is the particle effective radius, and $Q_{ext}(\lambda)$ and $Q_{abs}(\lambda)$ are the aerosol ~~particle~~ extinction and absorption coefficients, respectively. The size distribution and the spectral aerosol refractive index used to calculate $Q_{ext}(\lambda)$ and $Q_{abs}(\lambda)$ are assumed based on Global Aerosol Data Set (Koepke et al., 1997), with modifications for dust particles by including a spectral dependence for the imaginary part based on analysis of AERONET measurements (Dubovik et al., 2002b). Further, the particle optical properties $Q_{ext}(\lambda)$ and $Q_{abs}(\lambda)$ are calculated according to AERONET Kernel based on mixture of spheroids suggested in studies by Dubovik et al. (2002a, 2006). The particle density and ~~hydroscopic~~ hygroscopic growth rate are described in Chin et al. (2002) and Martin et al. (2003). Table 1 lists the detailed aerosol properties used in this study. Here we consider two cases of BC refractive index. Figure 2a demonstrates the relative humidity dependence of these two cases of BC aerosols extinction ($Q_{ext}(\lambda)/r_e$) at 565 nm, and Figure 2b presents the wavelength dependence of single scattering albedo (SSA) for these two cases. The Case 1 BC refractive index is based on

Chin et al. (2002) and Martin et al. (2003). More recent studies have recommended a BC refractive index of 1.95-0.79i (Schuster et al., 2005; Bond and Bergstrom, 2006; Koch et al., 2009; Arola et al., 2011), which has higher absorption and scattering ability than Case 1. Figure 2a shows that the extinctions calculated from AERONET Kernel for Case 2 BC particle are about a factor 1.5 higher than for Case 1. The difference of SSA is small (Case 2 is about 2% higher at 565 nm when RH=0%), however the difference increases when RH=95%, for which Case 2 is about 18% lower at 565 nm. Since the particle absorption efficiency $Q_{abs} = (1 - SSA) \cdot Q_{ext}$, the Case 2 BC particle shows a higher absorbing ability than Case 1. Sensitivity tests are conducted to evaluate how these two BC refractive indices influence the total BC emissions retrieval in Section 3.2.4. ~~The aerosol spectral extinction and absorption coefficients used in this study are all available online (http://esuchencheng.wixsite.com/chencheng/research-blog).~~ It should be noted that the particle morphologies can affect the computation of scattering and absorption properties (Liu and Mishchenko, 2007; Mishchenko et al., 2013). However, usually CTMs use external mixture of different aerosol components as described above for GEOS-Chem model used in present studies. The inclusion of more adequate internal mixing rules for calculating optical properties of resulted aerosol is a crucial for further improvements in CTMs aerosol simulation that is a subject for future developments. Indeed, since CTMs are aimed to account for all important chemical and physical transformations of aerosol particles. Therefore, in principle CTMs should provide all information about particles sizes and morphologies necessary for making complete and accurate ~~adequate~~ modelling of aerosol optical properties. However, at the current stage the level of details in CTMs is not sufficient to model fully adequate component mixing and, as a result, the conversion from aerosol mass to aerosol optical properties is based on simplified external mixing rule size distributions and refractive indices known from in situ and remote sensing observations.

Table 1. Aerosol refractive index, size distribution and particle density for DD, BC, OC, SU, SS and host water employed in this study

Aerosol	Complex refractive index			Size distribution (μm)			Density
	n	k(440/670/870/1020)		r_{mean}	r_{eff}	sigm	(g/cm^3)
DD	1.56	0.0029/0.0013/0.0001/0.0001	DST1	0.0421	0.14	2.0	2.5
			DST2	0.0722	0.24	2.0	2.5
			DST3	0.1354	0.45	2.0	2.5
			DST4	0.2407	0.80	2.0	2.5
			DST5	0.4212	1.40	2.0	2.65
			DST6	0.7220	2.40	2.0	2.65
			DST7	1.3540	4.50	2.0	2.65
BC (Case 1)	1.75	0.45		0.0118	0.039	2.0	1.0
BC (Case 2)	1.95	0.79		0.0118	0.039	2.0	1.0
OC	1.53	0.005		0.0212	0.087	2.2	1.8
SU	1.43	1.0e-8		0.0695	0.156	2.03	1.7
SS	1.5	1.55e-8	SSa	0.228	0.8	2.03	2.2
			SSc	1.64	5.73	2.03	2.2
Water	1.33	1.0e-8					1.0

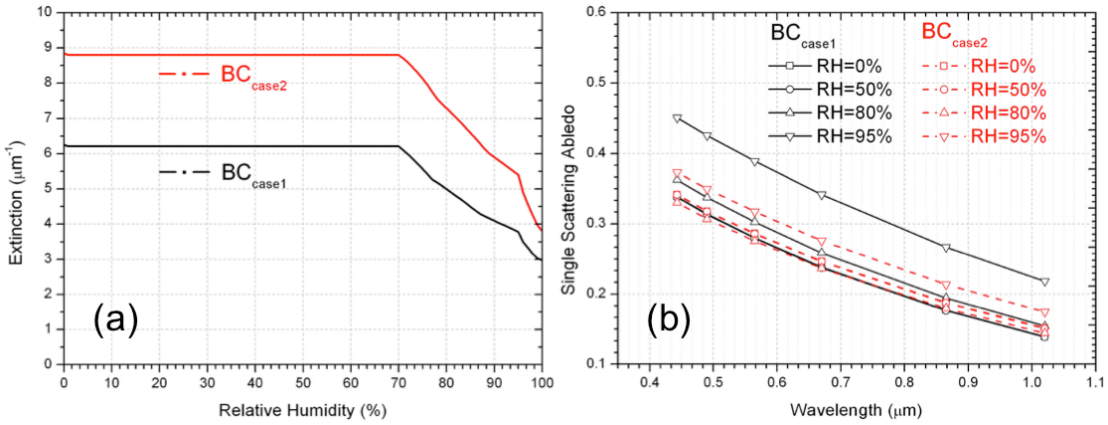

Figure 2. (a) The relative humidity dependence of BC particle extinction at 565 nm; (b) Wavelength dependence of BC particle single scattering albedo at six PARASOL wavelengths;

An adjoint model ~~is an efficient tool~~ can be used as a tool for calculating the gradient of a scalar model response function with respect to a large set of model parameters simultaneously (Fisher and Lary, 1995; Elbern et al., 1997, 2000, 2007; Henze et al., 2004; Sandu et al., 2005). The adjoint of the GEOS-Chem model was developed specifically for inverse modelling of aerosols or their precursors and gas emissions (Henze et al., 2007, 2009). The 4D-Variational data assimilation technique is used to optimize aerosol emissions by combining observations and model simulations. The adjoint of GEOS-Chem has been widely used to constrain emissions. For example, Kopacz et al. (2009) utilized MOPITT measurements of carbon monoxide (CO) columns to optimize Asian CO sources. Zhu et al. (2013) constrain ammonia emissions over the U.S. using TES (Tropospheric Emission Spectrometer) measurements. Zhang et al. (2015) use OMI AAOD to constrain anthropogenic BC emissions over East Asia. However, these studies have focused on a single aerosol or gas species and kept others constant during the inversion, since the satellites or other available observations of aerosols generally did not provide enough accurate information to estimate contributions from different species. The recent development of the PARASOL/GRASP retrieval, which retrieves more detailed and accurate aerosol information (see in section 2.3), thus presents a new opportunity for constraining emissions from different aerosol species simultaneously, which has only been considered in few studies (e.g., Xu et al., 2013).

2.3 PARASOL/GRASP aerosol products

GRASP is a recently developed ~~highly versatile and accurate~~ aerosol retrieval algorithm that processes properties of aerosol and land surface reflectance. The algorithm is developed for enhanced characterization of aerosol properties from spectral, multi-angular polarimetric remote sensing observations (http://www.grasp-open.com/) (Dubovik et al., 2011, 2014; Lopatin et al., 2013). The POLDER/PARASOL imager provides spectral information of angular distribution of both total and polarized components of solar radiation reflected to space. With the expectation of 3 gaseous absorption channels (763,

765 and 710 nm), the observations over each pixel include total radiance at 6 channels (443, 490, 565, 670, 865 and 1020 nm) and linear polarization among 3 channels (490, 670 and 865 nm). The number of viewing angle is similar for all spectral channels and varies from 14 to 16 depending on solar zenith and geographical location. Meanwhile, PARASOL provides global coverage about every 2 days. Comprehensive measurements (~144 independent measurements per pixel) from PARASOL allow GRASP to infer aerosol properties including spectral AOD and AAOD, the particle size distribution, single scattering albedo, spectral refractive index and the degree of sphericity (some description of GRASP aerosol products can be found in papers of Kokhanovsky et al. (2015) and Popp et al. (2016)). ~~Extensive information of aerosol distribution and their properties provides a means to constrain specific aerosol types, which is vital to characterizing emissions from different aerosol species.~~

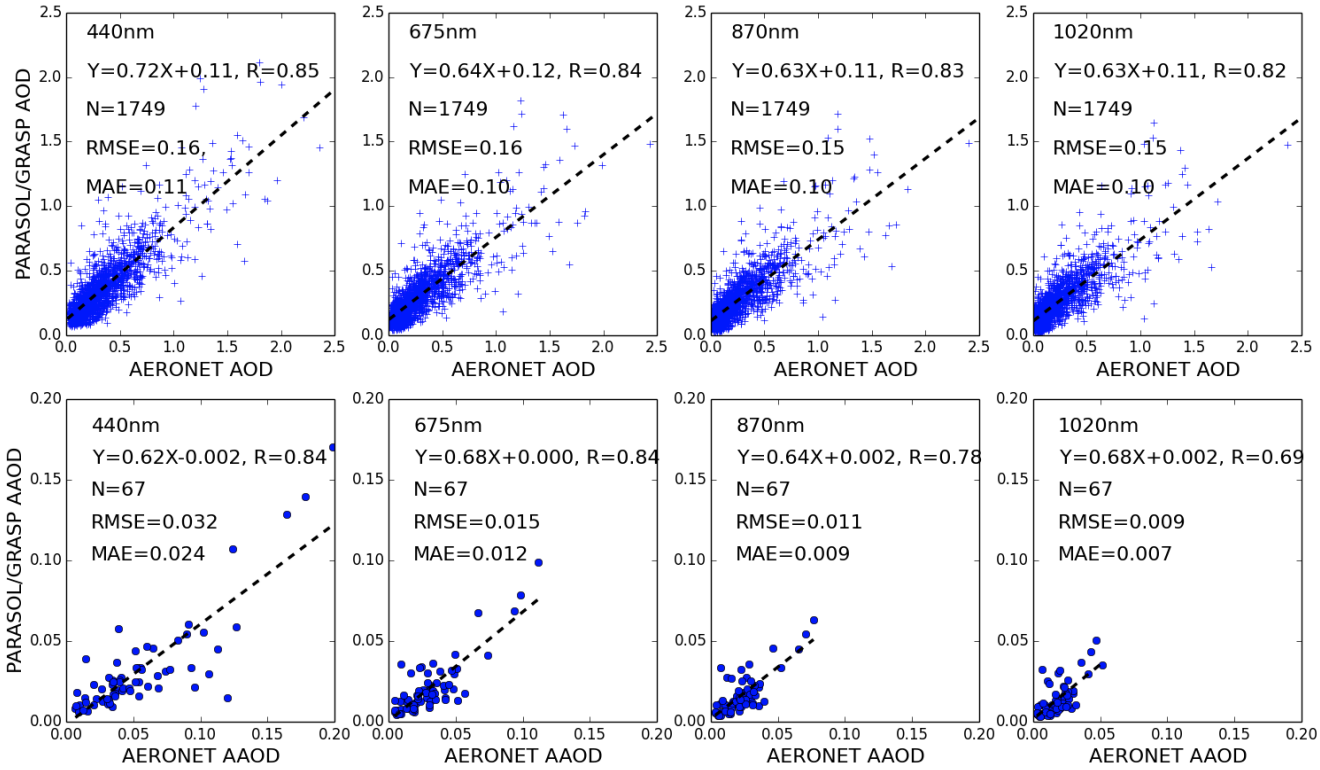

Figure 3. Validation of one-year of PARASOL/GRASP spectral AOD and AAOD rescaled to 2.0° x 2.5° horizontal resolution with AERONET 28 sites measurements at 440, 675, 870 and 1020 nm wavelengths over the study area; the number of matched pairs (N), correlation coefficient (R), root mean square error (RMSE) and mean absolute error (MAE) are provided in the top left corner.

In this study, we adopt one-year (December 2007 to November 2008) PARASOL products of spectral AOD and AAOD from GRASP to retrieve DD, BC and OC emissions over the study area in Section 4. In order to evaluate the

reliability of PARASOL aerosol products from GRASP, we compared PARASOL/GRASP retrievals with AERONET measured AOD and AAOD at 4 Sun photometer channels (440, 670, 870 and 1020 nm) in Figure 3. Here, we use level 2 AERONET Version 2 data, which are cloud screened and quality assured (Smirnov et al., 2000). From all one-year measurements collected from 28 sites, we extract data between 13:00 p.m. and 14:00 p.m. local time. This provides a 60 minute window centered at the PARASOL overpassing time of ~13:30 p.m. The averaged AERONET sun-direct AOD and AAOD by inversion of almucantar measurements (Dubovik et al., 2000; Dubovik and King, 2000) over this 60 minute window are averaged for comparison with PARASOL/GRASP retrievals. We aggregate the PARASOL/GRASP products into 2 ° latitude x 2.5° longitude horizontal resolution to match the spatial resolution used by GEOS-Chem; any 2° x 2.5° grid box with less than 500 available PARASOL/GRASP retrievals for averaging is omitted. Depending on geographical location, the number of GRASP retrievals in a single 2° x 2.5° grid box ranges from 500 to 1600. Figure 3 presents the validation of retrieved PARASOL AOD and AAOD by GRASP algorithm against the AOD and AAOD measured by AERONET. There is a solid correlation between PARASOL/GRASP and AERONET for AOD as well as AAOD. For example, the correlation coefficients (R) are 0.85 and 0.84, and the root mean square errors (RMSE) are 0.16 and 0.032, and the mean absolute errors (MAE $= \frac{1}{N}\sum_{i=1}^{N}|(M_i - O_i)|$) are 0.11 and 0.024 for AOD and AAOD at 440 nm respectively.

3 Methodology

3.1 Description of inverse modelling

Our inverse modelling approach optimizes BC, OC and DD emissions at the 2° x 2.5° horizontal resolution of the forward GEOS-Chem model, driven by GEOS-5 meteorological fields with 6h temporal resolution. It follows overall the assimilation concept described in many textbooks and articles (e.g. Talagrand and Courtier, 1987 and Bennett, 2002). The details of specific realization of the approach used here are discussed in the details by Henze et al. (2007) and Dubovik et al. (2008).

The algorithm iteratively seeks adjustments to emissions in order to minimize the differences between observations and simulations as quantified by the cost function, J, given by the sum of following quadratic form:

$$J(\boldsymbol{S}) = J_{obs}(\boldsymbol{S}) + J_{a\ priori}(\boldsymbol{S})$$
$$= \frac{1}{2}\sum(\boldsymbol{f}(\boldsymbol{S}) - \boldsymbol{f}_{obs})^{\mathrm{T}}\mathbf{C}_{obs}^{-1}(\boldsymbol{f}(\boldsymbol{S}) - \boldsymbol{f}_{obs}) + \frac{1}{2}\gamma_r(\boldsymbol{S} - \boldsymbol{S}_a)^{\mathrm{T}}\mathbf{C}_a^{-1}(\boldsymbol{S}^p - \boldsymbol{S}_a) \quad (3)$$

The first term characterizes the fitting of observation, where the vector $\boldsymbol{f}_{obs}$ is the vector of observed values used for inversion and $\boldsymbol{f}(\boldsymbol{S})$ is the vector of simulated values based on emission sources $\boldsymbol{S}$, while the vector $\boldsymbol{S}$ describes generally the four-dimensional distribution of emissions. ~~$\mathbf{C}_{obs}^{-1}$~~ $\mathbf{C}_{obs}$ is the error covariance matrix of $\boldsymbol{f}_{obs}$. The second term is introduced to constrain retrieval and it indicates the agreement with *a priori* estimates $\boldsymbol{S}_a$ of the emissions. ~~$\mathbf{C}_a^{-1}$~~ $\mathbf{C}_a$ is the error

covariance estimate of *a priori* emissions. ~~γ_r is a regularization parameter.~~ Indeed, in general the information content of observation is insufficient for unique retrieval of all parameters describing emissions, i.e. the problem is ill-posed and some *a priori* information is needed. In most applications "prior model" emission from bottom-up inventories $\boldsymbol{S}_a$ (i.e. standard model emissions) are used as *a priori* estimates of fundamentally unknown emissions. γ_r in Eq. (3) is a regularization parameter that is used for empirical adjustments of *a priori* term weight (see below).

The minimization of the quadratic form given by Eq. (3) can be obtained by steepest decent iterations:

$$\boldsymbol{S}^{p+1} = \boldsymbol{S}^p + \Delta\boldsymbol{S}^p,$$

$$\Delta\boldsymbol{S}^p = \nabla J_{obs}(\boldsymbol{S}^p) + \nabla J_{a\ priori}(\boldsymbol{S}^p) = \mathbf{K}_{obs}^T\mathbf{C}_{obs}^{-1}\Delta f^p + \gamma_r\mathbf{C}_a^{-1}(\boldsymbol{S}^p - \boldsymbol{S}_a), \quad (4)$$

where $\mathbf{K}_{obs}$ ~~$\mathbf{K}_{obs}^T$~~ denotes matrix of Jacobians of observation characteristics $\boldsymbol{f}$. Equations (3) and (4) are written using vectors and matrices, describing four-dimensional geophysical fields that are generally are very large. However, in practice neither transport models nor inverse modelling algorithms (if emissions retrieved at high resolution) explicitly utilize matrix and vectors. The transport models are generally organized as routines calculating continuous (i.e. with relatively small time step) time series of the geo characteristic resulted from time integration. For example, calculations of corrections $\Delta\boldsymbol{S}^p$ are obtained by running the adjoint model that directly produces the product of $\mathbf{K}_{obs}^T\mathbf{C}_{obs}^{-1}\Delta f^p$ without explicit calculation of the Jacobians $\mathbf{K}_{obs}$. For example, for inversion of observations of aerosol mass, i.e. $\boldsymbol{f}$=~~$\boldsymbol{M}$~~ $\boldsymbol{m}$, the computations of gradient $\nabla J^p(t,\boldsymbol{x})$ of cost function $J^p(t,\boldsymbol{x})$ using the adjoint model can be expressed as time integration operation (see derivations by Dubovik et al. (2008)) as following:

$$\nabla J^p(t,\boldsymbol{x}) = \int_t^{t_0} T^{\#}(t',\boldsymbol{x})(\nabla J^p(t',\boldsymbol{x}) + C_{obs}^{-1}\Delta m^{\boldsymbol{p}}(t',\boldsymbol{x}))(-\mathrm{d}t') \ + \gamma_r C_a^{-1}(s^p - s_a) \quad (5)$$

where

$$\Delta m^{\boldsymbol{p}}(t,\boldsymbol{x}) = m_{obs}(t,\boldsymbol{x}) - \int_{t_0}^{t} T(t',\boldsymbol{x})\big(m(t',\boldsymbol{x}) + s^p(t',\boldsymbol{x})\big)\,\mathrm{d}t' \quad (6)$$

and T represents transport operator. T and m are explicit functions of time t and spatial coordinates $\boldsymbol{x} = (x,y,z)$. $T^{\#}(t,\boldsymbol{x})$ is the adjoint of transport operator of $T(t,\boldsymbol{x})$, (the adjoint operation is a transformation of continuous function equivalent to matrix transposition operations) that is composed of adjoints $T_i^{\#}(t,\boldsymbol{x})$ of the component processes $T_i(t,\boldsymbol{x})$:

$$T^{\#}(t,\boldsymbol{x}) = T_1^{\#}T_2^{\#}T_3^{\#}\ldots T_{i-1}^{\#}T_i^{\#} \quad (7)$$

The above equations describe an approach to invert transport model based on the measurements of aerosol mass $\boldsymbol{m}_{obs}$, which is the direct simulation parameter in the chemical transport model. In our analysis, the aerosol data fields is available only in the form of AOD and AAOD from the satellite measurements:

$$\boldsymbol{f} = \boldsymbol{\tau}(t,\boldsymbol{x}) = f(m(t,\boldsymbol{x}),\lambda,Q_{ext},Q_{abs},\ldots) \quad (8)$$

where $f(\dots)$ is a function converting aerosol mass $m(t,\boldsymbol{x})$ to AOD and AAOD based on spectral characteristics λ, aerosol extinction Q_{ext} and absorption Q_{abs} coefficients, etc, see in Eq (1-2). The correction $\Delta\boldsymbol{S}^p(\boldsymbol{x}) = \nabla J^p(t,\boldsymbol{x})$ minimizing the form of Eq. (3) that relates for fitting of AOD and AAOD under *a priori* constraints can be written as:

$$\nabla J^p(t,\boldsymbol{x}) = \int_t^{t_0} T^{\#}(t',\boldsymbol{x})F^{\#}(t',\boldsymbol{x})(\nabla J^p(t',\boldsymbol{x}) + C_{obs}^{-1}\Delta\tau^{\boldsymbol{p}}(t',\boldsymbol{x}))(-\mathrm{d}t') + \gamma_r C_a^{-1}(s^p - s_a) \quad (9)$$

here $F^{\#}(t',\boldsymbol{x})$ is adjoint operator corresponding to matrix operation $\mathbf{F}^T$, where matrix $\mathbf{F}$ contains first derivatives $d\tau/dm$. It should be noted that GEOS-Chem adjoint model is developed for inversion of mass (or AOD at single wavelength), therefore the operator $F^{\#}(t',\boldsymbol{x})$ for inversion spectral AOD and AAOD was developed as a part of this work.

In principle, the methodology assumes that the *a priori* information is available, i.e. before the inversion, which here are the default model emissions. Unfortunately, the covariance matrix $\mathbf{C}_a$ of *a priori* emissions is not known accurately. As a result, this matrix is often assumed diagonal, where the elements of diagonal are equal or defined using rather simple strategies. In addition ~~Therefore~~, in order to address this fundamental lack of knowledge of $\mathbf{C}_a$, the contribution of the *a priori* term (second term) in Eq. (3) is weighted by a regulation parameter, γ_r that is determined by empirical tests. This strategy is adapted here.

In addition, the GEOS-Chem adjoint model previously has been used for calculation of the gradient of Eq. (9) with respect to a vector of emissions scaling factors $\boldsymbol{\sigma}$ ($\boldsymbol{S}^p = \boldsymbol{S}_0\boldsymbol{\sigma}^{p-1}$) (Henze et al., 2007). While the scaling factor formulation had the advantage of replace addition/subtraction correction of emissions (that can generate negative unphysical values) by division/multiplication of initial positive and non-zero $\boldsymbol{S}$, this can be realized in the inversion algorithm by transforming into log scale (see discussion by Dubovik and King, (2000), Dubovik, (2004) and Henze et al. (2009)). However, the latter approach is rather challenging and GEOS-Chem used in this study relies on ~~uses~~ empirically elaborated procedure (using equivalence ($\Delta\boldsymbol{S}/\boldsymbol{S}\sim\Delta ln(\boldsymbol{S})$)). Specifically, from the gradients of cost function with respect to aerosol emission scaling factors $\nabla_{\boldsymbol{\sigma}}J(t,\boldsymbol{x})$, the adjoint GEOS-Chem uses the L-BFGS-B optimization method (Byrd et al., 1995; Zhu et al., 1997), which affords bounded minimization of cost function, and ensuring positive values, to calculate the scaling factors for aerosol emissions. Figure 4 is the flowchart to illustrate the methodology.

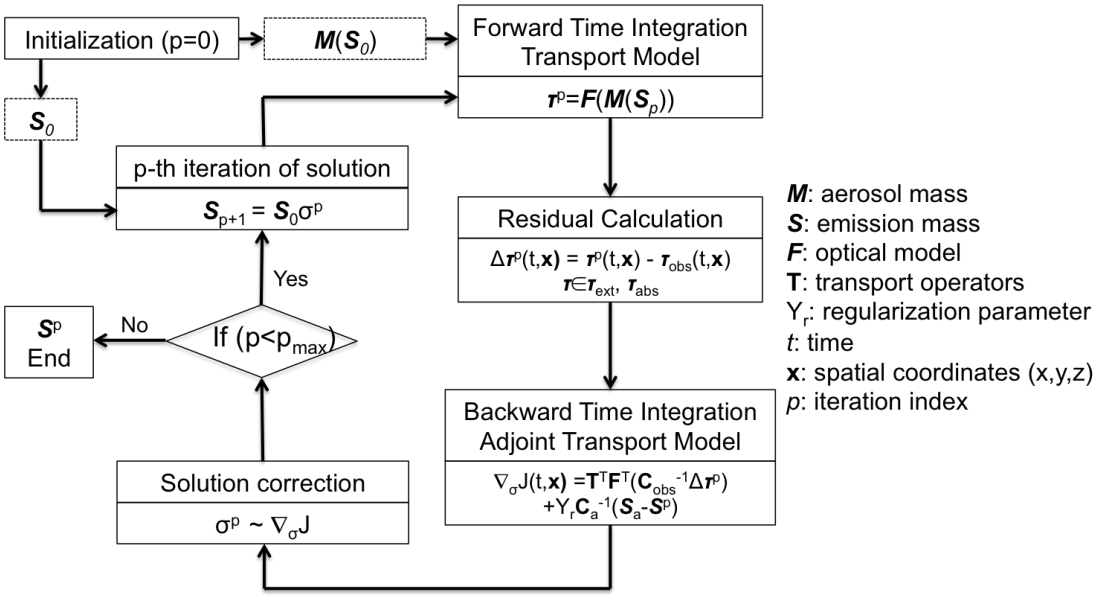

Figure 4. Diagram illustrating retrieval of aerosol emissions from satellite measurements

In order to optimize the specification of *a priori* constrains and initial guess, a number of synthetic tests were done in Section 3.2. It should be noted that using *a priori* estimate of emission $\boldsymbol{S}_0$ is not the only way of adding *a priori* constraints in the inverse modelling. For example, Dubovik et al. (2008) demonstrated used of *a priori* knowledge on spatial and temporal variability of emissions, i.e. *a priori* limitation on derivative of corresponding functions (smoothness constraints). The potential advantage of smoothness constraints is that these limitations are milder than direct assumptions about values of emissions and therefore they introduce less systematic errors in the retrieval. However, such constraints are not used in this study.

3.2 Inversion test using synthetic measurements

In this section, a series of numerical tests were performed to verify and illustrate how the algorithm inverts the synthetic measurements, and to tune the algorithm settings (e.g. initial guess, emission correction time resolution and BC refractive index). The retrieved results were compared with "True emissions". Synthetic measurements are PARASOL-like spectral AOD and AAOD at six PARASOL wavelengths, simulated from 16 days of BC, OC and DD emissions, which, for simplicity, are specified to be constant over the 16 days, yet different from the prior model emissions in order to test the algorithm performance under the circumstances that *a priori* knowledge of the emission distribution is limited. Figure 5 shows the design of the inversion test from synthetic measurements.

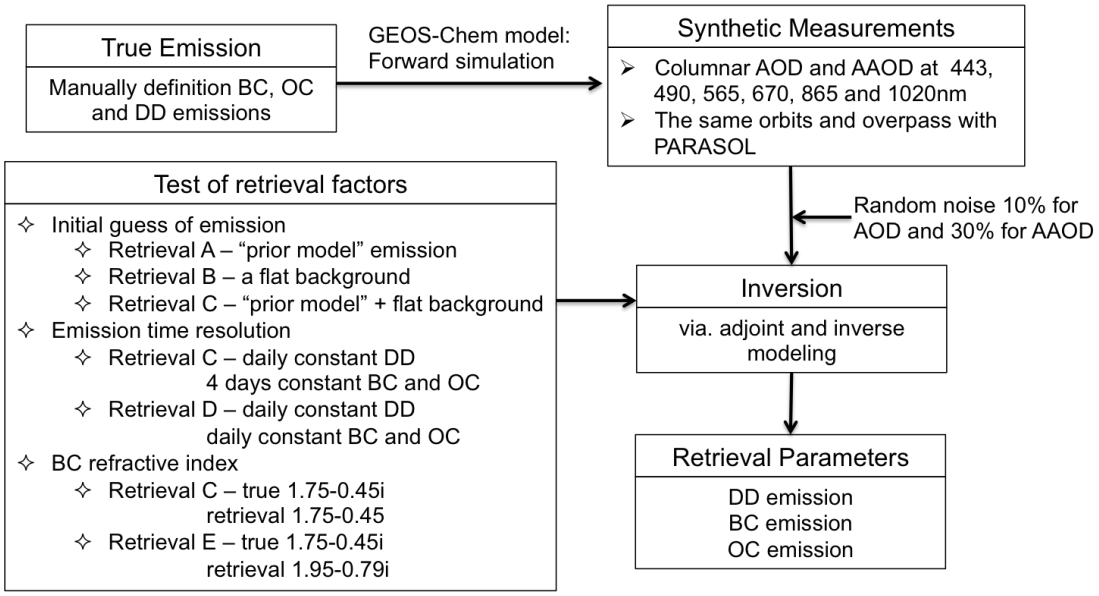

Figure 5. Diagram illustrating the inversion tests from synthetic measurements

3.2.1 ~~Spectrum weights~~ Assumption of C_{obs}, definitions of spectral weights in AOD and AAOD fitting

In our inversion framework, the observed aerosol parameters contain AOD and AAOD at six PARASOL wavelengths. In principle, the weighting of observations of AOD and AAOD at these different wavelengths should be defined ~~by~~ as $\mathbf{C}_{obs}^{-1}$. However, at present PARASOL/GRASP does not provide ~~the observation error~~ covariance matrix $\mathbf{C}_{obs}$ for operational retrieval, because it is computationally expensive and methodologically challenging. Indeed, GRASP inverts simultaneously large group of pixels and the covariance matrix should be joint, i.e. characterize all inverted data. Such matrix can be very large and it may have non-zero non-diagonal elements that are very difficult to use in practical applications. At the same time, GRASP AOD and AAOD were extensively evaluated against AERONET and there is overall understanding of accuracy. For example, usually AOD is about ten times higher than the AAOD at the same wavelength (~~SSA=1.0-AAOD/AOD~~ AAOD/AOD=1.0-SSA=~0.1). ~~and~~ Therefore in order to make contribution into cost function, the AAOD is expected to be ~~retrieved and~~ fitted about 10 times more accurate than AOD on an absolute scale. In addition, AAOD become very small at longer wavelengths. Based on these simple considerations we have defined different weighting for AOD and AAOD at different wavelengths. We have also assumed that retrieved AOD and AAOD are independent, i.e. $\mathbf{C}_{obs}$ is diagonal. Under such assumption the absolute values of $\mathbf{C}_{obs}$ diagonal are not of importance since minimization procedure searches for minimum and does not require knowledge of the cost function absolute value. In order to make some optimization of fitting weights, we have performed several sets of tests to optimize the fitting weights of observations. Specifically we have performed the retrievals with different assumptions and analysed the goodness of fit. ~~However, at present knowledge of this matrix is uncertain, so we thus perform the following sets of tests to optimize the observational~~

~~covariance weights.~~ The spectral residual values ~~are defined~~ to characterize the quality of spectral AOD and AAOD fit were defined as:

$$R_{AOD}(\lambda) = \sqrt{\frac{1}{N_i}\sum_{i=1,\dots,N_i}[\tau_{i,obs}(\lambda) - \tau_{i,model}(\lambda)]^2} \quad (10)$$

$$R_{AAOD}(\lambda) = \sqrt{\frac{1}{N_i}\sum_{i=1,\dots,N_i}[\tau_{a,i,obs}(\lambda) - \tau_{a,i,model}(\lambda)]^2} \quad (11)$$

The values of the spectral residuals $R_{AOD}(\lambda)$ and $R_{AAOD}(\lambda)$ are calculated after each iteration. The following options were tested using well-known qualitative tendencies. In sensitivity test, two scenarios of spectrum weights are analysed. Since we are fitting absolute value of AOD and AAOD, the relative accuracy of retrieved AOD and AAOD ($\Delta\tau/\tau$ and $\Delta\tau_a/\tau_a$) are expected to be the same. The spectrum weights are defined as follows:

Option A, Unity weights (the elements of $\mathbf{C}_{obs}^{-1}$) for AOD and AAOD at 6 wavelengths: $[1,1,1,1,1,1]^T$ for AOD and $[1,1,1,1,1,1]^T$ for AAOD.

Option B, Unity weights for AOD but more weights on AAOD: $[1,1,1,1,1,1]^T$ for AOD and $[5,10,15,20,25,30]^T$ for AAOD.

The retrievals are conducted with option A and option B respectively (the inversion is conducted under Retrieval C scenario, see in the following sections), with other settings held constant. Comparison of spectral residuals after 20 iterations are shown in Figure 6, which indicates that Option B have a better fit for AAOD than Option A by increasing the weights for AAOD, although spectral AOD can be fitted comparably well using either option.

In future studies, it is expected that more adequate information for $\mathbf{C}_{obs}$ of PARASOL/GRASP AOD and AAOD will be available and it will be accounted in future studies.

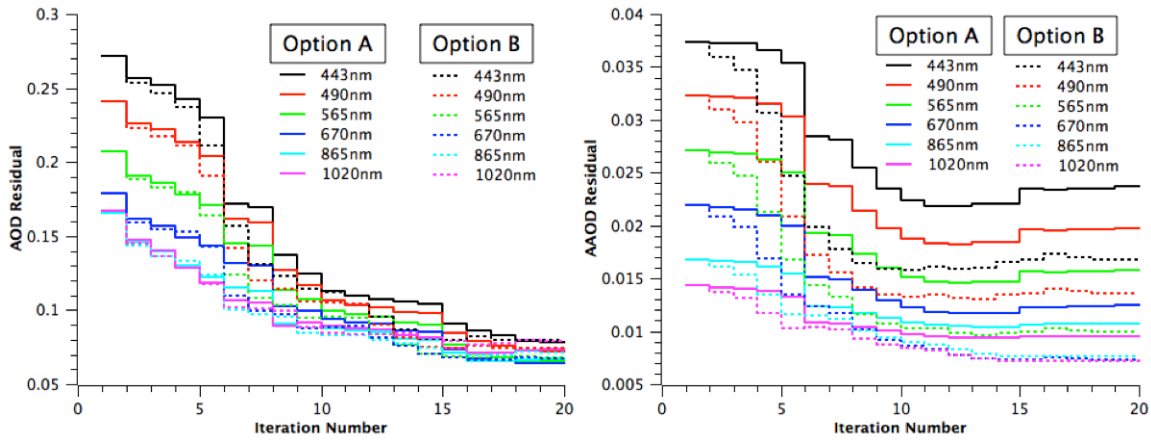

Figure 6. Comparison of spectral AOD and AAOD residual iteratively with two spectrum weight options

3.2.2 Effect of initial guess in emission retrieval

As mentioned in section 3.1, the emission retrieval is an ill-posed problem and utilization of *a priori* constraints and initial guesses are essential factors for the retrieval. In our retrieval framework, the emissions are adjusted using scaling factors that scaling for initial guess of emissions, $\boldsymbol{S}=\boldsymbol{S}_0\boldsymbol{\sigma}$. In principle, if the inverse problem is well-constrained the solution should be independent of the initial guess. Therefore, we analyse the dependence on initial guess using different retrieval settings. The inversion is conducted with three different initial guess schemes that we describe in detail in the following sections. In each of these three schemes, the input synthetic measurements are 6 wavelengths AOD and AAOD, and the spectrum weights use the Option B scenario, while the retrieved emission correction time variations are assumed to be daily constant for DD and 4-day constant for BC and OC (note that we will separately test the assumption of emission correction time resolution in section 3.2.3). Figure 7 shows the "True emissions" of DD, BC and OC and also the difference between true and retrieved emissions from three different initial guess schemes (Retrieval A, Retrieval B and Retrieval C). Figure 8 shows the scatter plots between BC, OC and DD emissions retrieved from Retrieval A, B, C versus true values.

Thus, the following tendencies were observed in the conducted test:

A. Prior model: Initial guess is equal to Prior model emissions

In this method, the prior model emissions are directly used as the initial guess, therefore the adjustments of emissions are limited to the grid boxes with prior model emissions $\boldsymbol{S}_0>0$. At the same time, the "True emissions" have difference with prior model. The upper panel in Figure 7 shows the assumed true BC, OC and DD emission distributions (units: kg/day) respectively. The second panel "Retrieval A - True" shows the differences between retrieved and true emissions from Retrieval A.

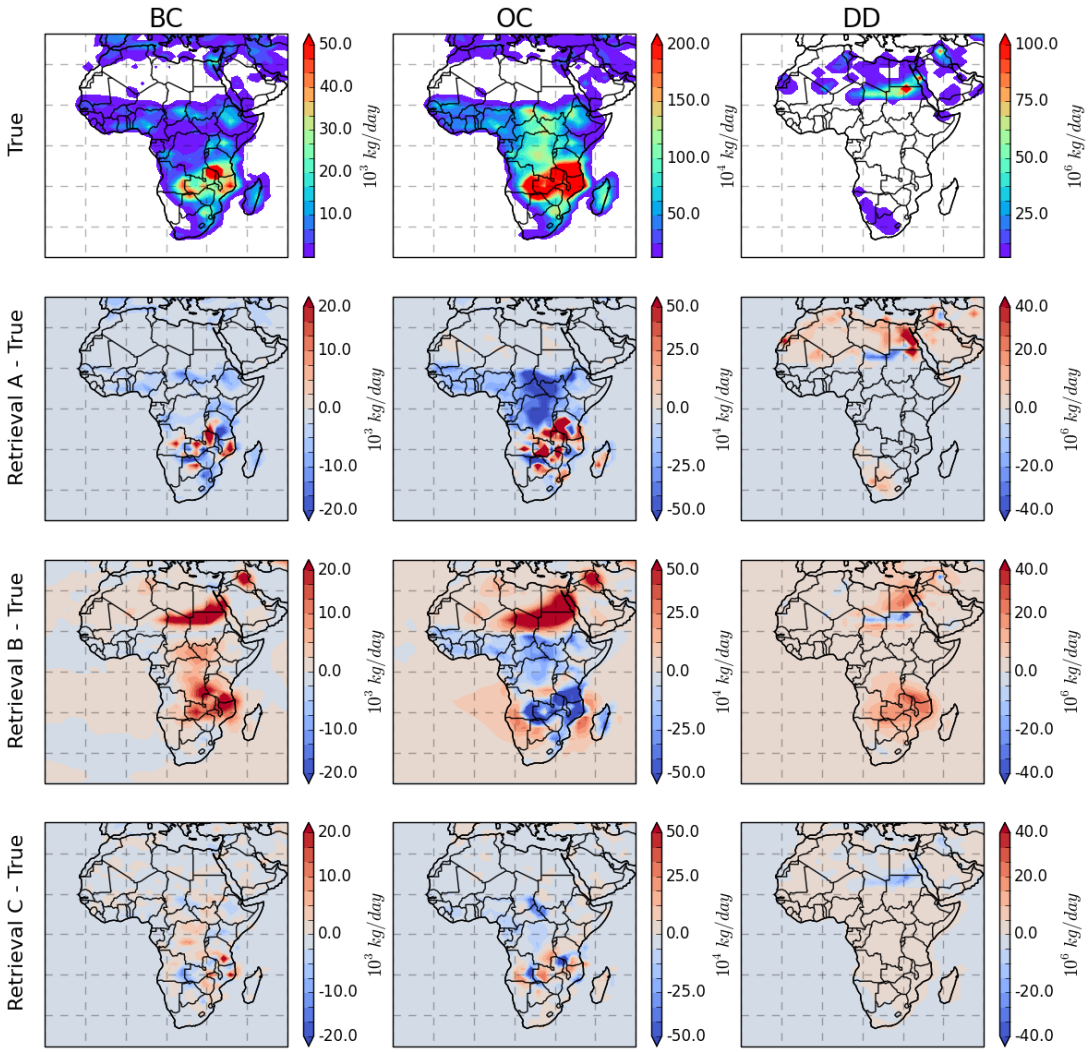

Figure 7. Inversion test for retrieving BC, OC and DD emissions from synthetic measurements with three different initial guess schemes: (A) Prior model emissions – Retrieval A; (B) Spatially uniform – Retrieval B; (C) Prior emission with spatially uniform background – Retrieval C;

5

For Retrieval A, the retrieval highly relies on the accurate distribution of model prior emissions, because the retrieval can only adjust the emissions on the grid boxes where the model prior emissions are non-zero, and thus the retrieval couldn't create new sources. In our inversion test, the model prior emissions are different from the truth both for distribution and strength. Therefore, as shown in Figure 8, the Retrieval A produces overestimations over the grid boxes that $\boldsymbol{S}_0$>0, while

$\boldsymbol{S}_{\text{true}}$=0, here $\boldsymbol{S}_{\text{true}}$ represent true emissions, however the underestimations occur over the grid boxes that $\boldsymbol{S}_0$=0, while $\boldsymbol{S}_{\text{true}}$>0.

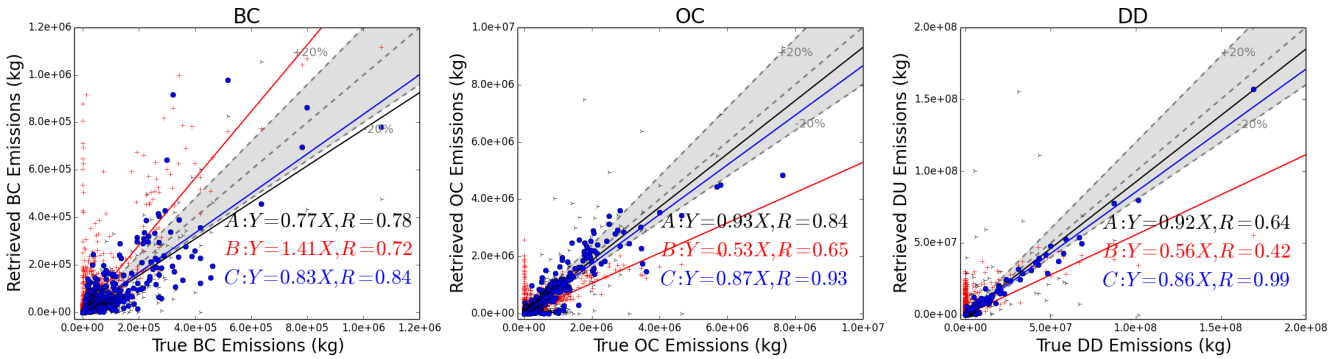

Figure 8. Scatter plots between BC, OC and DD emissions retrieved from Retrieval A, B, C versus true values

B. Flat background everywhere

For Retrieval B, we investigate the use of spatially uniform initial guesses for the emissions. With this initialization, we allow BC, OC and DD emission to be generated everywhere over land and ocean. In addition we are not using ~~which is equivalent to not using~~ *a priori* knowledge of aerosol emissions. From the Figure 7 panel "Retrieval B – True", the algorithm can determine the intensive aerosol emission grid boxes, where high aerosol loading is observed. However, the desert dust and carbonaceous aerosol sources were not correctly reproduced since a uniform emission is used everywhere. The scatter plots between retrieved emissions from Retrieval B and true values are also shown in Figure 8. In this case, the retrieval could produce overestimations over some grid boxes where $\boldsymbol{S}_{\text{true}}$=0. Although the uniform emission assumption gives the algorithm more freedom to find new sources, our tests indicate the retrieval could produce false sources in this assumption when the algorithm tries to determine BC, OC and DD emissions simultaneously. This misrepresentation indicates that the spectral AOD and AAOD are not sufficient to identify BC, OC and DD emission without any *a priori* knowledge.

C. Prior model emission with flat background

In retrieval C, the retrieval was initiated using prior model emissions but including a spatially uniform value over land grid boxes where $\boldsymbol{S}_0$=0. In this study, the flat value equals to 10^{-4} Tg/day/grid for DD, 10^{-6} Tg/day/grid for BC, and $5\text{x}10^{-6}$ Tg/day/grid for OC are used, which account for ~5% of the true emissions over entire area. This assumption allows retrieval of BC, OC and DD aerosol emissions everywhere over land (ship emissions over ocean are included in the model prior emissions), and at the same time it uses prior emission constraints to prevent false source generation that could occur due to inaccuracies in data or model processes. Figures 7 and 8 show that overall Retrieval C captures the emission distributions more accurately than Retrieval A and Retrieval B. The average ratio of retrieved emission to truth ($\sum_{N_{pixels}} \frac{\boldsymbol{S}_{\text{retrieval}}}{\boldsymbol{S}_{\text{true}}} / N_{pixels}$) for Retrieval C is 1.02 ± 1.05 for BC, 0.87 ± 1.42 for OC and 1.24 ± 1.80 for DD.

3.2.3 Assumption of emission correction time resolution

Aerosol sources are known to have high temporal and spatial variability. However, because PARASOL observations have limited temporal coverage (e.g. ~2 days global coverage, with observations once per day), the variability of aerosol emission at any given location can only be retrieved at a frequency no more than once per day. In order to investigate how assumptions regarding temporal variability of emission can affect the retrieval, we repeat the retrieval using two scenarios for emission correction: ET1, daily correction constant of DD, BC and OC emissions, and ET2, daily correction constant of DD emission and 4 days correction constant of BC and OC emissions. For each scenario, the input observations are 6 wavelengths of AOD and AAOD, and the retrieval is initialized by prior model emission with a uniform background emission (Retrieval C). Two scenarios are used. We test these two scenarios by conducting a 16-days retrieval, and Figure 9 shows the comparison between retrieved daily total DD, BC and OC emissions with the "True emissions". Note that the ET1 scenario uses the same settings with Retrieval C in section 3.2.2, and ET2 is named Retrieval D.

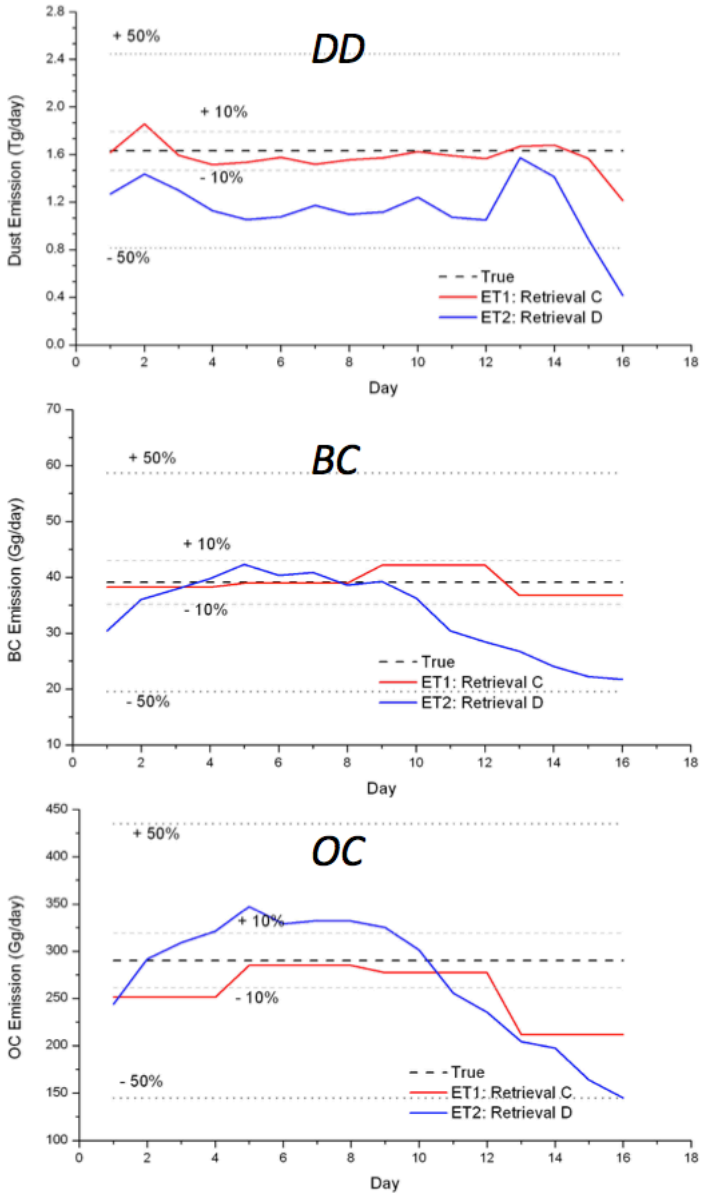

Figure 9. Sensitivity test for retrieving DD, BC and OC emissions over 16-days with two scenarios of assumption of emission correction time resolution

Figure 9 shows the retrieval maximum uncertainty ($\sum|S_{retrieval} - S_{true}| / \sum S_{true}$) for total daily DD emission over the study area is within 25.8% for Retrieval C, however this value reaches more than 50% for Retrieval D. For BC, the maximum uncertainty is within 5.9% for total daily emission from Retrieval C, while up to 40.8% for Retrieval D. The uncertainty of daily OC emission is within 26.9% for OC using Retrieval C, while about 38.6% for Retrieval D. Overall,

from this sensitivity test, the Retrieval C shows a better capability to capture the spatial distribution of DD, BC and OC emissions than Retrieval D, and it does not introduce false temporal variability.

It should be noted that the regularization parameter defining the contribution of *a priori* term in all tests was chosen very small (i.e. 0.0001) in order to make the retrieval relying mostly on the observations. Thus, the good convergence to the sought solution was obtained with minimum constraints. This aspect is planned to investigate in future studies.

3.2.4 Uncertainty in assumption of BC refractive index

Aerosol particles' light scattering and absorption efficiencies are determined by their complex refractive indices, expressed as m= n-ki, where n is the real part and k is the imaginary part. The real part of the complex refractive indices defines the light scattering property of an aerosol species, whereas the imaginary part of the complex refractive indices determines the absorbing ability. Black carbon aerosol is the strongest atmospheric absorber of solar radiation. Its imaginary refractive index is at least about two orders of magnitude higher than other aerosol species (see Table 1). To identify the impact of the uncertainties of BC refractive index in our results, we test another commonly used specification of 1.95-0.79i (Bond and Bergstrom, 2006) in our retrieval scheme (denoted as Retrieval E). Figure 10 compares the BC emission results from Retrieval E and Retrieval C (where the BC refractive index of 1.75-0.45i (Hess et al., 1998) was used) with the "true" BC emission.

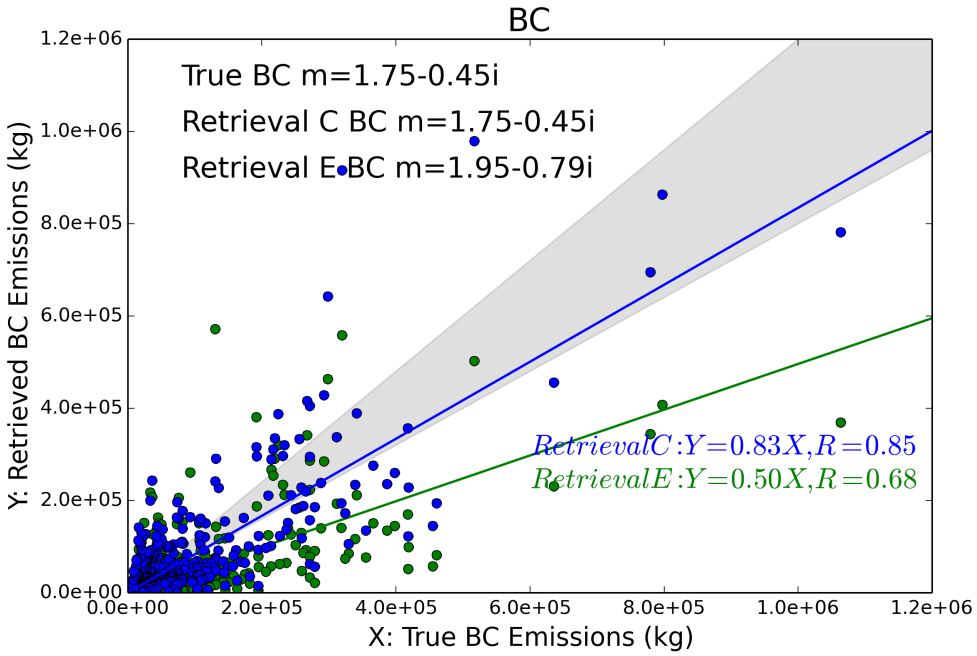

Figure 10. Test of BC particle refractive index influence on the retrieval of BC emissions. The scatter plots are grid-to-grid comparison of retrieved 16 days averaged emissions (blue: Retrieval C; green: Retrieval E) with the "true" BC emissions. The shade grey area represents ±20% differences around the true values.

The synthetic measurements of AOD and AAOD are simulated with BC refractive index m=1.75-0.45i, and the scenario Retrieval C uses the retrieval with the same BC refractive index; the slope of linear regression between the resulting retrieved and true BC emissions is 0.83, and the retrieved BC emission over study area is 39.0 Gg/day. In contrast, the Retrieval E scenario uses the retrieval with a higher BC absorption and scattering definition, m=1.95-0.79i, and as expected we get lower magnitudes of BC emissions (21.8 Gg/day), and the slope between retrieved and true BC emissions decreases to about 0.5. This sensitivity test demonstrates that uncertainty in the BC refractive index can lead to a factor of about 1.8 in total BC emissions.

Overall, these sensitivity tests suggest ~~show~~ that our inversion scheme is capable of determining the strength and spatial distribution of BC, OC and DD emissions simultaneously from the multispectral PARASPL/GRASP AOD and AAOD products in the following manner:

1. Six wavelengths (VIS-NIR) AOD and AAOD from PARASOL/GRASP are needed to retrieve BC, OC and DD emissions simultaneously.
2. The ~~improved~~ weighting spectral ~~weighting~~ factors for the PARASOL 6 wavelengths ~~are~~ ($[1,1,1,1,1,1]^T$ for AOD and $[5,10,15,20,25,30]^T$ for AAOD) were optimized to ~~, since it can~~ provide an improved ~~better~~ fit of both spectral AOD and AAOD.
3. The BC, OC and DD emissions are allowed everywhere over land. The retrieval is initialized by "prior model" emissions with a uniform background. The retrieval with this initialization could detect new sources and perform satisfactorily even when *a priori* knowledge of aerosol emission is not fully consistent with the assumed emissions. This scenario will be used in Sections 4 and 5.
4. The emission corrections are assumed daily constant for DD and 4 days constant for BC and OC. Owing to the limited observations available for assimilation, this assumption helps to make the retrieval sufficiently accurate and stable with rather generic initial guess. ~~more stable and accurate.~~
5. The BC emission retrieval is sensitive to BC refractive index assumption ~~is sensitive to BC emission retrieval~~, which could produce a factor of ~1.8 differences between the two sets of commonly used BC refractive index data for total BC emission. We will produce two BC emission datasets with two scenarios of BC refractive index, Case 1: m=1.75-0.45i and Case 2: m=1.95-0.79i.

4 Results

In this section, we discuss retrieval of DD, BC and OC emissions simultaneously from the actual PARASOL/GRASP

spectral AOD and AAOD data from December 2007 to November 2008. The SU and SS aerosol simulations are kept as the prior model. PARASOL/GRASP retrievals were aggregated to the same horizontal resolution as the GEOS-Chem model (2° x 2.5°) and averaged within the grid cells prior to assimilation. When iteratively minimizing Eq. (3), the maximum iteration number was chosen to be 40, which takes about 60 days to complete on a computer workstation with 32x3.3 GHz CPUs. Based on conducted tests, the decrease of the cost function is very minor starting from 20th iteration (e.g. see Figure 6).

4.1 Fitting of Aerosol Optical Depth

One of the important indicators of our inversion performance is the fitting of PARASOL/GRASP spectral AOD and AAOD. We evaluate the GEOS-Chem simulated spectral AOD at 443, 490, 565, 670, 865 and 1020 nm using prior or posterior emissions against the corresponding PARASOL/GRASP retrieved AOD in Figure 11. The posterior GEOS-Chem spectral AOD are simulated using retrieved DD, BC and OC emissions, which will be presented in section 4.2. Figure 11a presents the annual average of the PARASOL spectral AOD from GRASP algorithm, whereas Figure 11b and 11c show the same quantity from the GEOS-Chem simulations with prior and posterior emissions, respectively. Here we extract GEOS-Chem hourly AOD with the same PARASOL orbit partition at 13:00 p.m. local time, which is approximately the PARASOL overpass time of 13:30 p.m. Figure 11d and 11e display the grid-to-grid comparison between PARASOL/GRASP spectral AOD and prior and posterior GEOS-Chem simulation during one year, color-coded with the PARASOL Ångström exponent $\alpha_{443-865} = {\ln(\tau_{443}/\tau_{865})}/{\ln(865/443)}$. The Ångström exponent α is often used as a qualitative indicator of aerosol particle size; the smaller the α, the larger the particle size. For example, the α values for "pure" dust aerosols are usually near zero, whereas that for smoke or pollution aerosols are generally greater than 1 (Eck et al., 1999; Schuster et al., 2006).

One of the major discrepancies between the prior GEOS-Chem simulation and PARASOL/GRASP observation is that the model produces the highest annual average AOD values over the major dust source region of Northern Africa; however, satellite data show the maxima AOD in Central and the Southern Africa, where carbonaceous aerosols usually dominate (although Central Africa may also be influenced by dust events). Hence, compared to PARASOL/GRASP observations, the prior GEOS-Chem AOD is overestimated in Northern Africa, while it is underestimated in the Southern Africa biomass burning and Arabian Peninsula regions. Some recent studies by Ridley et al. (2012, 2016) and Zhang et al. (2015) also indicate that the GEOS-Chem model overestimates dust AOD in Northern Africa. Meanwhile, Ridley et al. (2012) and Zhang et al. (2013) propose a new and realistic dust particle size distribution according to the measurements from Highwood et al. (2003), which can partially adjust the misrepresentation of dust near the source and over transport areas. This new particle size distribution has been adopted in our prior and posterior GEOS-Chem simulation. In addition, the underestimation of model simulated AOD in biomass burning regions with the GFED emission database was also shown in other modeling studies (Chin et al., 2009; Johnson et al., 2016). The model simulated spectral AOD with the posterior emissions agree with the PARASOL observations much better, in spite of slight systematic overestimations from 565 nm to 1020 nm (about 13% on an annual average). This overestimation indicates some disagreement in modeling of AOD for these

bands that needs to be investigated and addressed in future studies.

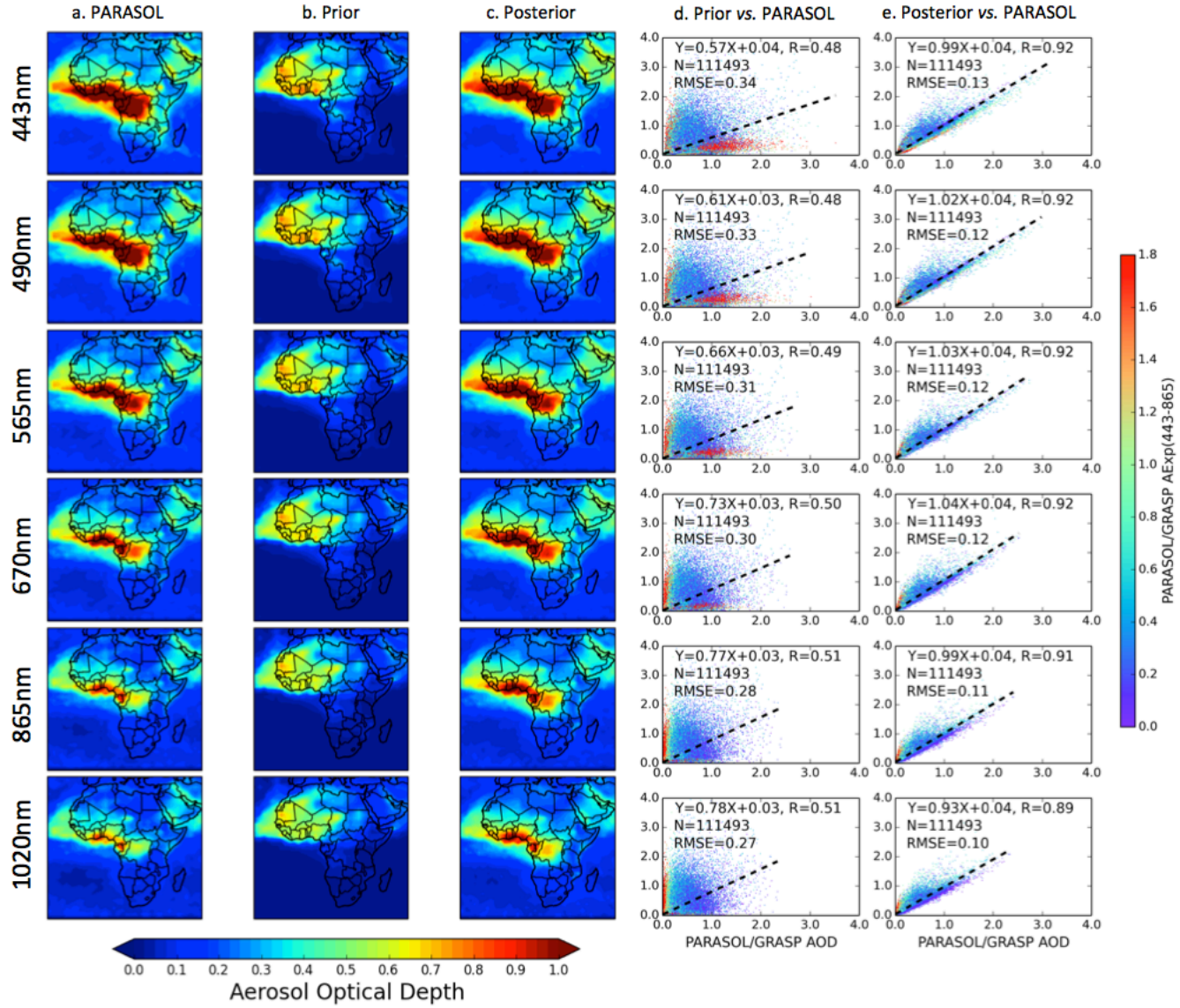

Figure 11. Comparison of the annual spatial distribution of prior (b) and posterior (c) GEOS-Chem simulated AOD at 443, 490, 565, 670 865 and 1020 nm with PARASOL/GRASP observations (a). The posterior spectral AOD are simulated using retrieved DD, BC and OC emissions. The scatter plots are grid-to-grid comparisons between PARASOL/GRASP spectral observations versus prior (d) and posterior (e) GEOS-Chem simulation during one year. The correlation coefficient (R) and root mean square error (RMSE) are provide in the top left corner.

Figure 11d and 11e show the statistics of prior and posterior GEOS-Chem simulated AOD versus PARASOL/GRASP

observed AOD at 6 wavelengths during the entire year. The number of matched pairs is 111,493. For the GEOS-Chem simulation with the posterior emissions, all the statistics parameters between model and observation are improved at all 6 wavelengths compared to the simulation with prior emissions. For example, the correlation coefficient has increased from 0.49-0.51 to 0.89-0.92 and the root mean square error has decreased from 0.27-0.34 to 0.10-0.13. Such improvements are expected as the posterior emissions are retrieved based on the PARASOL/GRASP AOD data. We will show further evaluations with other datasets in Section 5.

4.2 Fitting of Aerosol Absorption Optical Depth

Similar to the AOD analysis, here we evaluate the fitting of AAOD (Figure 12). From the annual-averaged spectral AAOD in Figure 12, the prior GEOS-Chem simulation (Figure 12b) shows significant underestimations of AAOD over the entire domain compared to PARASOL/GRASP observations (Figure 12a). On the other hand, the posterior GEOS-Chem simulation (Figure 12c) produces much better agreement with the PARASOL/GRASP data for all wavelengths, with a small overestimation of AAOD in the spectral range from 443 nm to 565 nm (about 6% on annual average) and a small underestimation at 865 nm and 1020 nm (about 9% on annual average). Linked with the ~13% overestimation of annual AOD from 565 nm to 1020 nm, this systematic phenomenon of fitting is possibly due to the model's relatively coarse resolution results in misrepresentations of DD, BC and OC emissions in some grid boxes.

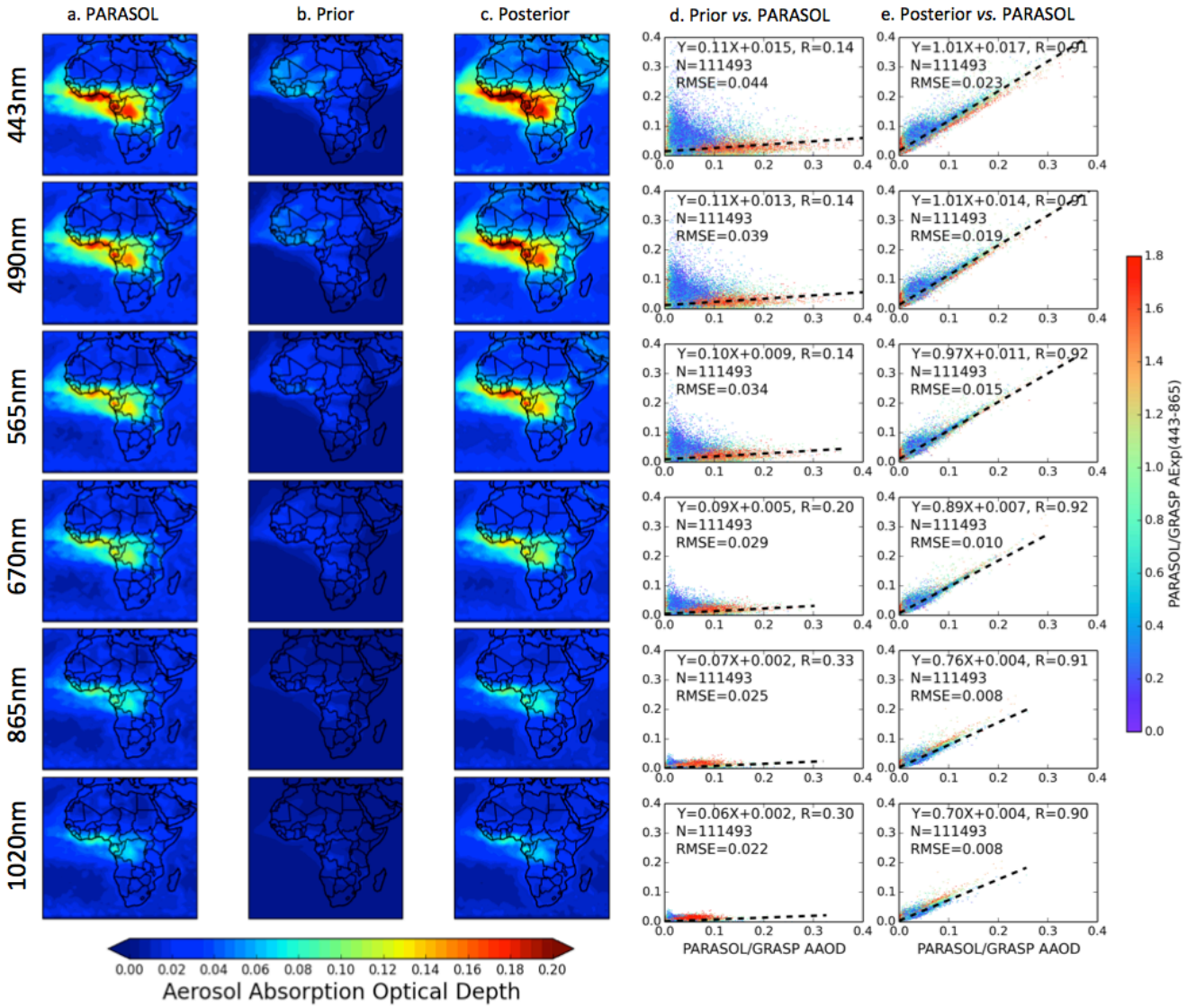

Figure 12. Same as Figure 11, but for AAOD.

Figures 12d and 12e show the comparisons of PARASOL/GRASP observed AAOD at 6 wavelengths with the corresponding GEOS-Chem simulated quantities using prior or posterior emissions. The very low linear regression slope between the model simulated AAOD using prior emissions with observations (less than 0.11 over all six wavelengths) indicates that the prior simulations significantly underestimate the AAOD. In contrast, model simulations with the posterior emissions ~~simulations~~ improve the slope to 1.01 at 443 nm and 0.70 at 1020 nm. Similar to the case of AOD, the agreements between the PARASOL/GRASP AAOD data and the model simulations are much better using the posterior emissions than using the prior emissions, with the correlation coefficients increased from 0.14-0.33 to 0.90-0.92 and the root mean square

error decreased from 0.022-0.044 to 0.008-0.023.

4.3 Emission sources

The retrieved and prior monthly total DD, BC and OC emission variations over the study area are shown in Figure 13.

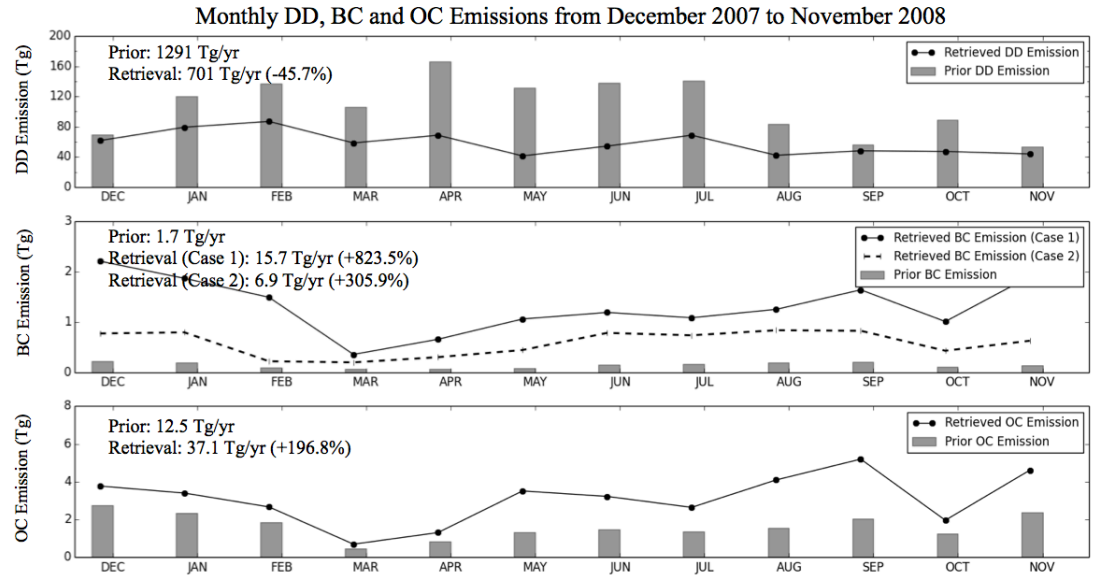

Figure 13. Comparison of monthly total DD, BC and OC emissions (unit: Tg ~~mon~~$^{-1}$) over the study area between prior model (GFED3 and Bond inventories for BC and OC, DEAD model for DD) and retrieved emissions, the annual values (unit: Tg yr^{-1}) are provided in the top left corner.

4.3.1 DD emissions

Figure 13 shows that the retrieved annual total DD emission in the study area is 701 Tg/yr (particle radius ranging from 0.1 to 6.0 microns, exclude super coarse mode dust particles), which is 45.7% smaller than the prior emissions of 1291 Tg/yr. Moreover, the retrieved total DD emissions show reduced emission amount from the prior values in every month, varying from 11.6% reduction in December to 68.5% in May. Figure 14 shows the comparison of the spatial distribution of seasonal DD emissions between the prior emissions (Figure 14a) and our retrievals (Figure 14b). As shown in Figure 14, the prior and the retrieved emissions show similar spatial and seasonal patterns; for example, the Bodélé Depression is the most active dust source area in DJF and SON and the Arabian Desert becomes active in MAM and JJA. One major discrepancy between the model and the retrieval is that the model has a much stronger DD sources over Algeria and Morocco in MAM and JJA, which is even stronger than the Bodélé Depression and the Arabian Desert. However, the retrieval still shows the dust emissions there, while the strength reduces a factor of 5-6.

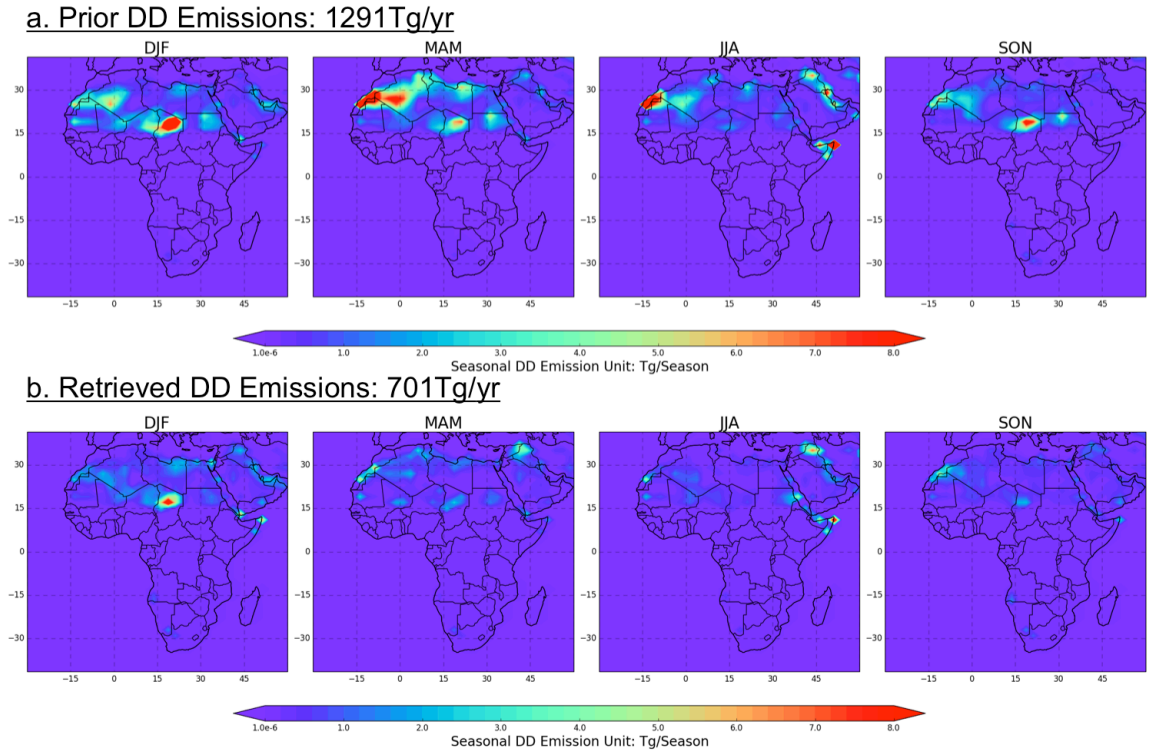

Figure 14. Spatial distribution of seasonal desert dust aerosol emission: (a) "prior model" DD emissions from DEAD model and (b) retrieved DD emissions.

4.3.2 BC emissions

As mentioned earlier, we considered two cases of BC aerosol refractive index to perform the retrieval (Case 1: m=1.75-0.45i; Case 2: m=1.95-0.79i), since the retrieved total BC emissions is very sensitive to the BC refractive index (our sensitivity test shows a factor of ~1.8 differences between Case 1 and Case 2, see section 3.2.4). Figure 13 shows the retrievals increase BC emissions for every month from the prior emissions by factors ranging from 5.9 in March to 14.4 in November with an annual averaged increase of a factor of ~8 in Case 1. For Case 2, the retrieved BC emissions have similar monthly variation as in Case 1 with a smaller magnitude of increase from the prior emissions, from a factor of 3.3 in March to 4.7 in November with an annual averaged increase of ~3.

The spatial comparison of seasonal BC emission is summarized in Figure 15. We plot model prior BC emission from GFED3 and Bond anthropogenic inventories in Figure 15a, retrieved BC emissions from Case 1 in Figure 15b, and Case 2 retrieved BC emissions in Figure 15c. Note that the color bar range in Figure 15b is 2.5 times larger than that of Figure 15a and Figure 15c. Not surprisingly, the patterns of model prior emission in Case 1 and Case 2 retrievals are similar, with the highest BC emission source areas located in biomass burning regions, such as Central Africa during DJF and Southern Africa JJA. The large increases in the BC emissions in the retrieval relative to the prior suggests that the current model

simulated AAOD is much too low, which is consistent with the PARASOL/GRASP observations in Section 4.2. Retrieval Case 2 shows a large increase over the Arabian Peninsula, indicating there is an emission ~5 times higher than the prior model in DJF, MAM and SON, where the latter shows only a small amount of carbonaceous fine particles. AERONET ground-based measurements indicate a moderate absorption phenomenon there (Seasonal AAOD at 550 nm about ~0.05, see Figure 21), which corroborates the retrieved values from the inversion.

4.3.3 OC emissions

The annual total OC emissions in Figure 13 shows that the retrieved annual OC emissions are higher than the prior model by a factor of ~2, with a minimum monthly increase found in March (1.54) and a maximum in May (5.71). Combined with BC emission, the retrieved total carbonaceous aerosol emissions are 52.8 Tg/yr (with Case 1 BC) and 44.0 Tg/yr (with Case 2 BC), which is 271.8% (Case 1) to 209.8% (Case 2) higher than prior model (14.2 Tg/yr). We compare the seasonal distribution of prior OC emissions with retrieved emissions in Figure 16. Both the retrieved and prior emissions have highest OC emissions in Southern Africa in JJA and in Central Africa in DJF.

4.3.4. Summary of retrieved emissions

Comparison of retrieved DD, BC and OC aerosol emissions over the study area with the GEOS-Chem prior model emission inventories show basically a consistent of spatial and temporal variation. However, the significant differences are in the emission strength. The PARASOL/GRASP based retrieval reduces the GEOS-Chem annual DD emission to 701 Tg/yr over the study area. A recent study by Escribano et al. (2017) estimated that the mineral dust flux for particle size less than 6.0 microns over northern Africa and the Arabian Peninsula is between 630 and 845 Tg/yr. Some other studies also show similar dust emission flux over Africa (Werner et al., 2002; Miller et al., 2004; Escribano et al., 2016, 2017). However, the overestimation of the prior model dust emission could also result from errors in particle size distribution, which is shown to biased toward smaller particle sizes compared to the observation in the atmosphere (Kok et al., 2017). Meanwhile, the retrieval increases the model annual carbonaceous aerosol emission by about 2.5 times. This value is close to the recommendation given in Bond et al. (2013) that increasing global BC absorption by a factor of 3 to fit the observation of columnar aerosol absorption. Kaiser et al. (2012) also recommend correcting the carbonaceous aerosol emission (GFED3) with a factor 3.4 when using them in the global aerosol forecasting system. In addition, there are many other efforts to improve the simulation of AAOD, e.g. treating hydrophilic BC as an internal aerosol core with other soluble hygroscopic aerosol species (Wang et al., 2016); including the light absorbing brown carbon in the simulation (Wang et al., 2014b). These studies are all crucial to improve current CTMs aerosol simulation, which should be adopted in our aerosol emission inversion framework in the future.

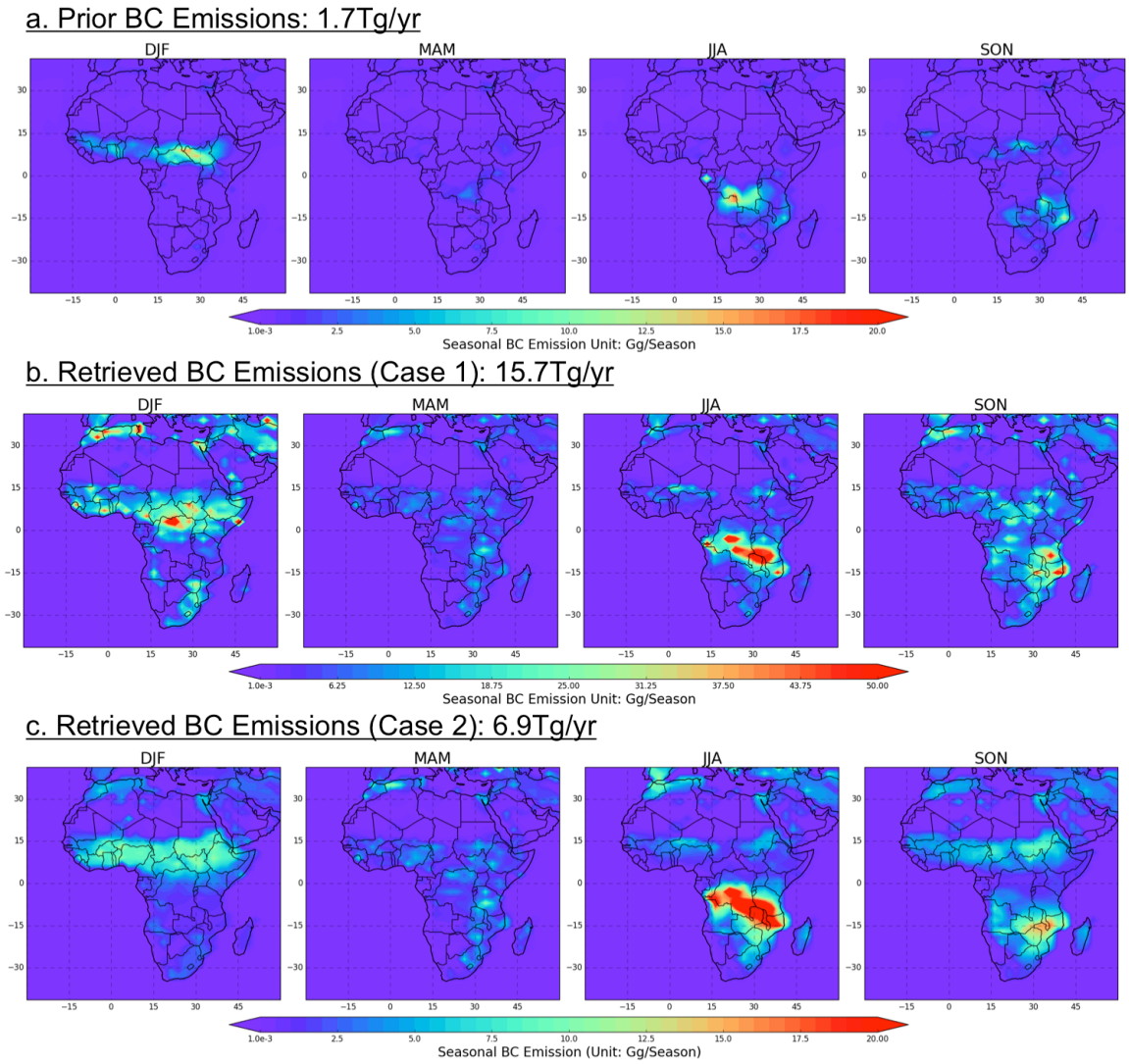

Figure 15. Spatial distribution of seasonal BC emissions: (a) prior model BC emissions from GFED3 and Bond inventories; (b) Case 1 retrieved BC emissions; (c) Case 2 retrieved BC emissions. Note that the color scale for (b) is different from (a) and (c) for better resolving the spatial contrasts.

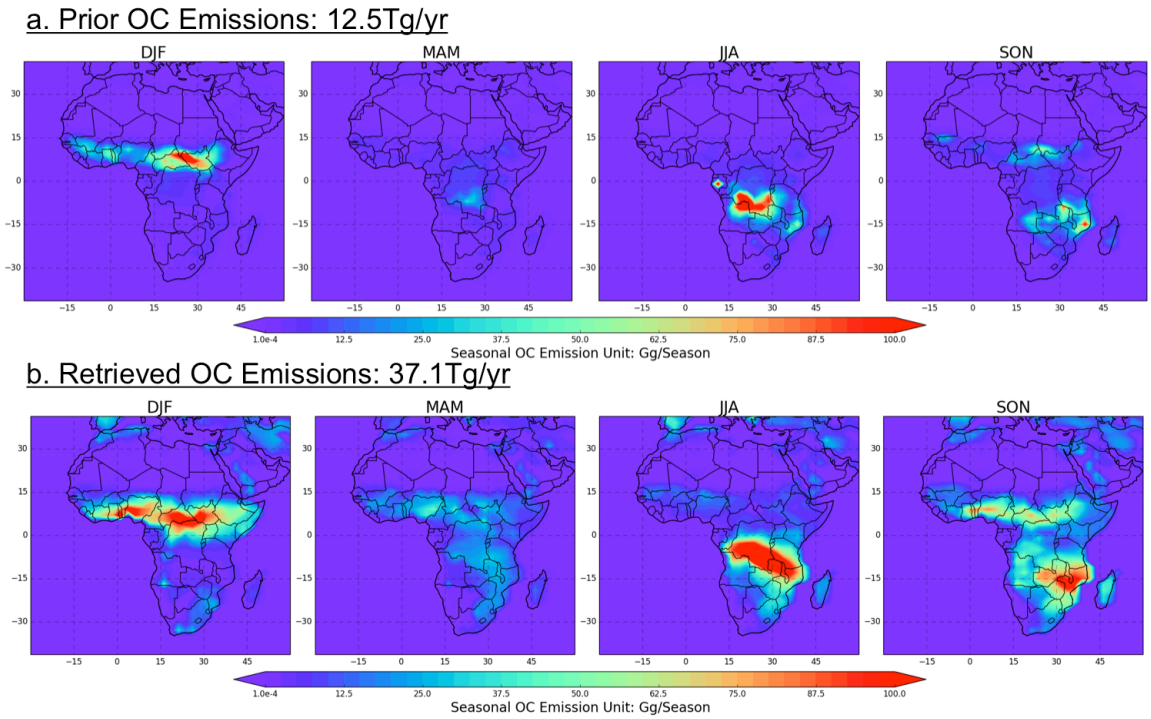

Figure 16. Spatial distribution of seasonal OC emissions: (a) prior model OC emissions using GFED3 and Bond inventories and (b) retrieved OC emissions.

5 Evaluation

5.1 Evaluation with AERONET

In order to objectively evaluate our retrieved aerosol emissions based on PARASOL/GRASP spectral AOD and AAOD, we made a series of evaluations using independent datasets and models not used by our inversion. First, the posterior simulated one-year AOD and AAOD (using Case 1 BC emission) are compared with the sun photometer measured AOD and AAOD at 28 AERONET sites (shown in Figure 1).

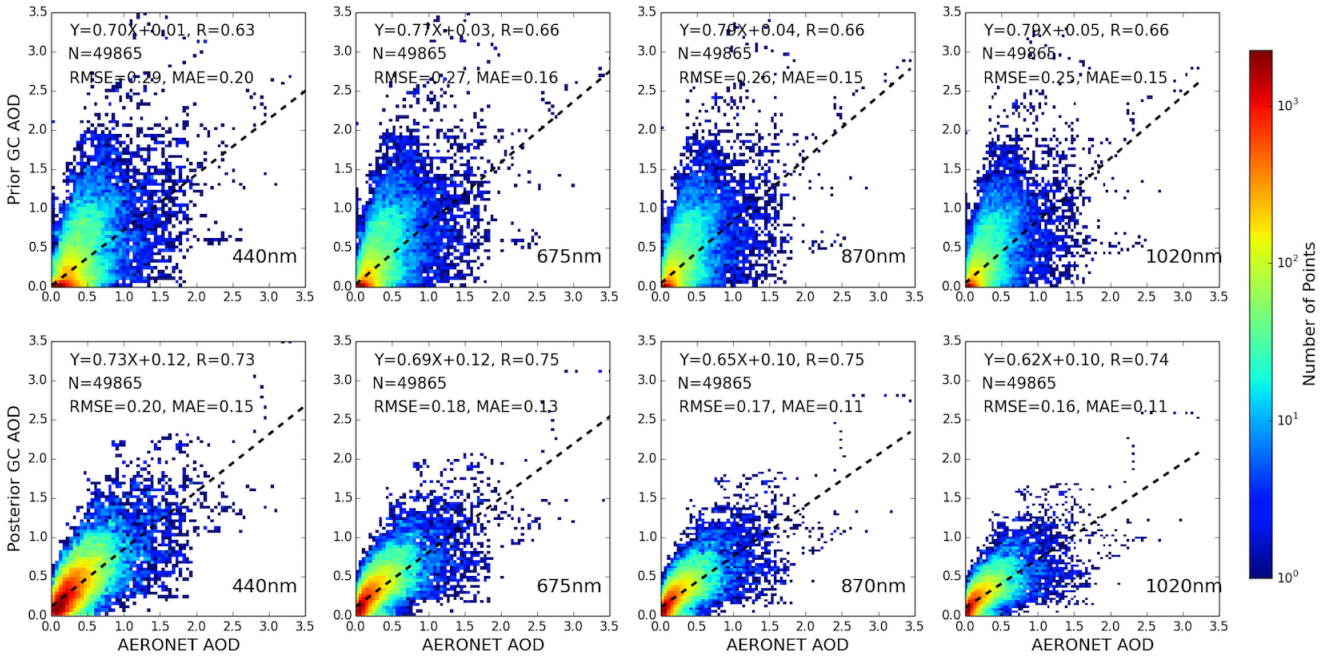

Figure 17. Density scatter plots of one-year GEOS-Chem simulated AOD using the prior emissions (top row) or the posterior emissions (bottom row) versus AERONET measured AOD at 440, 675, 870 and 1020 nm at 28 sites. The AOD data were aggregated into 80 bins on the both x- and y- directions spanning the range from 0.0 to 3.5 for AOD at four wavelengths. The number of matched pairs (N), correlation coefficient (R), root mean square error (RMSE) and mean absolute error (MAE) are shown on each panel.

Figure 17 and 18 show the comparison of GEOS-Chem simulations using prior and posterior emissions with AERONET measurements of AOD and AAOD, respectively. The evaluation was conducted at 4 wavelengths (440, 675, 870 and 1020 nm) and GEOS-Chem hourly spectral AOD and AAOD are interpolated based on the Ångström exponent. AERONET AOD and AAOD averaged ±30 minutes centered by model output time are used to compare with the model simulations over the grid box containing the AERONET sites. Density scatter plots of 49,865 matched pairs of AOD are shown in Figure 17. The correlation coefficients between GEOS-Chem simulations with prior emissions and AERONET data (shown in upper four panels) are 0.62, 0.67, 0.66 and 0.66 for the four wavelengths respectively, and the corresponding root mean square errors are 0.28, 0.25, 0.24 and 0.24. Yet, the correlation coefficients are increased to 0.73, 0.75, 0.75 and 0.74 when the posterior emissions are used in GEOS-Chem simulation (shown in lower four panels), and meanwhile the root mean square errors are decreased to 0.20, 0.18 0.17 and 0.16, respectively. Meanwhile, the mean absolute errors are also decreased from prior (0.20, 0.16, 0.15 and 0.15) to posterior (0.15, 0.13, 0.11 and 0.11).

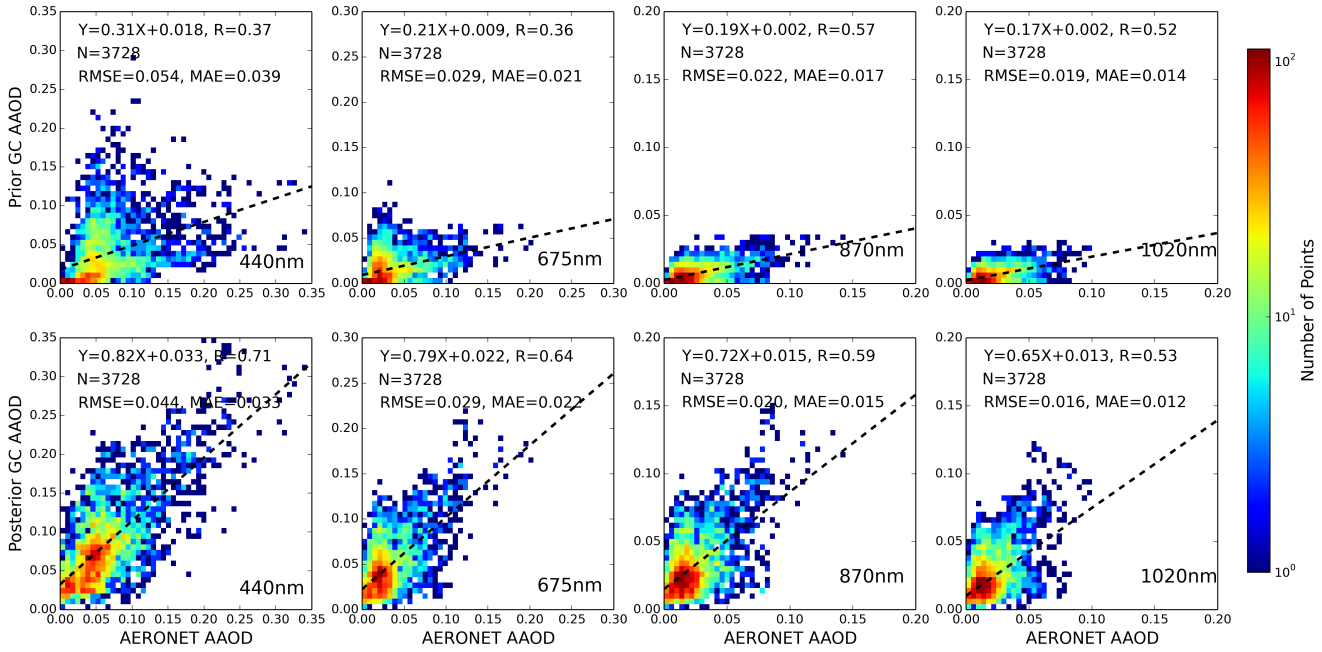

Figure 18. Same as Figure 17, but for AAOD. The AAOD data were aggregated into 50 bins on the both x- and y- directions spanning the range from 0.0 to 0.35 for AAOD at 440 nm; 0.0 to 0.3 at 675 nm; 0.0 to 0.2 at 870 and 1020 nm.

Figure 18 shows the density scatter plots comparisons for AAOD. However, unlike sun direct measurement of AOD, AERONET AAOD is inverted from almucantar measurements. To select sufficiently accurate retrievals, we applied standard quality-screening criteria (e.g. Dubovik et al., (2002b) and Holben et al., (2006)). Therefore, there are fewer AERONET AAOD that matched with GEOS-Chem simulations than for AOD. The number of matched pairs is 3,728. The low slope of the linear regression between prior model AAOD and AERONET (shown in upper four panels) indicates that the prior model significantly underestimates AAOD. The posterior GEOS-Chem simulations using retrieved emissions (shown in the lower four panels) shows the improvements validating with AERONET, with the correlation coefficients come to 0.71, 0.64, 0.59 and 0.53. In addition, the root mean square errors are also improved for posterior simulations.

Comparison between time series of AOD and AAOD at 440 nm from AERONET, PARASOL/GRASP, and prior and posterior GEOS-Chem simulations from December 2007 to November 2008 are made in two AERONET sites (Mongu and Ilorin), and the results are shown in Figure 19. The geo-locations of these two sites are already apparent in Figure 1. Ilorin is located close to the active dust sources in the Northern Africa, where are also influenced by seasonal biomass burning events, especially from November to February. Mongu is located close to the Southern Africa seasonal biomass burning sources. The posterior simulations better capture the time series variations and magnitude of AOD and AAOD from AERONET measurements. For example, in Mongu, the prior simulation underestimates AOD and AAOD significantly. In September, the underestimations are about 3 times (a bias of -0.56 for monthly average) for AOD and 4 times for AAOD (a bias -0.09).

Such bias is significantly reduced to -0.22 for AOD and +0.01 for AAOD in posterior simulation with retrieved emissions. In terms of correlation coefficients, the prior GEOS-Chem simulation shows a solid correlation with measurements in Mongu, while the slope of the linear regression (K) between prior simulation and AERONET (0.24 for AOD; 0.22 for AAOD) indicates that the model significantly underestimates the aerosol loading in Mongu. Furthermore, prior GEOS-Chem simulation can capture the variation and magnitude of AOD (R=0.79 and K=0.79) in Ilorin. However, for AAOD, the simulation shows underestimation with slope K=0.40, which is an indicator of the model underestimation of the aerosol absorption species, such as BC. Overall, the posterior GEOS-Chem simulation with retrieved emissions can better capture the time serial variation and magnitude of AOD and AAOD in both Mongu and Ilorin.

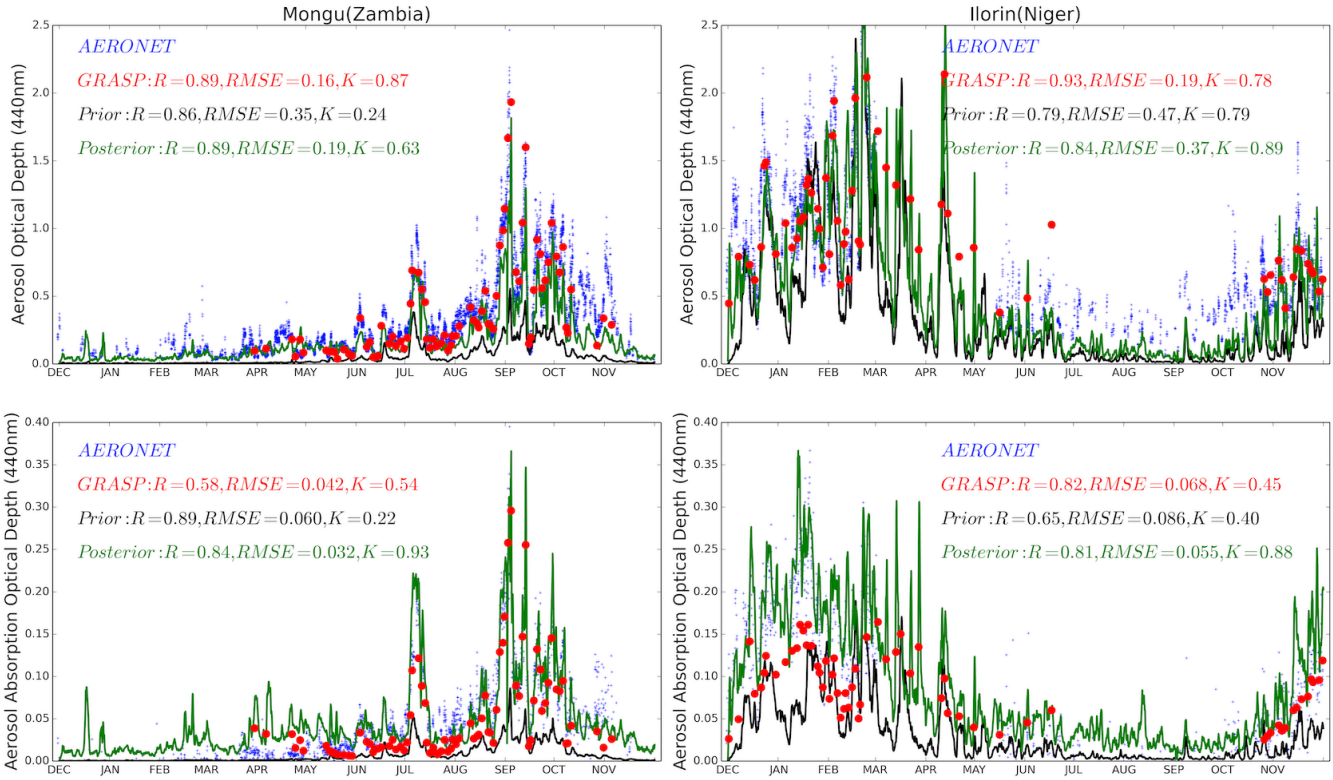

Figure 19. Time serial AOD (upper panel) and AAOD (lower panel) from AERONET (blue crosses), PARASOL/GRASP (red circles), prior GEOS-Chem (black line) and posterior (green line) GEOS-Chem simulations at 2 sites (Mongu and Ilorin). The error statistics parameters between PARASPOL/GRASP, prior and posterior GEOS-Chem simulations with AERONET are also shown in the figure.

5.2 Testing retrieved emission in the GEOS-5/GOCART model

All the evaluations considered thus far are ~~a~~ based on simulations in the GEOS-Chem model. To evaluate how such results may be impacted by model biases owing to factors other than BC, OC and DD emissions, here we ask - can aerosol

emissions retrieved from the GEOS-Chem based inversion improve the aerosol simulation for another chemical transport model? To investigate this, we implement our PARASOL/GRASP based aerosol emission database into the GEOS-5/GOCART model (Chin et al., 2002, 2009, 2014; Colarco et al., 2010). The prior and posterior GEOS-5/GOCART model simulated seasonal AOD are compared with MODIS observations in Figure 20. GEOS-5/GOCART uses similar meteorological fields as GEOS-Chem, with the prior anthropogenic emissions from the Hemispheric Transport of Atmospheric Pollution (HTAP) Phase 2, biomass burning emissions from the Fire Energetics and Emission Research (FEER) database (Ichoku and Ellison, 2014), dust emission calculated as a function of 10-m winds and surface characteristics (Ginoux et al., 2001), and volcanic emissions from OMI-based estimates (Carn et al., 2015). The PARASOL/GRASP retrieved DD, BC, and OC emissions over the study domain are used in the "posterior" simulations while other sources remain unchanged. On an annual average, the DD, BC, and OC posterior/prior emission ratios in the study area are 0.53, 5.3, and 1.2, respectively.

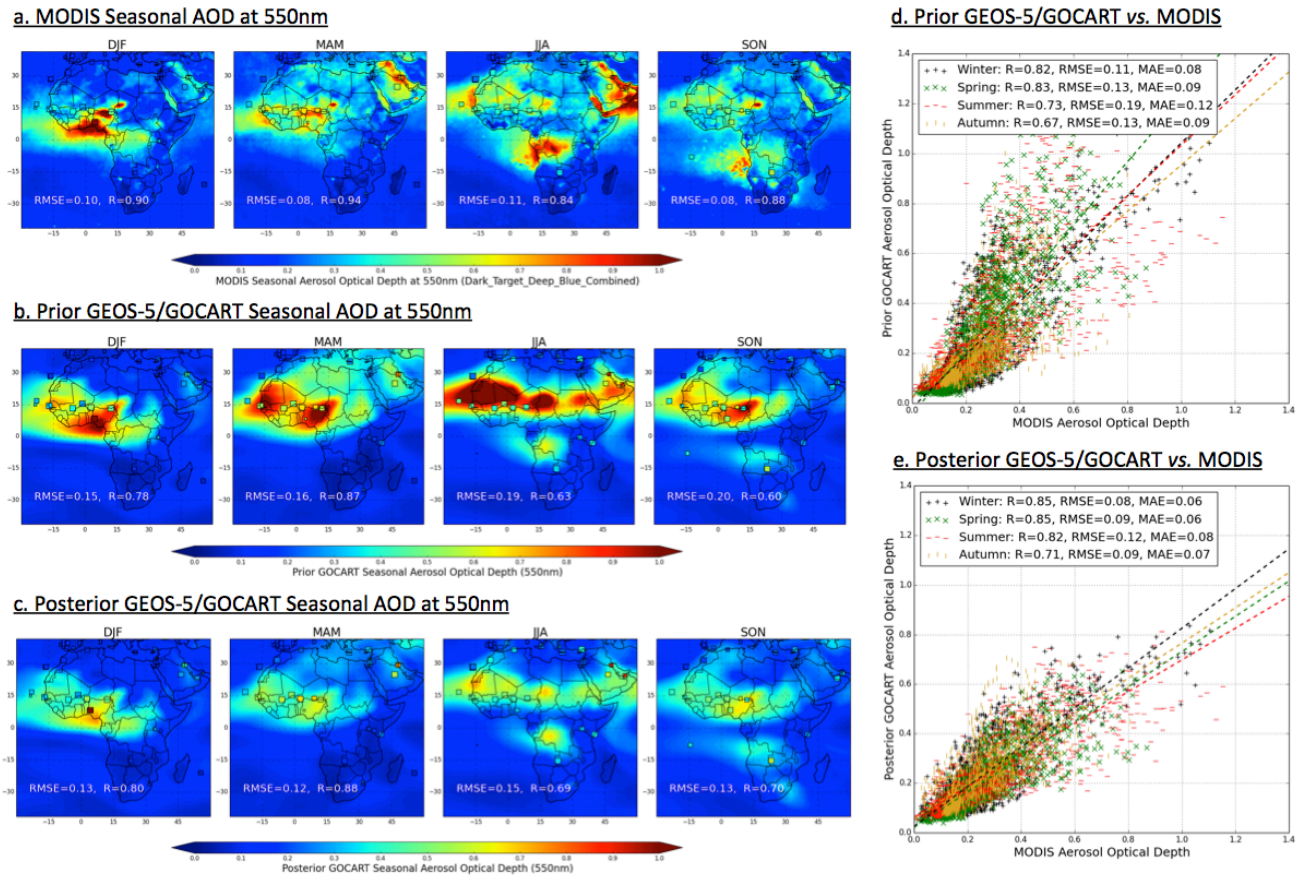

Figure 20. Comparison of the seasonal spatial distribution of prior (b) and posterior (c) GEOS-5/GOCART simulated AOD at 550 nm with MODIS observations (a). The scatter plots of grid-to-grid comparison between MODIS and prior GEOS-5/GOCART AOD (d) and posterior GEOS-5/GOCART AOD (e) are also shown. The ground-based measurements from

AERONET (squares) are over plotted over figures a-c. The MODIS and GEOS-5/GOCART versus AERONET correlation coefficient (R) and root mean square error (RMSE) are provided in figures a-c. Meanwhile, the GEOS-5/GOCART versus MODIS R, RMSE and MAE are also provided in figures (d-e).

Figure 20a shows the MODIS seasonal AOD at 550 nm. In order to have better spatial coverage, we take MODIS collection 6 combined dark target and deep blue AOD products at the spatial resolution of 1° x 1° (Hsu et al., 2004; Levy et al., 2013). Figure 20b presents prior GEOS-5/GOCART simulated seasonal AOD, and Figure 20c shows the posterior GEOS-5/GOCART simulation from our retrieved emissions (using Case 2 BC emission). In Figure 20d and 20e, we plot the grid-to-grid comparison between GEOS-5/GOCART prior and GEOS-5/GOCART posterior AOD with MODIS respectively; here the different colors represent different seasons. In order to carry out this grid-to-grid comparison, MODIS 1° x 1° AOD is re-gridded to the resolution 2.0° x 2.5°. The prior GEOS-5/GOCART simulate optical depth is comparable to MODIS observations with similar spatial pattern and correlation coefficient with MODIS R=~0.75 over a year. In addition, the simulation is better in DJF and MAM than in JJA and SON. The correlation coefficient with MODIS is about 0.82 and the root mean square error is about 0.12 in DJF and MAM, and it has a relatively low correlation in JJA and SON (~0.7); meanwhile the RMSE becomes high (~0.16). The prior GEOS-5/GOCART simulation somewhat overestimated observations over the Northern Africa dust region over 4 seasons, while it is underestimated in the southern Africa biomass burning area, especially in biomass burning seasons (JJA and SON), which can also be inferred from the validation with AERONET measurements (squares) over plotted in Figure 20a-c. With the posterior emissions, the GEOS-5/GOCART simulation shows improvements compared with AERONET and MODIS observations, with higher correlation coefficient and lower root mean square error in all 4 seasons than the prior GEOS-5/GOCART simulation. The posterior GEOS-5/GOCART simulated AOD is a little lower than MODIS on average 13% (Normalized Mean Bias, NMB=-13%, NMB=$\sum(M_i - O_i)/\sum O_i$, where sums are over the ensemble of all data i, and M_i and O_i are the modeled and observed values), likely associated with that the MODIS AOD is observed at noon, however the GEOS-5/GOCART AOD is average over 24 hours during a day.

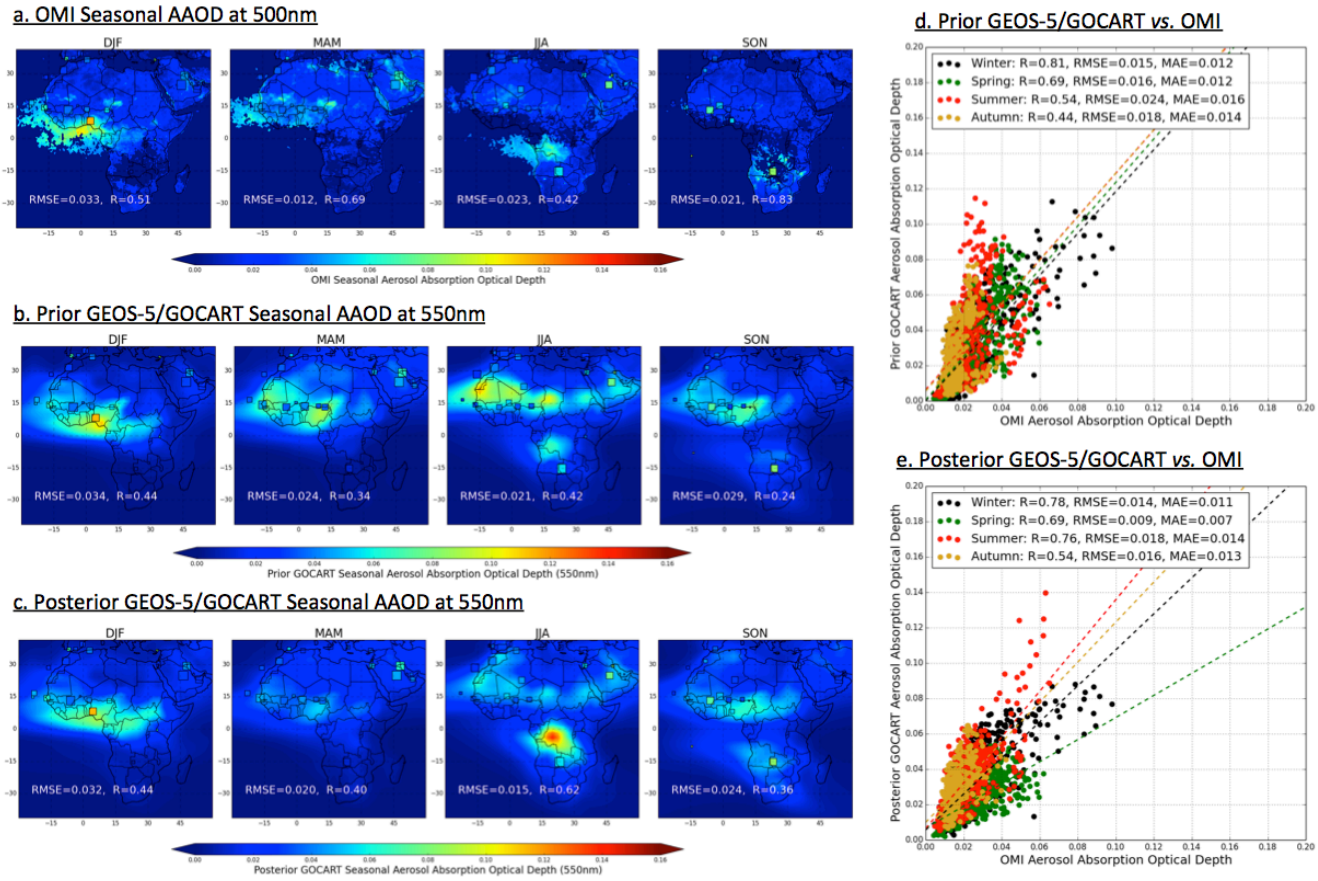

Figure 21. Comparison of the seasonal spatial distribution of prior (b) and posterior (c) GEOS-5/GOCART simulated AAOD at 550 nm with OMI observations (a). The scatter plots of grid-to-grid comparison between OMI and prior GEOS-5/GOCART AAOD (d) and posterior GEOS-5/GOCART AAOD (e) are also shown. The ground-based measurements from AERONET (squares) are plotted over figures a-c. The correlation coefficient (R) and root mean square error (RMSE) versus AERONET are provided in figures (a-c). Meanwhile, the GEOS-5/GOCART versus OMI R, RMSE and MAE are also provided in figures (d-e).

Commonly, ~~Because only~~ the ultraviolet, ~~and~~ shortwave visible channels and polarimeter measurements are considered as main observation types sensitive to aerosol absorption properties, therefore, AERONET, PARASOL/GRASP and OMI data sets are often used as major long-term records of AAOD. ~~are limited to AERONET, PARASOL/GRASP and OMI.~~ We use the latest OMI aerosol products (OMAERUV version 1.7.4) (Torres et al., 2007, 2013) to evaluate the GEOS-5/GOCART model simulated AAOD from prior aerosol emission inventories and our retrieved aerosol emission database. Meanwhile, collocated AERONET data over the study area are also employed to the evaluation. Detailed assessments of OMI aerosol products are described in other studies (Torres et al., 2013; Ahn et al., 2014; Jethva et al., 2014). Figure 21

shows the validation results. Figure 21a presents the OMI seasonal mean AAOD with original OMAERUV version 1.7.4 spatial resolution 0.5° x 0.5°. We plot grid-to-grid comparison between OMI and GEOS-5/GOCART AAOD in Figure 21d-e, here OMI AAOD are re-scaled to the same resolution with model simulation 2.0° x 2.5°. Any 2.0° x 2.5° grid box with less than 10 OMI original AAODs (~50% coverage) for averaging is abandoned. This evaluation highlights the following major findings:

1. The major discrepancy between OMI seasonal AAOD (Figure 21a) and the prior GEOS-5/GOCART simulated AAOD is that the simulated AAOD is higher than OMI values in the Northern Africa dust regions over all seasons, which can be attributed to the overestimation of dust particle absorption (Chin et al., 2009) and/or the total dust emissions. The posterior GEOS-5/GOCART simulated AAOD shows a similar spatial distribution and magnitude as OMI values over dust regions with reduced differences, although the model is still overall higher than OMI especially over the Southern Africa biomass regions in JJA.
2. As shown in Figure 21a, the correlation coefficients of OMI seasonal AAOD with AERONET vary from 0.42 in JJA to 0.83 in SON, meanwhile the root mean square error is smallest in MAM ~0.012 and largest in DJF ~0.033. Preliminary evaluations shows posterior GEOS-5/GOCART simulated seasonal AAOD (Figure 21c) have a slightly better correlation with AERONET than prior GEOS-5/GOCART simulation (Figure 21b) -- the mean correlation coefficient over entire year improves from ~0.36 to ~0.46 and the mean RMSE decreases from ~0.027 to ~0.023.
3. From the scatter plot of GEOS-5/GOCART simulated AAOD versus OMI AAOD in Figure 21d-e, the significant increase of correlation coefficient from prior to posterior simulations occurs in June-July-August (Prior: 0.54; Posterior: 0.76) as well as decreases of RMSE and MAE (Prior: RMSE=0.024, MAE=0.016; Posterior: RMSE=0.018, MAE=0.014), suggesting the reliability of posterior aerosol emission at high biomass burning aerosol loading season.

6 Conclusions

In this study, we designed a method to retrieve BC, OC and DD aerosol emissions simultaneously from satellite observed spectral AOD and AAOD based on the PARASOL/GRASP retrievals and the adjoint of GEOS-Chem chemical transport model. This method uses prior BC, OC and DD emissions as weak constraints in the inversion by initializing the retrieval with prior emissions added to uniform background values. A series of numerical tests were performed which show this assumption can provide a better fit to observations, meanwhile it allows the retrieval to produce rather good results even if *a priori* knowledge of emissions is poor. Admittedly, the satellite observations are sparse due to several factors, e.g., the clear-sky condition, global coverage orbit cycle. Nevertheless, the PARASOL 6 wavelengths AOD and AAOD from GRASP algorithm are shown to be sufficient to characterize the distribution and magnitude of BC, OC and DD aerosol emissions simultaneously under the assumption of DD emissions correction constant over 24h and 4 days correction constant carbonaceous aerosol emissions. The inversion test of synthetic PARASOL-like measurements results in about 25.8%

uncertainty for daily total DD emission, 5.9% for daily total BC emission and 26.9% for daily total OC emissions. In addition, it was shown that using two different assumptions for BC refractive index (Case 1: m=1.75-0.45i; Case 2: 1.95-0.79i) could lead to an additional factor of 1.8 differences in total BC emissions.

We evaluated the GRASP retrieved one-year PARASOL spectral AOD and AAOD with AERONET ground-based observations/retrievals at 28 sites across the study area (30°W-60°E, 40°S-40°N). Good agreements were found even using rescaling of the retrievals to the spatial resolution of 2.0° x 2.5°. Derimian et al. (2016) and Popp et al. (2016) show similar validation results of PARASOL/GRASP with AERONET. Therefore, we used PARASOL/GRASP retrieved spectral AOD and AAOD to optimize BC, OC and DD aerosol emissions in a year (December 2007 to November 2008) over the study area with horizontal resolution of 2.0° x 2.5° in order to match the adjoint GEOS-Chem spatial resolution. The retrieved emissions ~~are publically available at http://csuchencheng.wixsite.com/chencheng/research-blog; this dataset~~ will be publically available soon at the GEOS-Chem inventory findings website (http://wiki.seas.harvard.edu/geos-chem/index.php/Inventory_Findings).

Our analysis of the retrieved aerosol emissions indicates that the prior GEOS-Chem model overestimates annual desert dust aerosol emissions by a factor of about 1.8 (with the DEAD scheme) over the study area, similar to other previous modeling studies (Huneeus et al., 2012; Johnson et al., 2012; Ridley et al., 2012, 2016). The retrieved annual BC and OC emissions show a consistent seasonal variation with emission inventories (GFED3 for biomass burning and Bond for anthropogenic fossil fuel and biofuel combustions). However, we find these BC and OC emissions to have broad underestimations throughout the study area. For example, emissions from the emission inventories for BC are significant lower than our retrieved values up to factor of 8 ~~823.5%~~ (Case 1) and 3 ~~305.9%~~ (Case 2), and for OC they are about factor of 2 lower ~~196.8% lower~~. These results are reflected in the model bias of AOD and AAOD from the prior GEOS-Chem simulation, e.g. significant low bias over the biomass burning regions and high bias over the Sahara desert. Underestimation of BC and OC emissions in chemical transport models have been suggested previously (Sato et al., 2003; Zhang et al., 2015). However, we cannot rule-out the possibility that differences between model and observations could also be attributed to the errors in removal processes and aerosol microphysical properties, in addition to the deficiencies in emissions (Bond et al., 2013). Nevertheless, the fidelity of our results is confirmed by comparison of posterior simulations with measurements from AERONET that are completely independent from and more temporally frequent than PARASOL observations. Specifically, to analyze the PARASOL/GRASP based aerosol emission database further, we implemented these emissions in the GEOS-5/GOCART model and compared the resulting simulations of AOD and AAOD with independent MODIS and OMI observations. The comparisons show better agreements between model and observations with the posterior GEOS-5/GOCART results (lower biases and higher correlation coefficients) than prior simulations. In the future, we plan to apply our approach globally to longer records of observations to further investigate the inter-annual variability of aerosol emissions on global scales, and to test our retrieved emission database in other models.

Data availability. PARASOL/GRASP aerosol data are available from ICARE data distribution portal: http://www.icare.univ-lille1.fr/. The retrieved BC_V1, BC_V2, OC and DD emissions over study area can be requested directly from the lead author (cheng1.chen@ed.univ-lille1.fr).

Acknowledgments

This work is supported by the Laboratory of Excellence CaPPA – Chemical and Physical Properties of the Atmosphere – project, which is funded by the French National Research Agency (ANR). We would like to thank the GEOS-Chem and adjoint GEOS-Chem model developers; DKH recognizes support from NASA ACMAP NNX17AF63G. We also thank the entire AERONET team, and especially the principal investigators and site mangers of the 28 AERONET stations that we acquired data from. The authors are also grateful for the MODIS and OMI aerosol team (O. Torres and H. Jethva) for providing the data used in this investigation, and Huisheng Bian and Tom Kucsera for incorporating the PARASOL/GRASP emissions into the GEOS-5 model and provide the GEOS-5/GOCART simulation results.

References

Ahn, C., Torres, O. and Jethva, H.: Assessment of OMI near-UV aerosol optical depth over land, J. Geophys. Res. Atmos., 119(5), 2457–2473, doi:10.1002/2013JD020188, 2014.

Arola, A., Schuster, G., Myhre, G., Kazadzis, S., Dey, S. and Tripathi, S. N.: Inferring absorbing organic carbon content from AERONET data, Atmos. Chem. Phys., 11(1), 215–225, doi:10.5194/acp-11-215-2011, 2011.

Balkanski, Y. J., Jacob, D. J., Gardner, G. M., Graustein, W. C. and Turekian, K. K.: Transport and residence times of tropospheric aerosols inferred from a global three-dimensional simulation of 210 Pb, J. Geophys. Res., 98(D11), 20573–20586, doi:10.1029/93JD02456, 1993.

Bennett A.F., Inverse Modeling of the Ocean and Atmosphere, Cambirge University Press, 220 p. 2002.

Bellouin, N., Boucher, O., Haywood, J. and Reddy, M. S.: Global estimate of aerosol direct radiative forcing from satellite measurements, Nature, 438(7071), 1138–1141, doi:10.1038/nature04348, 2005.

Bessagnet, B., Hodzic, A., Vautard, R., Beekmann, M., Cheinet, S., Honoré, C., Liousse, C. and Rouil, L.: Aerosol modeling with CHIMERE—preliminary evaluation at the continental scale, Atmos. Environ., 38(18), 2803–2817, doi:10.1016/j.atmosenv.2004.02.034, 2004.

Bey, I., Jacob, D. J., Yantosca, R. M., Logan, J. A., Field, B. D., Fiore, A. M., Li, Q., Liu, H. Y., Mickley, L. J. and Schultz, M. G.: Global modeling of tropospheric chemistry with assimilated meteorology: Model description and evaluation, J. Geophys. Res. Atmos., 106(D19), 23073–23095, doi:10.1029/2001JD000807, 2001.

Bond, T. C. and Bergstrom, R. W.: Light Absorption by Carbonaceous Particles: An Investigative Review, Aerosol Sci. Technol., 40(1), 27–67, doi:10.1080/02786820500421521, 2006.

Bond, T. C., Streets, D. G., Yarber, K. F., Nelson, S. M., Woo, J. and Klimont, Z.: A technology-based global inventory of black and organic carbon emissions from combustion, J. Geophys. Res., 109(D14), D14203, doi:10.1029/2003JD003697, 2004.

Bond, T. C., Bhardwaj, E., Dong, R., Jogani, R., Jung, S., Roden, C., Streets, D. G. and Trautmann, N. M.: Historical emissions of black and organic carbon aerosol from energy-related combustion, 1850-2000, Global Biogeochem. Cycles, 21(2), GB2018, doi:10.1029/2006GB002840, 2007.

Bond, T. C., Doherty, S. J., Fahey, D. W., Forster, P. M., Berntsen, T., DeAngelo, B. J., Flanner, M. G., Ghan, S., Kärcher, B., Koch, D., Kinne, S., Kondo, Y., Quinn, P. K., Sarofim, M. C., Schultz, M. G., Schulz, M., Venkataraman, C., Zhang, H., Zhang, S., Bellouin, N., Guttikunda, S. K., Hopke, P. K., Jacobson, M. Z., Kaiser, J. W., Klimont, Z., Lohmann, U., Schwarz, J. P., Shindell, D., Storelvmo, T., Warren, S. G. and Zender, C. S.: Bounding the role of black carbon in the climate system: A scientific assessment, J. Geophys. Res. Atmos., 118(11), 5380–5552, doi:10.1002/jgrd.50171, 2013.

Byrd, R. H., Lu, P., Nocedal, J. and Zhu, C.: A Limited Memory Algorithm for Bound Constrained Optimization, SIAM J. Sci. Comput., 16(5), 1190–1208, doi:10.1137/0916069, 1995.

Carn, S. A., Yang, K., Prata, A. J. and Krotkov, N. A.: Extending the long-term record of volcanic SO2 emissions with the Ozone Mapping and Profiler Suite nadir mapper, Geophys. Res. Lett., 42(3), 925–932, doi:10.1002/2014GL062437, 2015.

Chin, M., Rood, R. B., Lin, S.-J., Müller, J.-F. and Thompson, A. M.: Atmospheric sulfur cycle simulated in the global model GOCART: Model description and global properties, J. Geophys. Res. Atmos., 105(D20), 24671–24687, doi:10.1029/2000JD900384, 2000.

Chin, M., Ginoux, P., Kinne, S., Torres, O., Holben, B. N., Duncan, B. N., Martin, R. V., Logan, J. A., Higurashi, A. and Nakajima, T.: Tropospheric Aerosol Optical Thickness from the GOCART Model and Comparisons with Satellite and Sun Photometer Measurements, J. Atmos. Sci., 59(3), 461–483, doi:10.1175/1520-0469(2002)059<0461:TAOTFT>2.0.CO;2, 2002.

Chin, M., Diehl, T., Ginoux, P. and Malm, W.: Intercontinental transport of pollution and dust aerosols: implications for regional air quality, Atmos. Chem. Phys., 7(21), 5501–5517, doi:10.5194/acp-7-5501-2007, 2007.

Chin, M., Diehl, T., Dubovik, O., Eck, T. F., Holben, B. N., Sinyuk, A. and Streets, D. G.: Light absorption by pollution, dust, and biomass burning aerosols: a global model study and evaluation with AERONET measurements, Ann. Geophys., 27(9), 3439–3464, doi:10.5194/angeo-27-3439-2009, 2009.

Chin, M., Diehl, T., Tan, Q., Prospero, J. M., Kahn, R. A., Remer, L. A., Yu, H., Sayer, A. M., Bian, H., Geogdzhayev, I. V., Holben, B. N., Howell, S. G., Huebert, B. J., Hsu, N. C., Kim, D., Kucsera, T. L., Levy, R. C., Mishchenko, M. I., Pan, X., Quinn, P. K., Schuster, G. L., Streets, D. G., Strode, S. A., Torres, O. and Zhao, X.-P.: Multi-decadal aerosol variations from 1980 to 2009: a perspective from observations and a global model, Atmos. Chem. Phys., 14(7), 3657–3690, doi:10.5194/acp-14-3657-2014, 2014.

Colarco, P., da Silva, A., Chin, M. and Diehl, T.: Online simulations of global aerosol distributions in the NASA GEOS-4 model and comparisons to satellite and ground-based aerosol optical depth, J. Geophys. Res., 115(D14), D14207, doi:10.1029/2009JD012820, 2010.

Dabberdt, W. F., Carroll, M. A., Baumgardner, D., Carmichael, G., Cohen, R., Dye, T., Ellis, J., Grell, G., Grimmond, S., Hanna, S., Irwin, J., Lamb, B., Madronich, S., McQueen, J., Meagher, J., Odman, T., Pleim, J., Schmid, H. P. and Westphal, D. L.: Meteorological Research Needs for Improved Air Quality Forecasting: Report of the 11th Prospectus Development Team of the U.S. Weather Research Program, Bull. Am. Meteorol. Soc., 85(4), 563–586, doi:10.1175/BAMS-85-4-563, 2004.

Derimian, Y., Dubovik, O., Huang, X., Lapyonok, T., Litvinov, P., Kostinski, A. B., Dubuisson, P. and Ducos, F.: Comprehensive tool for calculation of radiative fluxes: illustration of shortwave aerosol radiative effect sensitivities to the details in aerosol and underlying surface characteristics, Atmos. Chem. Phys., 16(9), 5763–5780, doi:10.5194/acp-16-5763-2016, 2016.

Drury, E., Jacob, D. J., Spurr, R. J. D., Wang, J., Shinozuka, Y., Anderson, B. E., Clarke, A. D., Dibb, J., McNaughton, C. and Weber, R.: Synthesis of satellite (MODIS), aircraft (ICARTT), and surface (IMPROVE, EPA-AQS, AERONET) aerosol observations over eastern North America to improve MODIS aerosol retrievals and constrain surface aerosol concentrations and sources, J. Geophys. Res., 115(D14), D14204, doi:10.1029/2009JD012629, 2010.

Dubovik, O.: Optimization of Numerical Inversion in Photopolarimetric Remote Sensing, in Photopolarimetry in Remote Sensing, pp. 65–106, Kluwer Academic Publishers, Dordrecht., 2004.

Dubovik, O. and King, M. D.: A flexible inversion algorithm for retrieval of aerosol optical properties from Sun and sky radiance measurements, J. Geophys. Res. Atmos., 105(D16), 20673–20696, doi:10.1029/2000JD900282, 2000.

Dubovik, O., Smirnov, A., Holben, B. N., King, M. D., Kaufman, Y. J., Eck, T. F. and Slutsker, I.: Accuracy assessments of aerosol optical properties retrieved from Aerosol Robotic Network (AERONET) Sun and sky radiance measurements, J. Geophys. Res. Atmos., 105(D8), 9791–9806, doi:10.1029/2000JD900040, 2000.

Dubovik, O., Holben, B. N., Lapyonok, T., Sinyuk, A., Mishchenko, M. I., Yang, P. and Slutsker, I.: Non-spherical aerosol retrieval method employing light scattering by spheroids, Geophys. Res. Lett., 29(10), 54-1-54–4, doi:10.1029/2001GL014506, 2002a.

Dubovik, O., Holben, B., Eck, T. F., Smirnov, A., Kaufman, Y. J., King, M. D., Tanré, D. and Slutsker, I.: Variability of Absorption and Optical Properties of Key Aerosol Types Observed in Worldwide Locations, J. Atmos. Sci., 59(3), 590–608, doi:10.1175/1520-0469(2002)059<0590:VOAAOP>2.0.CO;2, 2002b.

Dubovik, O., Sinyuk, A., Lapyonok, T., Holben, B. N., Mishchenko, M., Yang, P., Eck, T. F., Volten, H., Muñoz, O., Veihelmann, B., van der Zande, W. J., Leon, J.-F., Sorokin, M. and Slutsker, I.: Application of spheroid models to account for aerosol particle nonsphericity in remote sensing of desert dust, J. Geophys. Res., 111(D11), D11208, doi:10.1029/2005JD006619, 2006.

Dubovik, O., Lapyonok, T., Kaufman, Y. J., Chin, M., Ginoux, P., Kahn, R. A. and Sinyuk, A.: Retrieving global aerosol sources from satellites using inverse modeling, Atmos. Chem. Phys., 8(2), 209–250, doi:10.5194/acp-8-209-2008, 2008.

Dubovik, O., Herman, M., Holdak, A., Lapyonok, T., Tanré, D., Deuzé, J. L., Ducos, F., Sinyuk, A. and Lopatin, A.: Statistically optimized inversion algorithm for enhanced retrieval of aerosol properties from spectral multi-angle polarimetric satellite observations, Atmos. Meas. Tech., 4(5), 975–1018, doi:10.5194/amt-4-975-2011, 2011.

Dubovik, O., Lapyonok, T., Litvinov, P., Herman, M., Fuertes, D., Ducos, F., Torres, B., Derimian, Y., Huang, X., Lopatin, A., Chaikovsky, A., Aspetsberger, M. and Federspiel, C.: GRASP: a versatile algorithm for characterizing the atmosphere, SPIE Newsroom, doi:10.1117/2.1201408.005558, 2014.

Duncan, B. N., Martin, R. V., Staudt, A. C., Yevich, R. and Logan, J. A.: Interannual and seasonal variability of biomass burning emissions constrained by satellite observations, J. Geophys. Res., 108(D2), 4100, doi:10.1029/2002JD002378, 2003.

Ealo, M., Alastuey, A., Ripoll, A., Pérez, N., Cruz Minguillón, M., Querol, X. and Pandolfi, M.: Detection of Saharan dust and biomass burning events using near-real-time intensive aerosol optical properties in the north-western Mediterranean, Atmos. Chem. Phys, 16, 12567–12586, doi:10.5194/acp-16-12567-2016, 2016.

Eck, T. F., Holben, B. N., Reid, J. S., Dubovik, O., Smirnov, A., O'Neill, N. T., Slutsker, I. and Kinne, S.: Wavelength dependence of the optical depth of biomass burning, urban, and desert dust aerosols, J. Geophys. Res. Atmos., 104(D24), 31333–31349, doi:10.1029/1999JD900923, 1999.

Elbern, H., Schmidt, H. and Ebel, A.: Variational data assimilation for tropospheric chemistry modeling, J. Geophys. Res. Atmos., 102(D13), 15967–15985, doi:10.1029/97JD01213, 1997.

Elbern, H., Schmidt, H., Talagrand, O. and Ebel, A.: 4D-variational data assimilation with an adjoint air quality model for emission analysis, Environ. Model. Softw., 15(6), 539–548, doi:10.1016/S1364-8152(00)00049-9, 2000.

Elbern, H., Strunk, A., Schmidt, H. and Talagrand, O.: Emission rate and chemical state estimation by 4-dimensional variational inversion, Atmos. Chem. Phys., 7(14), 3749–3769, doi:10.5194/acp-7-3749-2007, 2007.

Engelstaedter, S., Tegen, I. and Washington, R.: North African dust emissions and transport, Earth-Science Rev., 79(1), 73–100, doi:10.1016/j.earscirev.2006.06.004, 2006.

Escribano, J., Boucher, O., Chevallier, F. and Huneeus, N.: Subregional inversion of North African dust sources, J. Geophys. Res. Atmos., 121(14), 8549–8566, doi:10.1002/2016JD025020, 2016.

Escribano, J., Boucher, O., Chevallier, F. and Huneeus, N.: Impact of the choice of the satellite aerosol optical depth product in a sub-regional dust emission inversion, Atmos. Chem. Phys., 17(11), 7111–7126, doi:10.5194/acp-17-7111-2017, 2017.

Fairlie, T. D., Jacob, D. J. and Park, R. J.: The impact of transpacific transport of mineral dust in the United States, Atmos. Environ., 41(6), 1251–1266, doi:10.1016/j.atmosenv.2006.09.048, 2007.

Fisher, M. and Lary, D. J.: Lagrangian four-dimensional variational data assimilation of chemical species, Q. J. R. Meteorol. Soc., 121(527), 1681–1704, doi:10.1002/qj.49712152709, 1995.

Generoso, S., Bréon, F.-M., Chevallier, F., Balkanski, Y., Schulz, M. and Bey, I.: Assimilation of POLDER aerosol optical thickness into the LMDz-INCA model: Implications for the Arctic aerosol burden, J. Geophys. Res., 112(D2), D02311, doi:10.1029/2005JD006954, 2007.

Geogdzhayev, I. V., Mishchenko, M. I., Rossow, W. B., Cairns, B. and Lacis, A. A.: Global Two-Channel AVHRR Retrievals of Aerosol Properties over the Ocean for the Period of NOAA-9 Observations and Preliminary Retrievals

Using NOAA-7 and NOAA-11 Data, J. Atmos. Sci., 59(3), 262–278, doi:10.1175/1520-0469(2002)059<0262:GTCARO>2.0.CO;2, 2002.

Ghan, S. J. and Schwartz, S. E.: Aerosol Properties and Processes: A Path from Field and Laboratory Measurements to Global Climate Models, Bull. Am. Meteorol. Soc., 88(7), 1059–1083, doi:10.1175/BAMS-88-7-1059, 2007.

Ginoux, P., Chin, M., Tegen, I., Prospero, J. M., Holben, B., Dubovik, O. and Lin, S.-J.: Sources and distributions of dust aerosols simulated with the GOCART model, J. Geophys. Res. Atmos., 106(D17), 20255–20273, doi:10.1029/2000JD000053, 2001.

Ginoux, P., Prospero, J. M., Gill, T. E., Hsu, N. C. and Zhao, M.: Global-scale attribution of anthropogenic and natural dust sources and their emission rates based on MODIS Deep Blue aerosol products, Rev. Geophys., 50(3), RG3005, doi:10.1029/2012RG000388, 2012.

Goloub, P., Tanré, D., Deuzé, J. L., Herman, M., Marchand, A. and Breon, F.-M.: Validation of the first algorithm applied for deriving the aerosol properties over the ocean using the POLDER/ADEOS measurements, IEEE Trans. Geosci. Remote Sens., 37(3), 1586–1596, doi:10.1109/36.763270, 1999.

Grell, G. A., Peckham, S. E., Schmitz, R., McKeen, S. A., Frost, G., Skamarock, W. C. and Eder, B.: Fully coupled "online" chemistry within the WRF model, Atmos. Environ., 39(37), 6957–6975, doi:10.1016/j.atmosenv.2005.04.027, 2005.

He, C., Li, Q., Liou, K.-N., Qi, L., Tao, S. and Schwarz, J. P.: Microphysics-based black carbon aging in a global CTM: constraints from HIPPO observations and implications for global black carbon budget, Atmos. Chem. Phys., 16(5), 3077–3098, doi:10.5194/acp-16-3077-2016, 2016.

Henze, D. K., Seinfeld, J. H., Liao, W., Sandu, A. and Carmichael, G. R.: Inverse modeling of aerosol dynamics: Condensational growth, J. Geophys. Res., 109(D14), D14201, doi:10.1029/2004JD004593, 2004.

Henze, D. K., Hakami, A. and Seinfeld, J. H.: Development of the adjoint of GEOS-Chem, Atmos. Chem. Phys., 7(9), 2413–2433, doi:10.5194/acp-7-2413-2007, 2007.

Henze, D. K., Seinfeld, J. H. and Shindell, D. T.: Inverse modeling and mapping US air quality influences of inorganic PM2.5 precursor emissions using the adjoint of GEOS-Chem, Atmos. Chem. Phys., 9(16), 5877–5903, doi:10.5194/acp-9-5877-2009, 2009.

Hess, M., Koepke, P. and Schult, I.: Optical Properties of Aerosols and Clouds: The Software Package OPAC, Bull. Am. Meteorol. Soc., 79(5), 831–844, doi:10.1175/1520-0477(1998)079<0831:OPOAAC>2.0.CO;2, 1998.

Highwood, E. J., Haywood, J. M., Silverstone, M. D., Newman, S. M. and Taylor, J. P.: Radiative properties and direct effect of Saharan dust measured by the C-130 aircraft during Saharan Dust Experiment (SHADE): 2. Terrestrial spectrum, J. Geophys. Res., 108(D18), 8578, doi:10.1029/2002JD002552, 2003.

Holben, B. N., Eck, T. F., Slutsker, I., Tanré, D., Buis, J. P., Setzer, A., Vermote, E., Reagan, J. A., Kaufman, Y. J., Nakajima, T., Lavenu, F., Jankowiak, I. and Smirnov, A.: AERONET—A Federated Instrument Network and Data Archive for Aerosol Characterization, Remote Sens. Environ., 66(1), 1–16, doi:10.1016/S0034-4257(98)00031-5, 1998.

Holben, B. N., Eck, T. F., Slutsker, I., Smirnov, A., Sinyuk, A., Schafer, J., Giles, D. and Dubovik, O.: Aeronet's Version 2.0 quality assurance criteria, vol. 6408, edited by S.-C. Tsay, T. Nakajima, R. P. Singh, and R. Sridharan, p. 64080Q, International Society for Optics and Photonics., 2006.

Hsu, N. C., Tsay, S.-C., King, M. D. and Herman, J. R.: Aerosol Properties Over Bright-Reflecting Source Regions, IEEE Trans. Geosci. Remote Sens., 42(3), 557–569, doi:10.1109/TGRS.2004.824067, 2004.

Huneeus, N., Boucher, O. and Chevallier, F.: Simplified aerosol modeling for variational data assimilation, Geosci. Model Dev., 2(2), 213–229, doi:10.5194/gmd-2-213-2009, 2009.

Huneeus, N., Schulz, M., Balkanski, Y., Griesfeller, J., Prospero, J., Kinne, S., Bauer, S., Boucher, O., Chin, M., Dentener, F., Diehl, T., Easter, R., Fillmore, D., Ghan, S., Ginoux, P., Grini, A., Horowitz, L., Koch, D., Krol, M. C., Landing, W., Liu, X., Mahowald, N., Miller, R., Morcrette, J. J., Myhre, G., Penner, J., Perlwitz, J., Stier, P., Takemura, T. and Zender, C. S.: Global dust model intercomparison in AeroCom phase i, Atmos. Chem. Phys., 11(15), 7781–7816, doi:10.5194/acp-11-7781-2011, 2011.

Huneeus, N., Chevallier, F. and Boucher, O.: Estimating aerosol emissions by assimilating observed aerosol optical depth in a global aerosol model, Atmos. Chem. Phys., 12(10), 4585–4606, doi:10.5194/acp-12-4585-2012, 2012.

Huneeus, N., Boucher, O. and Chevallier, F.: Atmospheric inversion of SO2 and primary aerosol emissions for the year 2010, Atmos. Chem. Phys., 13(13), 6555–6573, doi:10.5194/acp-13-6555-2013, 2013.

Ichoku, C. and Ellison, L.: Global top-down smoke-aerosol emissions estimation using satellite fire radiative power measurements, Atmos. Chem. Phys., 14(13), 6643–6667, doi:10.5194/acp-14-6643-2014, 2014.

Intergovernmental Panel on Climate Change (IPCC), Climate Change 2013: The Physical Science Basis, Cambridge Univ. Press, Cambridge, 2013.

Jaeglé, L., Quinn, P. K., Bates, T. S., Alexander, B. and Lin, J.-T.: Global distribution of sea salt aerosols: new constraints from in situ and remote sensing observations, Atmos. Chem. Phys., 11(7), 3137–3157, doi:10.5194/acp-11-3137-2011, 2011.

Jethva, H., Torres, O. and Ahn, C.: Global assessment of OMI aerosol single-scattering albedo using ground-based AERONET inversion, J. Geophys. Res. Atmos., 119(14), 9020–9040, doi:10.1002/2014JD021672, 2014.

Johnson, B. T., Haywood, J. M., Langridge, J. M., Darbyshire, E., Morgan, W. T., Szpek, K., Brooke, J. K., Marenco, F., Coe, H., Artaxo, P., Longo, K. M., Mulcahy, J. P., Mann, G. W., Dalvi, M. and Bellouin, N.: Evaluation of biomass burning aerosols in the HadGEM3 climate model with observations from the SAMBBA field campaign, Atmos. Chem. Phys., 16(22), 14657–14685, doi:10.5194/acp-16-14657-2016, 2016.

Johnson, M. S., Meskhidze, N. and Praju Kiliyanpilakkil, V.: A global comparison of GEOS-Chem-predicted and remotely-sensed mineral dust aerosol optical depth and extinction profiles, J. Adv. Model. Earth Syst., 4(3), M07001, doi:10.1029/2011MS000109, 2012.

Kahn, R. A., Nelson, D. L., Garay, M. J., Levy, R. C., Bull, M. A., Diner, D. J., Martonchik, J. V., Paradise, S. R., Hansen, E. G. and Remer, L. A.: MISR Aerosol Product Attributes and Statistical Comparisons With MODIS, IEEE Trans. Geosci. Remote Sens., 47(12), 4095–4114, doi:10.1109/TGRS.2009.2023115, 2009.

Kaiser, J. W., Heil, A., Andreae, M. O., Benedetti, A., Chubarova, N., Jones, L., Morcrette, J.-J., Razinger, M., Schultz, M. G., Suttie, M. and Van Der Werf, G. R.: Biomass burning emissions estimated with a global fire assimilation system based on observed fire radiative power, Biogeosciences, 9, 527–554, doi:10.5194/bg-9-527-2012, 2012.

Kaufman, Y. J., Tanré, D. and Boucher, O.: A satellite view of aerosols in the climate system, Nature, 419(6903), 215–223, doi:10.1038/nature01091, 2002.

King, M. D., Kaufman, Y. J., Tanré, D. and Nakajima, T.: Remote Sensing of Tropospheric Aerosols from Space: Past, Present, and Future, Bull. Am. Meteorol. Soc., 80(11), 2229–2259, doi:10.1175/1520-0477(1999)080<2229:RSOTAF>2.0.CO;2, 1999.

Kinne, S., Lohmann, U., Feichter, J., Schulz, M., Timmreck, C., Ghan, S., Easter, R., Chin, M., Ginoux, P., Takemura, T., Tegen, I., Koch, D., Herzog, M., Penner, J., Pitari, G., Holben, B., Eck, T., Smirnov, A., Dubovik, O., Slutsker, I., Tanré, D., Torres, O., Mishchenko, M., Geogdzhayev, I., Chu, D. A. and Kaufman, Y.: Monthly averages of aerosol properties: A global comparison among models, satellite data, and AERONET ground data, J. Geophys. Res., 108(D20), 4634, doi:10.1029/2001JD001253, 2003.

Kinne, S., Schulz, M., Textor, C., Guibert, S., Balkanski, Y., Bauer, S. E., Berntsen, T., Berglen, T. F., Boucher, O., Chin, M., Collins, W., Dentener, F., Diehl, T., Easter, R., Feichter, J., Fillmore, D., Ghan, S., Ginoux, P., Gong, S., Grini, A., Hendricks, J., Herzog, M., Horowitz, L., Isaksen, I., Iversen, T., Kirkevåg, A., Kloster, S., Koch, D., Kristjansson, J. E., Krol, M., Lauer, A., Lamarque, J. F., Lesins, G., Liu, X., Lohmann, U., Montanaro, V., Myhre, G., Penner, J., Pitari, G., Reddy, S., Seland, O., Stier, P., Takemura, T. and Tie, X.: An AeroCom initial assessment – optical properties in aerosol component modules of global models, Atmos. Chem. Phys., 6(7), 1815–1834, doi:10.5194/acp-6-1815-2006, 2006.

Koch, D., Schulz, M., Kinne, S., McNaughton, C., Spackman, J. R., Balkanski, Y., Bauer, S., Berntsen, T., Bond, T. C., Boucher, O., Chin, M., Clarke, A., De Luca, N., Dentener, F., Diehl, T., Dubovik, O., Easter, R., Fahey, D. W., Feichter, J., Fillmore, D., Freitag, S., Ghan, S., Ginoux, P., Gong, S., Horowitz, L., Iversen, T., Kirkevåg, A., Klimont, Z., Kondo, Y., Krol, M., Liu, X., Miller, R., Montanaro, V., Moteki, N., Myhre, G., Penner, J. E., Perlwitz, J., Pitari, G., Reddy, S., Sahu, L., Sakamoto, H., Schuster, G., Schwarz, J. P., Seland, Ø., Stier, P., Takegawa, N., Takemura, T., Textor, C., van Aardenne, J. A. and Zhao, Y.: Evaluation of black carbon estimations in global aerosol models, Atmos. Chem. Phys., 9(22), 9001–9026, doi:10.5194/acp-9-9001-2009, 2009.

Kok, J. F., Ridley, D. A., Zhou, Q., Miller, R. L., Zhao, C., Heald, C. L., Ward, D. S., Albani, S. and Haustein, K.: Smaller desert dust cooling effect estimated from analysis of dust size and abundance, Nat. Geosci., 10(4), 274–278, doi:10.1038/ngeo2912, 2017.

Kokhanovsky, A. A., Davis, A. B., Cairns, B., Dubovik, O., Hasekamp, O. P., Sano, I., Mukai, S., Rozanov, V. V., Litvinov, P., Lapyonok, T., Kolomiets, I. S., Oberemok, Y. A., Savenkov, S., Martin, W., Wasilewski, A., Di Noia, A., Stap, F. A., Rietjens, J., Xu, F., Natraj, V., Duan, M., Cheng, T. and Munro, R.: Space-based remote sensing of atmospheric aerosols: The multi-angle spectro-polarimetric frontier, Earth-Science Rev., 145, 85–116, doi:10.1016/j.earscirev.2015.01.012, 2015.

Kopacz, M., Jacob, D. J., Henze, D. K., Heald, C. L., Streets, D. G. and Zhang, Q.: Comparison of adjoint and analytical Bayesian inversion methods for constraining Asian sources of carbon monoxide using satellite (MOPITT) measurements of CO columns, J. Geophys. Res., 114(D4), D04305, doi:10.1029/2007JD009264, 2009.

Koepke P., Hess M., Schult I., and Shettle E. P.: Global aerosol dataset, Report N 243, Max-Plank-Institut für Meteorologie, Hamburg, 44 pp., September 1997.

Lenoble, J., Remer, L. and Tanré, D.: Aerosol Remote Sensing, edited by J. Lenoble, L. Remer, and D. Tanré, Springer Berlin Heidelberg, Berlin, Heidelberg., 2013.

Levy, R. C., Mattoo, S., Munchak, L. A., Remer, L. A., Sayer, A. M., Patadia, F. and Hsu, N. C.: The Collection 6 MODIS aerosol products over land and ocean, Atmos. Meas. Tech., 6(11), 2989–3034, doi:10.5194/amt-6-2989-2013, 2013.

Li, Z., Gu, X., Wang, L., Li, D., Xie, Y., Li, K., Dubovik, O., Schuster, G., Goloub, P., Zhang, Y., Li, L., Ma, Y. and Xu, H.: Aerosol physical and chemical properties retrieved from ground-based remote sensing measurements during heavy haze days in Beijing winter, Atmos. Chem. Phys., 13(20), 10171–10183, doi:10.5194/acp-13-10171-2013, 2013.

Liousse, C., Guillaume, B., Grégoire, J. M., Mallet, M., Galy, C., Pont, V., Akpo, A., Bedou, M., Castéra, P., Dungall, L., Gardrat, E., Granier, C., Konaré, A., Malavelle, F., Mariscal, A., Mieville, A., Rosset, R., Serça, D., Solmon, F., Tummon, F., Assamoi, E., Yoboué, V. and Van Velthoven, P.: Updated African biomass burning emission inventories in the framework of the AMMA-IDAF program, with an evaluation of combustion aerosols, Atmos. Chem. Phys., 10(19), 9631–9646, doi:10.5194/acp-10-9631-2010, 2010.

Liu, H., Jacob, D. J., Bey, I. and Yantosca, R. M.: Constraints from 210 Pb and 7 Be on wet deposition and transport in a global three-dimensional chemical tracer model driven by assimilated meteorological fields, J. Geophys. Res. Atmos., 106(D11), 12109–12128, doi:10.1029/2000JD900839, 2001.

Liu, L. and Mishchenko, M. I.: Scattering and radiative properties of complex soot and soot-containing aggregate particles, J. Quant. Spectrosc. Radiat. Transf., 106(1–3), 262–273, doi:10.1016/J.JQSRT.2007.01.020, 2007.

Lopatin, A., Dubovik, O., Chaikovsky, A., Goloub, P., Lapyonok, T., Tanré, D. and Litvinov, P.: Enhancement of aerosol characterization using synergy of lidar and sun-photometer coincident observations: the GARRLiC algorithm, Atmos. Meas. Tech., 6(8), 2065–2088, doi:10.5194/amt-6-2065-2013, 2013.

Mann, G. W., Carslaw, K. S., Spracklen, D. V., Ridley, D. A., Manktelow, P. T., Chipperfield, M. P., Pickering, S. J. and Johnson, C. E.: Description and evaluation of GLOMAP-mode: a modal global aerosol microphysics model for the UKCA composition-climate model, Geosci. Model Dev., 3(2), 519–551, doi:10.5194/gmd-3-519-2010, 2010.

Martin, R. V., Jacob, D. J., Yantosca, R. M., Chin, M. and Ginoux, P.: Global and regional decreases in tropospheric oxidants from photochemical effects of aerosols, J. Geophys. Res. Atmos., 108(D3), 4097, doi:10.1029/2002JD002622, 2003.

Meland, B. S., Xu, X., Henze, D. K. and Wang, J.: Assessing remote polarimetric measurement sensitivities to aerosol emissions using the geos-chem adjoint model, Atmos. Meas. Tech., 6(12), 3441–3457, doi:10.5194/amt-6-3441-2013, 2013.

Miller, R. L., Tegen, I. and Perlwitz, J.: Surface radiative forcing by soil dust aerosols and the hydrologic cycle, J. Geophys. Res. Atmos., 109(D4), doi:10.1029/2003JD004085, 2004.

Mishchenko, M. I., Liu, L. and Mackowski, D. W.: T-matrix modeling of linear depolarization by morphologically complex soot and soot-containing aerosols, J. Quant. Spectrosc. Radiat. Transf., 123, 135–144, doi:10.1016/J.JQSRT.2012.11.012, 2013.

Monks, P. S., Granier, C., Fuzzi, S., Stohl, A., Williams, M. L., Akimoto, H., Amann, M., Baklanov, A., Baltensperger, U., Bey, I., Blake, N., Blake, R. S., Carslaw, K., Cooper, O. R., Dentener, F., Fowler, D., Fragkou, E., Frost, G. J., Generoso, S., Ginoux, P., Grewe, V., Guenther, A., Hansson, H. C., Henne, S., Hjorth, J., Hofzumahaus, A., Huntrieser, H., Isaksen, I. S. A., Jenkin, M. E., Kaiser, J., Kanakidou, M., Klimont, Z., Kulmala, M., Laj, P., Lawrence, M. G., Lee, J. D., Liousse, C., Maione, M., McFiggans, G., Metzger, A., Mieville, A., Moussiopoulos, N., Orlando, J. J., O'Dowd, C. D., Palmer, P. I., Parrish, D. D., Petzold, A., Platt, U., Pöschl, U., Prévôt, A. S. H., Reeves, C. E., Reimann, S., Rudich, Y., Sellegri, K., Steinbrecher, R., Simpson, D., ten Brink, H., Theloke, J., van der Werf, G. R., Vautard, R., Vestreng, V., Vlachokostas, C. and von Glasow, R.: Atmospheric composition change – global and regional air quality, Atmos. Environ., 43(33), 5268–5350, doi:10.1016/j.atmosenv.2009.08.021, 2009.

Myhre, G., Shindell, D., Bréon, F.-M., Collins, W., Fuglestvedt, J., Huang, J., Koch, D., Lamarque, J.-F., Lee, D., Mendoza, B., Nakajima, T., Robock, A., Stephens, G., Takemura, T. and Zhang, H.: Anthropogenic and Natural Radiative Forcing, in Contribution of Working Group I to the Fifth Assessment Report of the Intergovernmental Panel on Climate Change [Stocker, T.F., D. Qin, G.-K. Plattner, M. Tignor, S.K. Allen, J. Boschung, A. Nauels, Y. Xia, V. Bex and P.M. Midgley (eds.)], Cambridge University Press, Cambridge, United Kindom and New York, NY, USA. [online] Available from: https://www.ipcc.ch/pdf/assessment-report/ar5/wg1/WG1AR5_Chapter08_FINAL.pdf, 2013.

Park, R. J., Jacob, D. J., Field, B. D., Yantosca, R. M. and Chin, M.: Natural and transboundary pollution influences on sulfate-nitrate-ammonium aerosols in the United States: Implications for policy, J. Geophys. Res., 109(D15), D15204, doi:10.1029/2003JD004473, 2004.

Popp, T., de Leeuw, G., Bingen, C., Brühl, C., Capelle, V., Chedin, A., Clarisse, L., Dubovik, O., Grainger, R., Griesfeller, J., Heckel, A., Kinne, S., Klüser, L., Kosmale, M., Kolmonen, P., Lelli, L., Litvinov, P., Mei, L., North, P., Pinnock, S., Povey, A., Robert, C., Schulz, M., Sogacheva, L., Stebel, K., Stein Zweers, D., Thomas, G., Tilstra, L., Vandenbussche, S., Veefkind, P., Vountas, M. and Xue, Y.: Development, Production and Evaluation of Aerosol Climate Data Records from European Satellite Observations (Aerosol_cci), Remote Sens., 8(5), 421, doi:10.3390/rs8050421, 2016.

Prospero, J. M. and Lamb, P. J.: African Droughts and Dust Transport to the Caribbean: Climate Change Implications, Science (80-.)., 302(5647), 1024–1027, 2003.

Pye, H. O. T., Liao, H., Wu, S., Mickley, L. J., Jacob, D. J., Henze, D. K. and Seinfeld, J. H.: Effect of changes in climate and emissions on future sulfate-nitrate-ammonium aerosol levels in the United States, J. Geophys. Res., 114(D1), D01205, doi:10.1029/2008JD010701, 2009.

Randerson, J. T., van der Werf, G. R., L. Giglio, Collatz, G. J. and Kasibhatla, P. S.: Global Fire Emissions Database, Version 3.1, , doi:doi:10.3334/ORNLDAAC/1191, 2013.

Ridley, D. A., Heald, C. L. and Ford, B.: North African dust export and deposition: A satellite and model perspective, J. Geophys. Res. Atmos., 117(D2), doi:10.1029/2011JD016794, 2012.

Ridley, D. A., Heald, C. L., Kok, J. F. and Zhao, C.: An observationally constrained estimate of global dust aerosol optical depth, Atmos. Chem. Phys., 16(23), 15097–15117, doi:10.5194/acp-16-15097-2016, 2016.

Sandu, A., Liao, W., Carmichael, G. R., Henze, D. K. and Seinfeld, J. H.: Inverse Modeling of Aerosol Dynamics Using Adjoints: Theoretical and Numerical Considerations, Aerosol Sci. Technol., 39(8), 677–694, doi:10.1080/02786820500182289, 2005.

Sato, M., Hansen, J., Koch, D., Lacis, A., Ruedy, R., Dubovik, O., Holben, B., Chin, M. and Novakov, T.: Global atmospheric black carbon inferred from AERONET., Proc. Natl. Acad. Sci. U. S. A., 100(11), 6319–6324, doi:10.1073/pnas.0731897100, 2003.

Schuster, G. L., Dubovik, O., Holben, B. N. and Clothiaux, E. E.: Inferring black carbon content and specific absorption from Aerosol Robotic Network (AERONET) aerosol retrievals, J. Geophys. Res., 110(D10), D10S17, doi:10.1029/2004JD004548, 2005.

Schuster, G. L., Dubovik, O. and Holben, B. N.: Angstrom exponent and bimodal aerosol size distributions, J. Geophys. Res., 111(D7), D07207, doi:10.1029/2005JD006328, 2006.

Smirnov, A., Holben, B. N., Eck, T. F., Dubovik, O. and Slutsker, I.: Cloud-Screening and Quality Control Algorithms for the AERONET Database, Remote Sens. Environ., 73(3), 337–349, doi:10.1016/S0034-4257(00)00109-7, 2000.

Spracklen, D. V., Pringle, K. J., Carslaw, K. S., Chipperfield, M. P. and Mann, G. W.: A global off-line model of size-resolved aerosol microphysics: II. Identification of key uncertainties, Atmos. Chem. Phys., 5(12), 3233–3250, doi:10.5194/acp-5-3233-2005, 2005.

Talagrand, O. and Courtier, P.: Variational assimilation of meteorological observations with the adjoint of the vorticity equations: Part I., Theory, Q. J. Roy. Meteor. Soc., 113, 1311–1328, 1987

Takemura, T., Okamoto, H., Maruyama, Y., Numaguti, A., Higurashi, A. and Nakajima, T.: Global three-dimensional simulation of aerosol optical thickness distribution of various origins, J. Geophys. Res. Atmos., 105(D14), 17853–17873, doi:10.1029/2000JD900265, 2000.

Tanré, D., Bréon, F. M., Deuzé, J. L., Dubovik, O., Ducos, F., François, P., Goloub, P., Herman, M., Lifermann, A. and Waquet, F.: Remote sensing of aerosols by using polarized, directional and spectral measurements within the A-Train: the PARASOL mission, Atmos. Meas. Tech., 4(7), 1383–1395, doi:10.5194/amt-4-1383-2011, 2011.

Tegen, I. and Lacis, A. A.: Modeling of particle size distribution and its influence on the radiative properties of mineral dust aerosol, J. Geophys. Res. Atmos., 101(D14), 19237–19244, doi:10.1029/95JD03610, 1996.

Textor, C., Schulz, M., Guibert, S., Kinne, S., Balkanski, Y., Bauer, S., Berntsen, T., Berglen, T., Boucher, O., Chin, M., Dentener, F., Diehl, T., Easter, R., Feichter, H., Fillmore, D., Ghan, S., Ginoux, P., Gong, S., Grini, A., Hendricks, J., Horowitz, L., Huang, P., Isaksen, I., Iversen, I., Kloster, S., Koch, D., Kirkevåg, A., Kristjansson, J. E., Krol, M., Lauer, A., Lamarque, J. F., Liu, X., Montanaro, V., Myhre, G., Penner, J., Pitari, G., Reddy, S., Seland, Ø., Stier, P., Takemura, T. and Tie, X.: Analysis and quantification of the diversities of aerosol life cycles within AeroCom, Atmos. Chem. Phys., 6(7), 1777–1813, doi:10.5194/acp-6-1777-2006, 2006.

Torres, O., Tanskanen, A., Veihelmann, B., Ahn, C., Braak, R., Bhartia, P. K., Veefkind, P. and Levelt, P.: Aerosols and surface UV products from Ozone Monitoring Instrument observations: An overview, J. Geophys. Res., 112(D24), D24S47, doi:10.1029/2007JD008809, 2007.

Torres, O., Ahn, C. and Chen, Z.: Improvements to the OMI near-UV aerosol algorithm using A-train CALIOP and AIRS observations, Atmos. Meas. Tech., 6(11), 3257–3270, doi:10.5194/AMT-6-3257-2013, 2013.

Veihelmann, B., Levelt, P. F., Stammes, P. and Veefkind, J. P.: Simulation study of the aerosol information content in OMI spectral reflectance measurements, Atmos. Chem. Phys., 7(12), 3115–3127, doi:10.5194/acp-7-3115-2007, 2007.

Wang, J., Cubison, M. J., Aiken, A. C., Jimenez, J. L. and Collins, D. R.: The importance of aerosol mixing state and size-resolved composition on CCN concentration and the variation of the importance with atmospheric aging of aerosols, Atmos. Chem. Phys., 10(15), 7267–7283, doi:10.5194/acp-10-7267-2010, 2010.

Wang, J., Xu, X., Henze, D. K., Zeng, J., Ji, Q., Tsay, S.-C. and Huang, J.: Top-down estimate of dust emissions through integration of MODIS and MISR aerosol retrievals with the GEOS-Chem adjoint model, Geophys. Res. Lett., 39(8), L08802, doi:10.1029/2012GL051136, 2012.

Wang, R., Tao, S., Balkanski, Y., Ciais, P., Boucher, O., Liu, J., Piao, S., Shen, H., Vuolo, M. R., Valari, M., Chen, H., Chen, Y., Cozic, A., Huang, Y., Li, B., Li, W., Shen, G., Wang, B. and Zhang, Y.: Exposure to ambient black carbon derived from a unique inventory and high-resolution model., Proc. Natl. Acad. Sci. U. S. A., 111(7), 2459–63, doi:10.1073/pnas.1318763111, 2014a.

Wang, R., Balkanski, Y., Boucher, O., Ciais, P., Schuster, G. L., Chevallier, F., Samset, B. H., Liu, J., Piao, S., Valari, M. and Tao, S.: Estimation of global black carbon direct radiative forcing and its uncertainty constrained by observations, J. Geophys. Res. Atmos., 121(10), 5948–5971, doi:10.1002/2015JD024326, 2016.

Wang, X., Heald, C. L., Ridley, D. A., Schwarz, J. P., Spackman, J. R., Perring, A. E., Coe, H., Liu, D. and Clarke, A. D.: Exploiting simultaneous observational constraints on mass and absorption to estimate the global direct radiative forcing of black carbon and brown carbon, Atmos. Chem. Phys., 14(20), 10989–11010, doi:10.5194/acp-14-10989-2014, 2014b.

Wang, Y., Jacob, D. J. and Logan, J. A.: Global simulation of tropospheric O3-NOx hydrocarbon chemistry: 3. Origin of tropospheric ozone and effects of nonmethane hydrocarbons, J. Geophys. Res. Atmos., 103(D9), 10757–10767, doi:10.1029/98JD00156, 1998.

Watson, J. G., Zhu, T., Chow, J. C., Engelbrecht, J., Fujita, E. M. and Wilson, W. E.: Receptor modeling application framework for particle source apportionment, Chemosphere, 49(9), 1093–1136, doi:10.1016/S0045-6535(02)00243-6, 2002.

van der Werf, G. R., Randerson, J. T., Giglio, L., Collatz, G. J., Kasibhatla, P. S. and Arellano, A. F.: Interannual variability in global biomass burning emissions from 1997 to 2004, Atmos. Chem. Phys., 6(11), 3423–3441, doi:10.5194/acp-6-3423-2006, 2006.

van der Werf, G. R., Randerson, J. T., Giglio, L., Collatz, G. J., Mu, M., Kasibhatla, P. S., Morton, D. C., DeFries, R. S., Jin, Y. and van Leeuwen, T. T.: Global fire emissions and the contribution of deforestation, savanna, forest, agricultural, and peat fires (1997–2009), Atmos. Chem. Phys., 10(23), 11707–11735, doi:10.5194/acp-10-11707-2010, 2010.

Werner, M., Tegen, I., Harrison, S. P., Kohfeld, K. E., Prentice, I. C., Balkanski, Y., Rodhe, H. and Roelandt, C.: Seasonal and interannual variability of the mineral dust cycle under present and glacial climate conditions, J. Geophys. Res., 107(D24), 4744, doi:10.1029/2002JD002365, 2002.

Wesely, M. L.: Parameterization of surface resistances to gaseous dry deposition in regional-scale numerical models, Atmos. Environ., 23(6), 1293–1304, doi:10.1016/0004-6981(89)90153-4, 1989.

Xu, X., Wang, J., Henze, D. K., Qu, W. and Kopacz, M.: Constraints on aerosol sources using GEOS-Chem adjoint and MODIS radiances, and evaluation with multisensor (OMI, MISR) data, J. Geophys. Res. Atmos., 118(12), 6396–6413, doi:10.1002/jgrd.50515, 2013.

Zender, C. S., Bian, H. and Newman, D.: Mineral Dust Entrainment and Deposition (DEAD) model: Description and 1990s dust climatology, J. Geophys. Res., 108(D14), 4416, doi:10.1029/2002JD002775, 2003.

Zhang, L., Gong, S., Padro, J. and Barrie, L.: A size-segregated particle dry deposition scheme for an atmospheric aerosol module, Atmos. Environ., 35(3), 549–560, doi:10.1016/S1352-2310(00)00326-5, 2001.

Zhang, L., Jacob, D. J., Kopacz, M., Henze, D. K., Singh, K. and Jaffe, D. A.: Intercontinental source attribution of ozone pollution at western U.S. sites using an adjoint method, Geophys. Res. Lett., 36(11), L11810, doi:10.1029/2009GL037950, 2009.

Zhang, L., Kok, J. F., Henze, D. K., Li, Q. and Zhao, C.: Improving simulations of fine dust surface concentrations over the western United States by optimizing the particle size distribution, Geophys. Res. Lett., 40(12), 3270–3275, doi:10.1002/grl.50591, 2013.

Zhang, L., Henze, D. K., Grell, G. A., Carmichael, G. R., Bousserez, N., Zhang, Q., Torres, O., Ahn, C., Lu, Z., Cao, J. and Mao, Y.: Constraining black carbon aerosol over Asia using OMI aerosol absorption optical depth and the adjoint of GEOS-Chem, Atmos. Chem. Phys., 15(18), 10281–10308, doi:10.5194/acp-15-10281-2015, 2015.

Zhao, C., Liu, X., Leung, L. R., Johnson, B., McFarlane, S. A., Gustafson, W. I., Fast, J. D. and Easter, R.: The spatial distribution of mineral dust and its shortwave radiative forcing over North Africa: modeling sensitivities to dust emissions and aerosol size treatments, Atmos. Chem. Phys., 10(18), 8821–8838, doi:10.5194/acp-10-8821-2010, 2010.

Zhu, C., Byrd, R. H., Lu, P. and Nocedal, J.: Algorithm 778: L-BFGS-B: Fortran subroutines for large-scale bound-constrained optimization, ACM Trans. Math. Softw., 23(4), 550–560, doi:10.1145/279232.279236, 1997.

Zhu, L., Henze, D. K., Cady-Pereira, K. E., Shephard, M. W., Luo, M., Pinder, R. W., Bash, J. O. and Jeong, G.-R.: Constraining U.S. ammonia emissions using TES remote sensing observations and the GEOS-Chem adjoint model, J. Geophys. Res. Atmos., 118(8), 3355–3368, doi:10.1002/jgrd.50166, 2013.